STUDY ON THE FORMATION OF NITROGENOUS DISINFECTION BY PRODUCTS FROM THE REACTION BETWEEN DICHLOROACETALDEHYDE AND MONOCHLORAMINE

BY

TRANG NHA VU

DISSERTATION

Submitted in partial fulfillment of the requirements
for the degree of Doctor of Philosophy in Environmental Engineering in Civil Engineering
in the Graduate College of the
University of Illinois at Urbana-Champaign, 2018

Urbana, Illinois

Doctoral Committee:

Professor Benito Jose Mariñas, Chair
Professor Michael Jacob Plewa
Associate Professor Thanh Huong Nguyen
Professor Susan D. Richardson, University of South Carolina

ABSTRACT

Disinfection is a mandatory step in drinking water treatment to inactivate harmful pathogens found in source waters and minimize health risks for human consumers. Among many powerful oxidants commonly used as disinfectants, chlorine has been widely utilized at many water treatment facilities due to low cost and high efficiency in reducing waterborne diseases such as cholera and typhoid. However, the major downside of this process is the formation of a group of compounds known as disinfection by-products (DBPs) when chlorine unintentionally reacts with some constituents naturally occurring in source water. To prevent the negative health effects of chlorinated DBPs such as trihalomethanes (THMs) and haloacetic acids (HAAs), regulations that stipulate their maximum contaminant levels have been established since 1970s and gradually become more stringent. For this reason, switching to alternative disinfectants (i.e. ozone, UV or chloramine) helps to significantly reduce the concentration of chlorinated DBPs in finished water. Although this strategy allows water utilities to comply the stricter regulation recently proposed, the alternative disinfectants introduce new DBP classes that are not well studied and can also cause severe human health effects.

Among newly found DBPs which are introduced to disinfected water by using alternative disinfectant, nitrogen containing DBPs (N-DBPs) are of growing concern to human consumers due to their relatively high toxicity compared to regulated DBPs mostly produced by chlorination. Occurrence studies have shown that haloacetonitriles (HANs) and haloacetamides (HAMs), two unregulated N-DBP groups, were commonly found in drinking water with chloramine disinfection. Although these N-DBP groups occur at lower levels than chlorinated DBPs, they are shown to be more toxic and can significantly contribute to the overall toxicity of disinfected drinking water. In addition, haloaldehydes were also observed in the finished water from several water facilities and they are identified as the third largest DBP group by weight, only behind THMs and HAAs.

For the first time, this study confirms the predominant formation of HAN and HAM dominant species, dichloroacetonitrile (DCAN) and dichloroacetamide (DCAM), from the reaction between monochloramine and dichloroacetaldehyde via the aldehyde reaction pathway. Initial reactants reacted quickly and reached equilibrium with carbinolamine 2,2-dichloro-1-(chloroamino)ethanol. Then, the carbinolamine underwent two parallel reactions where, (1) it

slowly dehydrated to 1,1-dichloro-2-(chloroimino)ethane and further decomposed to dichloroacetonitrile and (2) it was oxidized by monochloramine to form a newly discovered *N*-haloacetamide *N*,2,2-trichloroacetamide. Additionally, labelled ^{15}N-monochloramine experiments with natural water reveals the prevalence of the aldehyde pathway in real drinking water conditions as 60-70% DCAN and DCAM contain ^{15}N atom which was contributed by ^{15}N-monochloramine. Furthermore, free chlorine pretreatment followed by chloramination was shown to enhance the formation of ^{15}N-DBPs. A kinetic model was developed that predicted up to 90% of N-DBPs in natural waters.

This thesis of dedicated to my mom, dad, brother and my husband for their love and support throughout these years.

ACKNOWLEDGEMENTS

Firstly, I would like to express my sincere gratitude to Professor Benito J. Mariñas, my adviser, for his warm encouragement and insightful comments throughout these years. I would have never been able to attend this study program at UIUC and finish the project without the dedicated support and considerable help from Professor Mariñas. Also, I would like to offer my special thanks to Dr. Susana Kimura who has been extraordinarily tolerant and supportive to train me on the lab protocol and techniques. She helped me to get adapted to a new academia environment with numerous advices and useful instructions for research and courses. I owe a very important debt to Susana for her generous support in academic research as well as in life. Moreover, I want to thank Professor Michael Plewa for his guidance and wonderful stories when instructing me about toxicity experiment in his lab. I also would like to thank Professor Susan Richardson for her excellent advice and generosity when allowing me to work in her lab and learn about analysis extraction methods. I am so thankful to Professor Helen Nguyen for her advice and comments as a member of my dissertation committee.

I also would like to thank Professor Vern Snoeyink and Dr. Ana Martinez for their helpful advices on the classes, research and my presentation skills in CASE group. I want to thank Dr. Shaoying Qi at the 4th floor for the lab maintenance and Dr. Alex Ulanov from Metabolomics Center for their help on the instrumentation. Furthermore, I am very thankful to many colleagues and students that have worked with me and helped me a lot throughout the years of my PhD life. I would like to express my deep appreciation to my officemate, Lauren Valentino for her kindness, huge support and always being a great listener. I am very thankful to Dr. Yukako Komaki, Gabrielle Levato, Andrea Vozar and Aimee Gall for interesting talks about research and life; to Bernardo Vazquez, Oki Abiodun, Daniel Mosiman and Bryan Smith for their valuable comments, great helps and encouragements. A special thank also goes to the rest of the students in Mariñas research group. I feel very lucky to be a part of this group and be able to meet these amazing people. Besides, I want to thank Anna Yang for her help and guidance on NMR analysis. I also thank Kentaro, Apeksha and other students in CEE department and also in the 4th floor who have helped and worked together with me to go through the courses.

My appreciation goes to Tan Nguyen, my dear husband for doing housework, running errands, and baby-sitting our son while I am working in the lab and writing the thesis. I also would like to show my greatest appreciation to my parents, my brother, and other family members. I would have never finished this work without their help and understanding.

Lastly, I would like to thank Vietnam Education Foundation (VEF) for their fellowship and CEE department at UIUC for their generous department fellowship.

TABLE OF CONTENTS

CHAPTER 1

INTRODUCTION

In drinking water treatment, disinfection is a mandatory step to inactivate pathogens found in source waters and minimize health risks for human consumers. In this stage, some powerful oxidants (e.g., chlorine, ozone, UV) are often used as disinfectants to eliminate disease-causing bacteria and virus in finished water. Since its introduction in 1900s, chlorine has been widely utilized at many water treatment facilities for disinfection due to low cost and high efficiency in reducing waterborne diseases such as cholera and typhoid [1]. However, chlorine has been shown to react with some constituents naturally occurring in source water to unintentionally produce a group of compounds known as disinfection by-products (DBPs) [2-4]. Several studies in the 1970s have reported that chloroform and three other trihalomethanes (THMs), the first group of DBPs discovered, can be considered possible carcinogenic compounds for human [5, 6]. For this reason, regulations that stipulate maximum contaminant levels (MCLs) for THMs, haloacetic acids (HAAs), chlorite ion and bromate ion were established [7].

In Stage 1 of the D/DBP Rule (1998), the MCL for THMs was set to 80 µg/L, and the MCLs for the total concentration of five HAAs, bromate and chlorite were also established to 60 µg/L, 10 µg/L and 1 mg/L, respectively [8]. Some revised points in Stage 2 of the D/DBP Rule (2006) (i.e. locational running annual average) make it harder for the water utilities to comply with the standards of THMs and HAAs even though the MCLs did not change [9]. This has led the water facilities to switch to other disinfectants (i.e. ozone, UV or chloramine) to meet the stricter regulations on chlorinated DBPs. Although the switch to alternative disinfectants reduces the formation of THMs and HAAs, which are mainly formed during chlorination, these alternative strategies can also increase the formation of other types of DBPs that are still unknown [10-13]. Since the discovery of THMs and HAAs in 1970s, more than 600 DBP species have been identified in finished waters which were treated with commonly used disinfectants; yet, about 70% of the total halogenated organic carbon remains unidentified [14].

Among newly found DBPs which are introduced by using alternative disinfectant, nitrogen containing DBPs (N-DBPs) are of growing concern to human health due to their relatively high toxicity compared to regulated DBPs. The presence of N-DBPs in post-disinfected drinking water

can result from the use of combined chlorine as the alternative disinfectant or from the chlorination of water sources impacted by wastewater secondary effluents with high nitrogen levels [15-17]. In an occurrence study that monitored unregulated and priority DBPs at several US water treatment utilities from 2000 – 2002, haloacetonitriles (HANs), haloacetamides (HAMs) and halonitromethanes (HNMs) were commonly found in treated water samples [15]. Among 12 water utilities at which different water disinfectants were employed, the median concentrations of these DBPs were 3, 1.4, and 1 μg/L, respectively [11, 15]. For each subgroup, di-chlorinated species were shown to occur at higher concentrations than the mono-chlorinated or tri-chlorinated analogues. In particular, dichloroacetonitrile was one of the most predominant compounds among these groups with a median and maximum concentrations of 1 and 12 μg/L, respectively. The second most prevalent species in these studies was dichloroacetamide (median and maximum concentrations of 1.3 and 5.6 μg/L, respectively). The highest occurrences of these priority DBPs were observed at a treatment plant using prechlorination followed by chloramination [11, 18].

Moreover, the occurrence study also reported that haloaldehydes (HAL) were observed in disinfected water from several water utilities beside HANs and HAMs [11]. Most aldehydes resulted from ozone treatment in which natural organic matter was broken down into less complex and more biodegradable compounds [19, 20]. Depending on the treatment stages employed, total aldehyde concentration, including both haloaldehydes and non-halogenated aldehyde, ranged from 5 – 300 μg/L in finished drinking water [21]. Typical formaldehyde and acetaldehyde concentrations were reported to be 28.3 μg/L and 9.7 μg/L, respectively [22]. According to the nationwide occurrence and study of unregulated priority DBPs, the third largest DBP group by weight was identified as haloaldehydes, behind THMs and HAAs [11]. Within this group, dichloroacetaldehyde and trichloracetaldehyde (chloral hydrate) were the predominant species with maximum concentrations of 14 μg/L and 16 μg/L, respectively [11].

Previous research on the toxicity of N-DBPs suggested that N-DBPs are more toxic than THMs and HAAs [4, 12, 23-26]. For this reason, current studies are focusing on the occurrence, formation and toxicity of major N-DBP groups including halonitromethanes, haloacetonitriles, haloacetamides and N-nitrosamines. As shown in Figure 1, HANs and HAMs are significantly more genotoxic than regulated DBPs such as THMs and HAAs. The genotoxicity of DBP species shown in the figure was evaluated with the Chinese hamster ovary (CHO) cell assay which reveal genomic damage caused by the examined compounds [24]. The halogen atoms attached to the

alpha carbon have an important effect on the toxicity of the compounds. Particularly, the toxicity can increase dramatically in the order of halogen substitution of Cl < Br << I. In general, iodo species were found to be more toxic than their bromo- or chloro- analogues [4]. Among HANs, iodoacetonitrile was found to be slightly more toxic than bromoacetonitrile which was followed by chloroacetonitrile. Iodoacetonitrile at the concentration of 37.1 μM can cause as much genomic damage on CHO cells as 38.5 μM bromoacetonitrile or 601 μM chloroacetonitrile [23]. Among the HAcAms, iodoacetamide was observed to have the highest toxicity with 34.1 μM iodoacetamide producing a similar level of damage on CHO cells as 36.8 μM bromoacetonitrile or 1.38 mM chloroacetonitrile [24]. The difference in concentration causing DNA damage between iodoacetamide and chloroacetamide was more than two orders of magnitude. As a result, these unregulated N-DBPs may provide a significant contribution to the toxicity of drinking water after disinfection in addition to regulated DBPs even though N-DBPs are found at low concentrations.

In short, dichloroacetaldehyde, dichloroacetonitrile (DCAN) and dichloroacetamide (DCAM) are the most prevalent compounds of HALs, HANs and HAMs group that were commonly found in chlorinated drinking water. Preliminary results in occurrence studies showed that HANs and HAMs were more likely produced from chloramination as an alternative usage of free chlorine. Although these N-DBPs are more toxic than the regulated ones, their formation mechanisms have not been well studied. Therefore, it is important to explore the chemical formation of HANs and HAMs during chloramine disinfection. The purpose of this study is to verify the formation of DCAN and DCAM from the reaction between dichloroacetaldehyde and monochloramine. A reaction scheme was proposed and kinetic rate constants were determined according to the identified intermediates and products from this reaction. Another goal of this research is to evaluate the relevance of this reaction pathway and that reported previously for the monochlorinated species under drinking water conditions and in natural waters of various qualities by using labelled $^{15}NH_2Cl$ technique. The results from this study will provide more information about the formation pathway of HANs and HAMs, two dominant N-DBP groups under drinking water conditions. Therefore, it also efficiently contributes to the development of N-DBP control strategies and regulations in order to minimize the health risks of these compounds on human consumers.

Tables and Figures

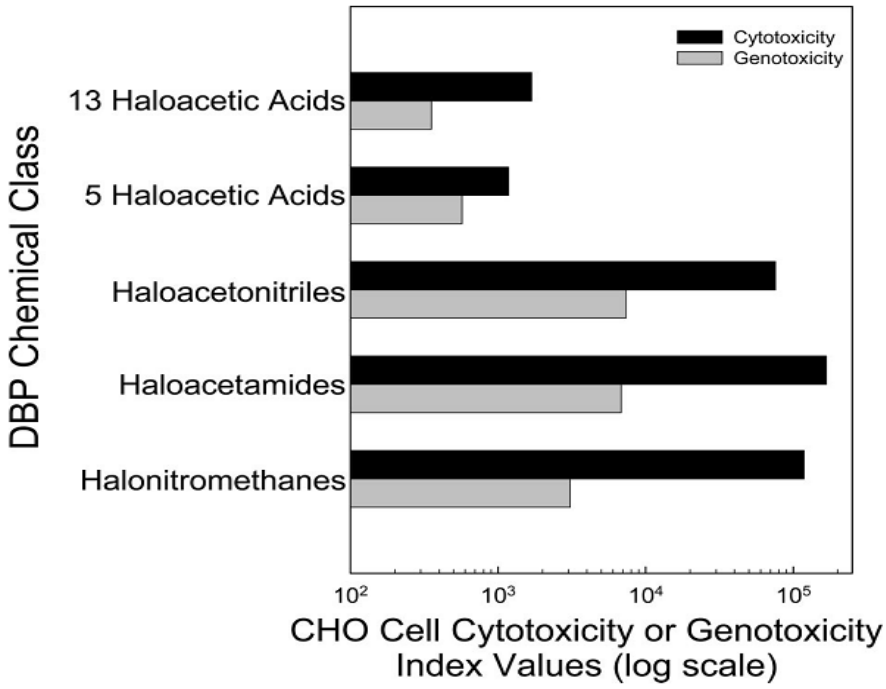

Figure 1.1 CHO cell cytotoxicity and genotoxicity index values for some DBP chemical classes [24].

References

1. Calderon, R., *The epidemiology of chemical contaminants of drinking water.* Food Chem. Toxicol., 2000. **38**: p. S13-S20.
2. Bellar, T.A., J.J. Lichtenberg, and R.C. Kroner, *The occurrence of organohalides in chlorinated drinking waters.* J. Am. Water Works Assoc., 1974. **66**: p. 703-706.
3. Rook, J.J., *Haloforms in drinking water.* J. Am. Water Works Assoc., 1976. **68**: p. 168-172.
4. Richardson, S.D., et al., *Occurrence, genotoxicity, and carcinogenicity of regulated and emerging disinfection by-products in drinking water: a review and roadmap for research.* Mutat. Res., 2007. **636**(1): p. 178-242.
5. Page, N.P., *Report on carcinogenesis bioassay of chloroform*. 1976, Bethesda, MD: U.S. Dept. of Health, Education, and Welfare, Public Health Service, National Institutes of Health, National Cancer Institute, Division of Cancer Cause and Prevention, Carcinogenesis Program, Carcinogen Bioassay and Program Resources Branch.
6. Fawell, J., *Risk assessment case study—chloroform and related substances.* Food Chem. Toxicol., 2000. **38**: p. S91-S95.
7. U.S.EPA, *National interim primary drinking water regulations: control of trihalomethanes in drinking water: final rules.* Federal register, 1979. **44**: p. 68624-68705.
8. U.S.EPA, *National primary drinking water regulations: disinfectants and disinfection by-products: final rule.* Fed. Regist., 1998. **63**: p. 69390-69476.
9. U.S.EPA, *National primary drinking water regulations: Stage 2 disinfectants and disinfection byproducts rule.* Fed. Regist., 2006. **71**: p. 387-493.
10. Weinberg, H.S., et al., *The occurrence of disinfection by-products (DBPs) of health concern in drinking water: results of a nationwide DBP occurrence study*. 2002, EPA National Exposure Research Laboratory: Athens, GA.
11. Krasner, S.W., et al., *Occurrence of a new generation of disinfection byproducts.* Environ. Sci. Technol., 2006. **40**(23): p. 7175-7185.

12. Plewa, M., et al., *Occurrence, formation, health effects and control of disinfection by-products in drinking water*, in *Comparative Mammalian Cell Toxicity of N-DBPs and C-DBPs*. 2008, American Chemical Society Washington, DC. p. 36-50.

13. Chu, W., et al., *Formation and speciation of nine haloacetamides, an emerging class of nitrogenous DBPs, during chlorination or chloramination.* J. Hazard. Mater., 2013. **260**: p. 806-812.

14. Richardson, S. and R. Meyers, *Encyclopedia of environmental analysis and remediation.* Hoboken, New Jersey: John Wiley & Sons, 1998: p. 1398.

15. Westerhoff, P. and H. Mash, *Dissolved organic nitrogen in drinking water supplies: a review.* Aqua, 2002. **51**: p. 415-448.

16. Joo, S.H. and W.A. Mitch, *Nitrile, aldehyde, and halonitroalkane formation during chlorination/chloramination of primary amines.* Environ. Sci. Technol., 2007. **41**(4): p. 1288-1296.

17. Mitch, W.A., et al., *Occurrence and formation of nitrogenous disinfection by-products*. 2009, Denver, CO: Water Research Foundation.

18. Lee, W., P. Westerhoff, and J.-P. Croué, *Dissolved organic nitrogen as a precursor for chloroform, dichloroacetonitrile, N-nitrosodimethylamine, and trichloronitromethane.* Environ. Sci. Technol., 2007. **41**(15): p. 5485-5490.

19. Weinberg, H.S., et al., *Formation and removal of aldehydes in plants that use ozonation.* Journal (American Water Works Association), 1993: p. 72-85.

20. Schechter, D.S. and P.C. Singer, *Formation of aldehydes during ozonation.* Ozone Sci. Eng., 1995. **17**(1): p. 53-69.

21. Krasner, S.W., et al., *The occurrence of disinfection by-products in US drinking water.* J. Am. Water Works Assoc., 1989. **81**(8): p. 41-53.

22. Glaze, W.H., et al. *Trends in aldehyde formation and removal through plants using ozonation and biological active filters*. in *American Water Works Association. Proceedings, A W W A Annual Conference*. 1991.

23. Muellner, M.G., et al., *Haloacetonitriles vs. regulated haloacetic acids: are nitrogen-containing DBPs more toxic?* Environ. Sci. Technol., 2007. **41**(2): p. 645-651.

24. Plewa, M.J., et al., *Occurrence, synthesis, and mammalian cell cytotoxicity and genotoxicity of haloacetamides: an emerging class of nitrogenous drinking water disinfection byproducts.* Environ. Sci. Technol., 2008. **42**(3): p. 955-961.

25. Plewa, M.J., et al., *Comparative Mammalian Cell Toxicity of N-DBPs and C-DBPs*, in *Disinfection By-Products in Drinking Water*. 2008, American Chemical Society. p. 36-50.

26. Komaki, Y., B.J. Mariñas, and M.J. Plewa, *Toxicity of drinking water disinfection byproducts: cell cycle alterations induced by the monohaloacetonitriles.* Environ. Sci. Technol., 2014. **48**(19): p. 11662-11669.

CHAPTER 2

FORMATION OF HALOACETONITRILE, HALOACETAMIDE AND N-HALOACETAMIDE FROM THE REACTION BETWEEN DICHLOROACETALDEHYDE AND MONOCHLORAMINE

Abstract

In drinking water disinfection, switching from chlorination to alternative disinfectants may introduce new classes of disinfection byproducts (DBPs) that can cause negative human health effects. Haloacetonitriles (HANs) and haloacetamides (HAMs), two unregulated nitrogen-containing DBP (N-DBP) groups, are commonly found with monochloramine and have been shown to be more toxic than regulated DBPs. For the first time, this study confirms the predominant formation of HAN and HAM dominant species, dichloroacetonitrile and dichloroacetamide, from the reaction between monochloramine and dichloroacetaldehyde via the aldehyde reaction pathway. Labelled ^{15}N-monochloramine experiments with natural water were employed to confirm the relevance of the aldehyde pathway in drinking water conditions. A kinetic model was developed that predicted up to 90% of N-DBPs in natural waters. Initial reactants reacted quickly and reached equilibrium with carbinolamine 2,2-dichloro-1-(chloroamino)ethanol (K_1=1.87x10^4 $M^{-1}s^{-1}$). Then, 2,2-dichloro-1-(chloroamino)ethanol underwent two parallel reactions where, (1) it slowly dehydrated to 1,1-dichloro-2-(chloroimino)ethane (k_2=1.09x10^{-5} s^{-1}) and further decomposed to dichloroacetonitrile and (2) it was oxidized by monochloramine (k_3= 4.87x10^{-2} $M^{-1}s^{-1}$) to form a newly discovered *N*-haloacetamide *N*,2,2-trichloroacetamide. At high pH, dichloroacetonitrile hydrolyzed to dichloroacetamide (k_4^0=3.12x10^{-7} s^{-1}, k_4^{OH}=3.54 $M^{-1}s^{-1}$). Additionally, trichloroacetaldehyde was also produced from the reaction of dichloracetaldehyde and monochloramine (k_5=2.12x10^{-2} $M^{-1}s^{-1}$) under the presence of monochlorammonium ion, a product of monochloramine disproportionation. Within the *N*-haloacetamide family, *N*,2,2-trichloroacetamide (LC_{50}=3.90x10^{-4} M) was found to be more cytotoxic than *N*-chloroacetamide but slightly less potent than *N*,2-dichloroacetamide.

Introduction

Chlorination has been widely used since the last century protecting against waterborne pathogens making water safe to drink [1]. However, chlorine reacts with organic matter to unintentionally form disinfection by-products (DBPs), such as trihalomethanes (THMs) and haloacetic acids (HAAs) [2-4]. Because THMs and HAAs were shown to be carcinogenic, chronic exposure to DBPs can potentially increase human health risk [5, 6]. As a result, maximum DBP concentrations in drinking water were established to minimize health risks for consumers [7-9]. For this reason, alternative disinfectants such as chloramines have been increasingly applied by water utilities to reduce the formation of regulated DBPs. A switch of disinfectant however, may increase the formation of other unregulated DBP classes, including haloacetonitriles (HANs) and haloacetamides (HAMs)[10-13] that are more toxic than DBPs predominantly produced by chlorination [4, 14].

According to occurrence studies, nitrogen-containing DBPs (N-DBPs) have been detected at slightly higher levels in drinking water samples collected from water utilities that use chloramines compared to chlorine [10-12] Among HANs and HAMs, dichloroacetonitrile (DCAN) and dichloroacetamide (DCAM) were reported as predominant species with median of 1 µg/L and 1.3 µg/L and up to maximum concentrations of 12 µg/L and 5.6 µg/L, respectively [10, 11]. Although HANs and HAMs are found at low levels, they were demonstrated to be more cyto- and genotoxic compared to regulated DBPs, and could contribute significantly to the overall toxicity of disinfected waters [4, 13, 15-17].

Because of the occurrence and elevated toxicity of HANs and HAMs [18], there is an emphasis on research efforts to characterize their formation mechanism relevant in drinking waters [19-29]. The formation of HANs and HAMs in drinking water has been hypothesized based on the origin of nitrogen atom in their molecule. Nitrogen-containing organic matter (i.e., amino acids, algal matter) could serve as a major precursor to form N-DBPs when it reacts with chlorine or chloramine via the decarboxylation pathway [19-21]. On the other hand, the nitrogen atom of the nitrile group or the amide group of HANs or HAMs could also be contributed from monochloramine, an inorganic source, from the reaction with aldehydes [25-27] or aromatic compounds [22, 24, 30, 31]. All of these formation pathways may occur simultaneously and one pathway may become the dominant at certain conditions. In two previous studies using ^{15}N-

labelled-monochloramine, one reported >70% DCAN produced contained ^{15}N atom [21] while another work demonstrated >92% of DCAN produced contained ^{15}N atom [28]. Of importance in both studies, a large majority of the ^{15}N from the labelled monochloramine was transferred to DCAN. These results indicated the importance of the aldehyde pathway on the formation of these N-DBPs under drinking water disinfection conditions.

The reaction of monochloramine with aldehydes, commonly formed as byproducts from ozone and chlorine disinfection [32-35], that can lead to the formation of HANs, HAMs, and *N*-haloacetamides (*N*-HAMs), a recently discovered group, is known as the aldehyde pathway. The formation mechanisms of chloroacetonitrile, chloroacetamide, and *N*,2-dichloroacetamide were characterized from the reaction between monochloramine and chloroacetaldehyde in a recent study [26]. Monochloramine reacted with chloroacetaldehyde by nucleophilic addition, to form the carbinolamine 2-chloro-(1-chloroamino)ethanol in a reversible reaction. The carbinolamine dehydrated and produced imine 1-chloro-(2-chloroimino)ethane that subsequently decomposed to chloroacetonitrile. The reaction was acid and base catalyzed. In a parallel reaction, the carbinolamine was oxidized to form *N*,2-dichloroacetamide, which was identified for the first time as a new N-DBP subgroup, *N*-HAMs family. A similar mechanism was observed for the formation of acetonitrile, acetamide, and *N*-chloroacetamide from the reaction of monochloramine with acetaldehyde [27].

Although several formation mechanisms for HAN, HAM, and *N*-HAM formation were proposed [20, 21, 25-28], the predominance of a specific pathway has not been identified in natural waters. The formation of DCAN and DCAM via the aldehyde pathway has also not been determined. The possible formation of *N*-HAM *N*,2,2-trichloroacetamide (*N*,2,2-TCAM) has not been shown. It is possible that DCAN, N,2,2-TCAM and DCAM may be produced from the reaction between dichloroacetaldehyde (DCAL) and monochloramine. This hypothesis is supported by the fact that DCAL and choral hydrate are two species with the highest concentration amongst the haloaldehyde group quantified in drinking water [11].

The main objective of this study was to determine the predominance of DCAN and DCAM formation from the reaction between DCAL and monochloramine via the aldehyde pathway. To achieve this, three approaches were conducted. (1) The reaction pathway was confirmed through the identification of intermediates and products, including *N*,2,2-TCAM. Cytotoxicity of *N*,2,2-

TCAM was compared to other species from the *N*-HAM and HAM groups. (2) ^{15}N-labeled monochloramine was used on natural waters to evaluate the relevance of the aldehyde pathway on the formation of DCAN, *N*,2,2-TCAM, and DCAM under drinking water conditions. (3) Reaction rate constants for the proposed pathway were determined via batch experiments using synthetic buffered water. DCAN, *N*,2,2-TCAM, and DCAM concentrations were simulated using the kinetic model determined previously. Experimental and simulated data were compared to determine the occurrence of DCAN, *N*,2,2-TCAM, and DCAM through the aldehyde pathway.

Experimental methods

Reagents of the highest purity grade commercially available were used in this study. Potassium biphosphate (99%), sodium perchlorate (>98%), sodium hydroxide (97%), perchloric acid (70%), ammonium chloride (99.9%), sodium bicarbonate (99%), sodium hypochlorite (5-6%), chloral hydrate (>97%), 2,2-dichloroacetonitrile (>99.5%), sodium sulfate (99%), methyl tertiary butyl ether (HPLC grade 99.9%), hexane (>98.5%) and ethyl acetate (HPLC grade 99.9%) were purchased from Sigma-Aldrich (St. Louis, MO) and Fisher Scientific (Pittsburgh, PA). Commercial DCAL hydrate solid stock (>95%) was purchased from Tokyo Chemical Industry (TCI) – America (Portland, OR). Acetamide 2,2-dichloroacetamide (>98%) was purchased from Alfa Aesar (Ward Hill, MA).

All solutions were prepared with MiliQ water (>18 MΩ.cm, Millipore, Billerica, MA) with a total phosphate buffer concentration of 0.02 M and ionic strength of 0.1 M. Phosphate buffer solution was prepared daily by dissolving potassium biphosphate in pure water. pH was adjusted with perchloric acid and a sodium hydroxide solution that was prepared every month. Ionic strength was adjusted with a 1 M sodium perchlorate solution prepared monthly.

Monochloramine stock solution was prepared daily for each set of experiments by a slow drop-wise addition of sodium hypochlorite solution into an ammonium chloride solution (N/Cl molar ratio = 1.1) under fast stirring at pH of 8.5. Monochloramine (ε_{243} = 461 $M^{-1}cm^{-1}$) [36] and sodium hypochlorite (ε_{292} = 362 $M^{-1}cm^{-1}$) were standardized with a spectrophotometer.

A 1-2 M DCAL stock solution was freshly prepared for each experimental set by diluting DCAL hydrate in oxygen-free pure water. The aldehyde solution was stored at 4^{o}C for several hours before use. Chloral hydrate and 2,2-dichloroacetonitrile were prepared by diluting in

acetonitrile and were used to prepare calibration curves for gas chromatography (GC) - mass spectrometry (MS) analysis.

N,2,2-Trichloroacetamide was prepared by slowly mixing equal volumes of a 20 mM sodium hypochlorite with 20 mM DCAM aqueous solution at pH 9.5 and 25^{o}C. This reaction was monitored by UV-Vis spectroscopy for 7 days and ^{1}H NMR for 3 days and shown in Figure 2.1 and 2.2. Sodium hypochlorite disappeared quickly after 15 min to form *N*,2,2-TCAM and remained stable for several days. A 16 mL *N*,2,2-TCAM aliquot was removed and extracted with liquid-liquid extraction (LLE) with 3 mL of ethyl acetate and 4.6 g of sodium sulfate. The extract was immediately analyzed by GC-high resolution mass spectrometry (HRMS). Details about this synthetic procedure was described elsewhere [26, 27, 37].

Controlled Reactions

Reaction intermediates and products were identified by reacting excess DCAL (10 and 50 mM) with monochloramine (1 and 15 mM) at pH 9.5. Sample aliquots without quenching were extracted by LLE and analyzed by GC-MS and GC-HRMS. Suspect intermediate and products were confirmed by analysis of pure standards or by mass spectral interpretation.

Experiments conducted for this study are shown in Table 2.1. Experiments under drinking water conditions (GC-1) were tested in triplicate to evaluate the relevance of the aldehyde pathway to form *N*,2,2-trichloroacetamide and dichloroacetonitrile. ^{15}N-labeled monochloramine was added to treated surface waters from Bloomington, IL collected after filtration and before disinfection. Kinetic constants of the proposed reaction pathway were determined using batch reactors for experiments GC-2, GC-3, GC-4, UV-1, UV-2, HR-1, and HR-2. Fast reactions, including the reversible reaction of DCAL with monochloramine to form the corresponding carbinolamine, were studied under experimental conditions SF-1 with stop flow analysis (SF-1). All experiments where maintained at 25.0 ± 0.1^{o}C throughout the whole reaction.

Instrumentation and Methods

A Thermo Electron Orion ROSS Ultra pH electrode connected to an Accumet AB15 Plus pH meter were used to measure pH. The pH meter was calibrated daily with commercial 4, 7, and 10 pH standard solutions. Measured pH values were adjusted to actual hydrogen ion concentration

using the Davis equation (μ=0.1 M). A water bath re-circulator (PolyScience, Niles, IL) was used to maintain a constant temperature (25.0 ± 0.1°C) for all reactions.

A 2550 UV-Vis spectrophotometer (Shimadzu Scientific Instruments, Columbia, MD) was used to standardize solutions and monitor reactions. Samples were placed in 10 mm quartz cuvettes and absorbance spectra were taken at wavelengths between 200 – 400 nm.

A SX20 stopped flow spectrophotometer (Applied Photophysics, Surrey, UK) was used to study fast reactions of experimental set SF-1. Equal volumes of each reactant were mixed and monitored at monochloramine's λ_{max} of 243 nm. Five replicates were taken for each experiment. The resulting data was analyzed by the chemical relaxation method shown in Appendix A [27]. Micromath Scientist 3.0 (St. Louis, MO) was used to fit the experimental data to kinetic models.

GC-MS (Agilent Technologies GC 6850-MSD 5975C) was employed to identify and quantify intermediates and products from experimental set GC-1 to GC-4 shown in Table 1. A 7 mL aliquot was sampled from the reactor over time and extracted by LLE with 1 mL of ethyl acetate and 2 g of sodium sulfate. Extracts were injected under split mode (2:1 split ratio) at 230°C. Compounds were separated with a 30 m DB-624 column (J&W Scientific) by initially holding the oven temperature at 35°C for 3 min, then ramping at 10°C/min to 90°C and held for 1 min, and finally ramped at 10°C/min to 240°C and held for 5 min. Helium was used as carrier gas with a flow of 1.0 mL/min. Electron ionization (EI) was used to ionize the compounds in the sample and performed under full scan mode at m/z 30-350.

Labeled ^{15}N-monochloramine and GC-MS analysis was also applied in drinking water experiments to verify the dominance of the aldehyde pathway in the competition with the decarboxylation pathway. Surface water from the city of Bloomington, IL treated with conventional treatment after filtration and before disinfection was used for these experiments. Monochloramine was added to a reactor with a dose of 10 mg/L as Cl_2. Aliquots of 200 mL were quenched with sodium thiosulfate and analyzed for HANs, HAMs, and HALs over time. HANs and HAMs were extracted from an aliquot of 100 mL by LLE with 2 mL of methyl tert-butyl ether (MTBE), 30 g of sodium sulfate, and 1,2-dibromopropane as an internal standard.[38] The mixture was shaken for 30 min and the top layer was transferred to a vial after a 5 min rest. HALs were derivatized with O-2,3,4,5,6-pentafluorobenzylhydroxylamine (PFBHA) and extracted from another 100 mL aliquot according to a procedure described elsewhere [39]. The GC-MS program

was slightly modified to analyze both extracts with a 30 m Rtx-200, 0.25mm ID, 1 µm film thickness (Restek Corporation, Bellefonte, PA). A 2 µL extract was injected into the inlet under split mode (2:1 split ratio) at 230^{o}C. The oven was held at 40^{o}C for 3 min, increased to 70^{o}C (ramped 10^{o}C/min) and held for 2 min, then risen to 240^{o}C (ramped 10^{o}C/min) and held for 5 min. EI was used and the scan range was m/z 30-450. MS source and quad temperature were 230oC and 150oC, respectively. For DCAN, the fragments m/z 74 and 75 were used to distinguish DCAN containing ^{14}N and DCAN containing ^{15}N, respectively (Figure 2.3a). Similarly, m/z 127 and 128 were applied to differentiate DCAM containing ^{14}N and DCAM containing ^{15}N, respectively (Figure 2.3b).

GC-HRMS analysis was done with a HP 5890 GC (Agilent Technologies, Santa Clara, CA) coupled to a Synapt G2-Si high resolution time-of-flight mass spectrometer with an atmospheric pressure chemical ionization (APCI) source (Waters Cooperation, Milford, MA). The resolution of this instrument was 50,000, and it was operated in full scan mode. The GC oven program was as follows: hold for 2 min at 50^{o}C and ramped at 15^{o}C per min to 280^{o}C and held for 5 min. A 30 m DB-5MS GC column with 0.25 mm ID and 1 µm film thickness (J&W Scientific) was used. The ion source and transfer line were 150 and 200^{o}C, respectively.

Mammalian Cell Cytotoxicity

Chinese Hamster Ovary (CHO) cells were used to determine the chronic cytotoxicity of 20 mM *N*,2,2-TCAM stock solution buffered with 14 mM $NaHCO_3$. In this test, Ham's F12 medium was added to *N*,2,2-TCAM solution. F12 medium was initially prepared with 5% fetal bovine serum, 1% antibiotic-antimycotic solution (10 units/mL penicillin G sodium, 10 µg/mL streptomycin sulfate, 25 µg/mL amphotericin B, 0.85% saline; Introgen, Carlsbad, CA) and 1% L-glutamine. CHO cells were exposed to increasing concentrations of *N*,2,2-TCAM for 72 h to obtain the concentration vs. response curve. 8 replicates were conducted for the measurement of the cell density exposed to each chemical concentration. These results were then converted into the mean percentage of the cell density of the negative control. Data analysis and nonlinear regression fitting were obtained by Sigmaplot 12.0 (Sytat Software Inc., San Jose, CA). The LC_{50} value at which the exposed chemical concentration causes a 50% reduction of the negative control's cell density was also determined from the above calculation. Details about the experimental procedure of this test were mentioned elsewhere [18, 40].

Results and discussions

N-haloacetamide and haloacetonitrile formation via the aldehyde reaction pathway

Similar to other aldehydes previously reported,[26, 27] DCAL was shown to react with monochloramine in a fast and reversible reaction to form carbinolamine 2,2-dichloro-1-(chloroamino)ethanol (Figure 2.4). Monochloramine attacks DCAL's carbonyl carbon via nucleophilic addition. The carbinolamine subsequently follows two parallel reactions. In the first reaction, the carbinolamine dehydrates to form imine 1,1-dichloro-2-(chloroimino)ethane that further decomposes to DCAN. Intermediate 1,1-dichloro-2-(chloroimino)ethane and product DCAN were observed in GC-MS results as shown in Figure 2.5 and 2.6. The identity of imine 1,1-dichloro-2-(chloroimino)ethane was identified from the m/z fragmentation pattern shown in Figure 2.6. A three chlorine isotope pattern was observed from 1,1-dichloro-2-(chloroimino)ethane's molecular ion cluster of 145 (M), 147 (M+2), and 149 (M+4). Additionally, isotope patterns from clusters 110/112/114 and 83/85/87 pertain to fragments of the imine that have two chlorines. Intermediate carbinolamine 2,2-dichloro-1-(chloroamino)ethanol was not observed, possibly because it could have dehydrated to the imine at the GC inlet (230°C). Reaction products, including DCAN, DCAM, and chloral hydrate, were identified by comparing their retention times and mass spectra from those obtained from the pure commercially standards.

In the second reaction, carbinolamine 2,2-dichloro-1-(chloroamino)ethanol was oxidized by monochloramine to form an *N*-HAM, *N*,2,2-trichloroacetamide (*N*,2,2-TCAM). To confirm this reaction and the product, a pure *N*,2,2-TCAM standard was prepared in this study and compared to reaction products. Both extracts were analyzed with the same method by GC-APCI-HRMS. The *N*,2,2-TCAM standard had a $[M + H]^+$ ion of m/z 161.9283 (100% relative abundance) with isotopes of m/z 163.9250 (96%), m/z 165.9224 (31%) and m/z 167.9202 (3%) as shown in Figure 2.7. The isotopic pattern indicated the presence of 3 chlorine atoms in the molecular structure of *N*,2,2-TCAM. The mass error of the observed molecular ion was 1.2 ppm. Total ion chromatograms from the reaction extracts and pure standards are shown in Figure 2.8. The $[M + H]^+$ ion cluster from the *N*,2,2-TCAM standard were also observed in the reaction products with a retention time of 12.1 min. A possible isomer of *N*,2,2-TCAM, 2,2,2-trichloroacetamide, was also analyzed as a pure standard to compare with the reaction extract. The peak of this isomer had an later retention time of 16.21 min and was not observed in the reaction mixture, therefore,

eliminating the possibility of 2,2,2-trichloroacetamide as a product from the aldehyde reaction pathway between dichloroacetaldehyde and monochloramine. These results confirmed that *N*,2,2-TCAM was produced from the reaction between monochloramine and DCAL. The formation of *N*-HAMs via the aldehyde pathway has been reported in recent studies [26, 27].

Additionally, GC-MS analyses also suggested that DCAM was a product from the reaction between DCAL and monochloramine as shown in Figure 2.6 and 2.8. One possible reaction could be the hydrolysis of DCAN to DCAM. Previous studies have shown that haloacetonitriles hydrolyze to haloamides and haloacetic acids [23, 41]. Control experiments (HR-1 in Table 1, Figure 2.9) of DCAN at different pH conditions showed that DCAN quickly hydrolyzed corresponding to the increasing formation of DCAM from the solution at high pH (pH > 9). Even though DCAN hydrolysis was negligible at pH 7.8, DCAM was observed in experiments conducted at this pH range (GC-1, GC-2, GC-4, and HR-1 from Table 1). Another reaction that has been shown in previous studies [26, 27] is that the addition of a quencher to reduce monochloramine and stop the reaction will also reduce *N*-HAMs to HAMs. Sodium thiosulfate, quencher used in this study, reduced the chlorine attached to the amide nitrogen, and *N*,2,2-TCAM was identified and quantified as DCAM. *N*,2,2-TCAM was quantified as DCAM in GC-MS experiments conducted in this study.

High levels of trichloroacetaldehyde (TCAL) were also found as a product from the reaction between DCAL and monochloramine, especially at neutral pH. However, the formation of TCAL at high pH (pH> 9) was negligible compared to the formation of DCAN and *N*,2,2-TCAM. The formation of more substituted haloaldehydes found in the reaction between DCAL and monochloramine was not observed with other aldehydes [26, 27]. Experimental set GC-4 showed increasing formation rate of TCAL with decreasing pH (data not shown). Some studies have hypothesized that the halogenation of DCAL leading to the formation of TCAL involved monochlorammonium ion (NH_3Cl^+) resulting from monochloramine disproportionation [42, 43]. At low pH, monochlorammonium ion would occur at a higher concentration and thereby enhance the formation of TCAL. Monochlorammonium ion has also been suggested as a possible halogenation agent at low pH [44].

Relevance of the aldehyde reaction pathway under drinking water conditions

The relevance of the aldehyde reaction pathway in Figure 1 that leads to the formation of DCAN, *N*,2,2-TCAM, and DCAM was tested in drinking water conditions. ^{15}N-labeled monochloramine ($^{15}NH_2Cl$) can react with natural organic matter and can be incorporated into ^{15}N-labeled DCAN and ^{15}N-labeled DCAM through the aldehyde reaction pathway. $^{15}NH_2Cl$ was added to Bloomington lake waters which previously treated by sedimentation and recarbonation with no disinfection (TOC = 1.8 mg/L, pH= 7.8-8.1) and analyzed by GC-MS over the course of 5 days, representing an average residence time in a water distribution system. Results are shown in Figure 2.10. In the first sample taken at 4 h, ^{15}N-DCAN concentration was 44% of the total DCAN concentration of 0.24 μg/L. At 95 h, total DCAN increased to a maximum concentration of 1.05 μg/L with 64% attributed to ^{15}N-DCAN. Similarly, total DCAM was relatively low (0.32 μg/L) at 4 h with 51% as ^{15}N-DCAM. Total DCAM reached a maximum concentration of 4.6 μg/L at 5 days with 67% as ^{15}N-DCAM. Our findings show that about 60-70% of the total DCAN and DCAM produced from the chloramination of the feed water contain an ^{15}N atom in their structures which can only be provided by the $^{15}NH_2Cl$ spike. These findings are also consistent with other studies [21, 28] that used $^{15}NH_2Cl$ in natural waters and NOM models and observed greater than 50% formation of ^{15}N-DCAN and ^{15}N-DCAM of the total DCAN and DCAM.

The concentration of *N*,2,2-TCAM, quantified as ^{15}N-DCAM, was also found to be higher than ^{15}N-DCAN throughout the chloramination experiment. ^{15}N-DCAM (or *N*,2,2-TCAM) reached a maximum concentration after 5 days (3.0 μg/L) which is 4.7x times higher than ^{15}N-DCAN concentration (0.63 μg/L). The predominant formation of DCAM over DCAN suggests that DCAM was produced independently from the hydrolysis of DCAN, which was insignificant at neutral pH range in this experiment. These results are consistent with a previous study[21] that showed independent formation of DCAM and DCAN during chloramination of drinking water and wastewater effluents.

A kinetic model that predicts the formation of *N*,2,2-TCAM, DCAM, and DCAN as the product from the aldehyde pathway under drinking water conditions can validate the proposed mechanism in Figure 2.4. In this experiment set, the feed water initially did not contain any detectable amount of DCAL, an initial reactant in the aldehyde pathway. However, reactions between $^{15}NH_2Cl$ and NOM during chloramination produced DCAL, which then reacted with $^{15}NH_2Cl$ via the aldehyde pathway and consequently forming ^{15}N-DCAN and ^{15}N-DCAM. The apparent formation rate of DCAL was experimentally determined from the quantified DCAL

residue and its products (i.e., DCAN and DCAM) assuming that DCAL was only consumed by the aldehyde pathway reactions proposed in this study (Figure 2.4). To predict the formation of ^{15}N-DCAN and ^{15}N-DCAM in drinking water, equilibrium and reaction rate constants were determined as shown in the following sections.

Kinetic rate constant determination

Equilibrium constant and formation of carbinolamine 2,2-dichloro-1-(chloroamino)ethanol

In aqueous solution, DCAL exists as two species in equilibrium: the aldehyde and a hydrated form. Therefore, total DCAL concentration ($C_{T,\,Cl_2CHCHO}$) is expressed as the sum of these two compounds. The dissociation constant for hydrated species of DCAL, K_d, was estimated according to a predictive model specific for the aldehydes and ketones[45] and is equal to:

$$K_d = \frac{[Cl_2CHCHO]}{[Cl_2CHCH(OH)_2]} = \ 4.46 \times 10^{-4} \qquad (1)$$

The hydration constant reveals that DCAL will predominantly exist as the hydrated species ($Cl_2CHCH(OH)_2$) in solution. The fractions of DCAL and it hydrated form of the total concentration $C_{T,Cl2CHCHO}$ were determined as 4.45 x 10^{-4} and 0.99955, respectively.

The DCAL and monochloramine reversible reaction was fast and reached equilibrium with carbinolamine 2,2-dichloro-1-(chloroamino)ethanol within 10 – 20 seconds. The equilibrium expression for this reaction K_1 is expressed as

$$K_1 = \frac{k_1}{k_{-1}} = \frac{[Cl_2CHCH(OH)NHCl]_e}{[NH_2Cl]_e[Cl_2CHCHO]_e} \qquad (2)$$

where, K_1 is the equilibrium constant, k_1 and k_{-1} are the forward and reverse reaction rate constants. $[Cl_2CHCH(OH)NHCl]_e$, $[NH_2Cl]_e$, and $[Cl_2CHCHO]_e$ are the 2,2-dichloro-1-(chloroamino)ethanol, monochloramine and DCAL concentrations at equilibrium state, respectively.

Experimental set SF-1 in Table 2.1 were used to study this fast reaction between DCAL and monochloramine. The chemical relaxation method [27, 46] was used to determine the forward and reverse reaction rate constants described in the Appendix A. The reaction was monitored at absorbance 243 nm (monochloramine's λ_{max}) until it reached the equilibrium. Results from each experimental condition were fitted to eq 3 to obtain the values of Abs_e, Abs_0 and $1/\tau$

$$Abs_t = (Abs_0 - Abs_e)\exp\left(-\frac{t}{\tau}\right) + Abs_e \quad (3)$$

where, Abs_e and Abs_0 are the absorbance values at equilibrium and at t = 0, and $(1/\tau)$ is a constant defined by eq 4.

$$\frac{1}{\tau} = k_1' + k_{-1} = k_1[Cl_2CHCHO]_0 + k_{-1} \quad (4)$$

For each initial DCAL concentration used, a $(1/\tau)$ value was obtained from data fitting. Results are plotted in Figure 2.11 as $(1/\tau)$ versus initial unhydrated DCAL concentration $[Cl_2CHCHO]_0$. A linear relationship was observed according to eq 4 where, the slope represents k_1 and the intercept at $[Cl_2CHCHO]_0 = 0$ is k_{-1}. Reaction rate constants k_1 and k_{-1} are 1.73±0.08 x 10^4 $M^{-1}s^{-1}$ and 0.922±0.016 s^{-1}, respectively.

Equilibrium constant K_1 was calculated with eq 2 to be 1.87 x 10^4 M^{-1}. In the presence of monochloramine and DCAL, K_1 predicts that carbinolamine will exist as the predominant species predominantly. Equilibrium constant K_1 was also found to be one to two orders of magnitude higher compared to the equilibrium constants of the reactions of acetaldehyde and chloroacetaldehyde with monochloramine which were reported as 109 and 1468 M^{-1}, respectively [26, 27]. An increased substitution of electron-withdrawing chlorine on the aldehyde's beta carbon will create a partially positive carbonyl carbon making it more electrophilic and susceptible to nucleophilic attack by monochloramine. As a result, the equilibrium constant K_1 of DCAL is significantly higher than chloroacetaldehyde followed by acetaldehyde. Because of this phenomenon, the dissociation rate constant k_{-1} of 6.71 x 10^{-1}, 2.70 x 10^{-2}, and 4.46 x 10^{-4} s^{-1} becomes slower with increasing chlorine substitution in the order of acetaldehyde, chloroacetaldehyde and DCAL, respectively [26, 27].

Dichloroacetonitrile, dichloroacetamide, *N*,2,2-trichloroacetamide, and trichloroacetaldehyde formation

Carbinolamine 2,2-dichloro-1-(chloroamino)ethanol quickly reached equilibrium and slowly decomposed through parallel dehydration and oxidation reactions as shown in Figure 2.4. The total monochloramine concentration ($C_{T,NCl}$) is expressed as the sum of monochloramine and carbinolamine concentration at a given time.

$$C_{T,NCl} = [NH_2Cl] + [Cl_2CHCH(OH)NHCl] \quad (5)$$

Monochloramine and carbinolamine concentrations are expressed as a fraction of $C_{T,NCl}$, α_0 and α_1, respectively.

$$\alpha_0 = \frac{[NH_2Cl]}{C_{T,NCl}} = \frac{1}{1 + K_1[Cl_2CHCHO]} \quad (6a)$$

$$\alpha_1 = \frac{[Cl_2CHCH(OH)NHCl]}{C_{T,NCl}} = \frac{K_1[Cl_2CHCHO]}{1 + K_1[Cl_2CHCHO]} \quad (6b)$$

The $C_{T,NCl}$ decomposition rate is composed by the loss of carbinolamine by dehydration and oxidation and the reacted monochloramine to produce TCAL expressed as:

$$-\frac{dC_{T,NCl}}{dt} = k_2[Cl_2CHCH(OH)NHCl] + k_3[Cl_2CHCH(OH)NHCl][NH_2Cl] + k_5[Cl_2CHCHO][NH_2Cl] \quad (7)$$

The individual rate expressions for the formation of products DCAN, DCAM, *N*,2,2-TCAM, and TCAL are:

$$\frac{d[Cl_2CHCN]}{dt} = k_2\alpha_1 C_{T,NCl} - k_4[Cl_2CHCN] \quad (8)$$

$$\frac{d[Cl_2CHC(O)NH_2]}{dt} = k_4[Cl_2CHCN] \quad (9)$$

$$\frac{d[Cl_2CHC(O)NHCl]}{dt} = k_3\alpha_1\alpha_0\left(C_{T,NCl}\right)^2 \quad (10)$$

$$\frac{d[Cl_3CCHO]}{dt} = k_5[Cl_2CHCHO]\alpha_0 C_{T,NCl} \quad (11)$$

Because excess aldehyde compared to monochloramine was used in this study, the reaction rate is $k_5' = k_5[Cl_2CHCHO] \cong k_5[Cl_2CHCHO]_0$ and eq 11 can be simplified to a pseudo-first order equation.

Experimental sets UV-1 and UV-2 (Table 2.1) were used to determine concentrations at time *t* of monochloramine ($[NH_2Cl]_t$), carbinolamine 2,2-dichloro-1-(chloroamino)ethanol ($[Cl_2CHCH(OH)NHCl]$) and *N*,2,2-TCAM ($[Cl_2CHC(O)NHCl]_t$). These concentrations will be used to determine reaction rate constants. For neutral pH condition (UV-1), DCAN hydrolysis to

DCAM was negligible and was not included in the kinetic model. Reactions were monitored at two wavelengths, 210 and 243 nm, and the measured absorbance is expressed as:

$$Abs_{\lambda,t} = \left(\varepsilon_{\lambda,NH_2Cl} + \varepsilon_{\lambda,Cl_2CHCH(OH)NHCl} K_1 [Cl_2CHCHO]_o\right)[NH_2Cl]_t + \varepsilon_{\lambda,Cl_2CHC(O)NHCl}[Cl_2CHC(O)NHCl]_t \quad (12)$$

where, $\varepsilon_{\lambda,NH_2Cl}$, $\varepsilon_{\lambda,Cl_2CHCH(OH)NHCl}$, and $\varepsilon_{\lambda,Cl_2CHC(O)NHCl}$ are the molar extinction coefficients previously determined from the absorbance of the pure standards at varying concentration levels (Table 2.2). Concentrations for $[Cl_2CHCH(OH)NHCl]$ and $C_{T,NCl}$ at time *t* were determined according to eq 2 and 5.

DCAN and TCAL were not included in eq 12 because their individual absorbance values at the concentration levels that were produced in the studied reaction were negligible compared to the measured absorbance of other reactants and products. Instead, DCAN and TCAL concentrations were determined by GC-MS (GC-2) at the exact times samples were collected and analyzed with UV-Vis. To ensure samples where taken at the same time for both method, reaction aliquots were quenched with sodium thiosulfate.

Experimental data obtained from UV-Vis and GC-MS were fitted to the kinetic model to determine the kinetic rate constants k_2, k_3, and k_5 (Figure 2.12). *N*,2,2-TCAM was quantified by GC-MS indirectly as DCAM. *N*,2,2-TCAM was also quantified by UV-Vis and results show a good agreement between both measurements as shown in Figure 2.13. The fitted rate constants at neutral pH 7.8 were $k_2 = (1.09 \pm 0.06) \times 10^{-5}$ s^{-1}, $k_3 = (4.87 \pm 0.25) \times 10^{-2}$ $M^{-1}s^{-1}$ and $k_5 = (2.12 \pm 0.15) \times 10^{-2}$ $M^{-1}s^{-1}$ for 25°C.

At pH >9 range, the hydrolysis reaction of DCAN to form DCAM was dominant and the formation of TCAL was not significant. In this case, DCAN, DCAM and *N*,2,2-TCAM were the main products from the reaction between DCAL and monochloramine. However, the carbonate buffer used at high pH range experiments caused an interference signal that affected the UV-VIS data analysis to obtain accurate kinetic rate values. In future work, we will employ different buffers and reaction conditions that will minimize its interference with our data analysis. This will enhance the applicability of our kinetic model as a predictive tool for the formation of HANs and HAMs at a wider pH range.

Dichloroacetonitrile hydrolysis to dichloroacetamide

DCAN hydrolysis was found to be significant at high pH values. For this reason, DCAN's hydrolysis rates at different pH values were determined. The reaction was monitored at wavelength 210 nm where the absorbance is equal to DCAN and DCAM concentration over time (HR-1 in Table 2.1). Absorbance is expressed as

$$Abs_{210,t} - Abs_{210,0} = \left(\varepsilon_{210,DCAM} - \varepsilon_{210,DCAN}\right)([DCAN]_0 - [DCAN]_t) \qquad (13)$$

where, $Abs_{210,0}$ is the absorbance of the DCAN sample at *t*=0, $Abs_{210,t}$ is the absorbance of DCAN and DCAM at time *t*, and $\varepsilon_{210,DCAM}$ and $\varepsilon_{210,DCAN}$ are the molar extinction coefficients of DCAM and DCAN that were previously determined (Table 2.2). $[DCAN]_0$ and $[DCAN]_t$ are the concentration of DCAN at t=0 and at time *t*.

The rate expression for DCAN hydrolysis is

$$-\frac{d[DCAN]}{dt} = k_4[DCAN] = \{k_4^0 + k_4^{OH}[OH^-]\}[DCAN] \qquad (14)$$

The concentration of DCAN over time from each experiment at different pH values were fitted to eq 14 and plotted the observed reaction rate k_4 versus $[OH^-]$ as shown in Figure 2.14. Results show a linear relationship between with a coefficient of determination (R^2) of 0.998 that indicates a base catalyzed reaction. Observed k_4 values were fitted to $k_4^0 + k_4^{OH}[OH^-]$ to obtain rate constants k_4^0 = (2.86 ± 0.90) x 10^{-7} s^{-1} and k_4^{OH} = 3.69 ± 0.09 $M^{-1}s^{-1}$ for 25°C. These rate constant results are consistent and in good agreement with the hydrolysis rate constants of DCAN reported in literature (k_4^0 = (1.78 ± 0.35) x 10^{-7} s^{-1} and k_4^{OH} = 3.42 ± 0.31 $M^{-1}s^{-1}$ for 20°C) [47]. The effect of monochloramine on the hydrolysis of DCAN (HR-2) was also examined, but results (data not shown) suggested that the role of monochloramine was not significant in this reaction.

***N*,2,2-trichloroacetamide cytotoxicity**

A mammalian cell cytotoxicity analysis was performed to determine the in vitro toxicity characteristics of *N*,2,2-TCAM. After a 72 h exposure, *N*,2,2-TCAM induced a concentration-response curve . The data were analyzed with an ANOVA test statistic with a Holm-Sidak comparison test with the control group ($1 - \beta \geq 0.8$, $\alpha = 0.05$). The lowest significant cytotoxic concentration of *N*,2,2-TCAM was 250 µM. The concentration, which reduced 50% of the cell density (LC_{50}) compared to the negative control group, was estimated by nonlinear regression analysis (R^2 = 0.99, illustrated in Figure 2.15).

Among the *N*-HAM family, mammalian cell cytotoxicity of *N*,2,2-TCAM (LC_{50} = 3.90 × 10^{-4} M) was found to be more toxic than *N*-chloroacetamide (LC_{50} = 1.78 × 10^{-3} M) but shown slightly less potent than *N*,2-dichloroacetamide (LC_{50} = 2.56 × 10^{-4} M). In comparison with other HAMs, *N*,2,2-TCAM was more toxic than dichloroacetamide and trichloroacetamide (LC_{50} = 1.92 × 10^{-3} M and LC_{50} = 2.05 × 10^{-3} M, respectively) but less potent than chloroacetamide (LC_{50} = 1.48 × 10^{-4} M).

Kinetic model validation and predominance of the aldehyde reaction pathway

The kinetic model and reaction rate constants determined in this study were used to predict the formation of *N*,2,2-TCAM and DCAN from experiment GC-1. Quantified DCAL and NH_2Cl initial dose of 10 mg/L as Cl_2 were used as inputs for the kinetic model. Modeled and experimental data for a period of 5 days are plotted in Figure 2.16. Results show a very good agreement between the measured DCAN-^{15}N and DCAM-^{15}N (indirectly for *N*,2,2-TCAM-^{15}N) and their prediction provided by the kinetic model. The model accounted for 81-99% of the experimental data suggesting that these compounds are predominantly formed through the aldehyde reaction pathway proposed in this study. Additionally, these results also validate our initial assumption that DCAL is produced from the reaction of NH_2Cl with NOM in waters that do not contain DCAL.

This study has shown for the first time that the aldehyde reaction pathway is a major pathway for the formation of DCAN, *N*,2,2-TCAM and DCAM, the most commonly found N-DBP species among HANs and HAMs group in drinking water. Additionally, our kinetic model could be applied as a useful tool to predict the formation of DCAN, *N*,2,2-TCAM and DCAM under drinking water conditions. This reaction pathway could also extend to our preceding work with other aldehydes [26, 27].

Quenchers and Practical Implications

The use of quenchers, such as ascorbic acid and sodium thiosulfate, brings into question how much HAMs and HANs are actually present in drinking water versus an artifact of sample and preservation methods. For example, in occurrence studies, *N*,2,2-TCAM would mistakenly be quantified as DCAM because grab samples will often use quenchers (i.e. sodium thiosulfate) to reduce the main disinfectant but will also quench *N*,2,2-TCAM to DCAM. These new findings indicate that drinking water consumers are predominantly exposed to *N*,2,2-TCAM, which was

found to be more toxic than DCAM and trichloroacetamide and in similar toxicity as other *N*-haloacetamides tested in our preceding work [26, 27].

Ammonium chloride, another commonly used quencher for free chlorine, will react with free chlorine to form chloramines which will then continue to react with organic matter present in samples to potentially form HANs and HAMs while being held for several days to weeks before extraction. While quenchers might be appropriate for the detection and quantification of certain DBPs it might not be appropriate for another set of DBP. For this reason, sampling and preservation methods used for DBP analysis must be carefully designed to minimize artifacts caused by such methods.

Tables and Figures

Table 2.1. Experimental conditions and instrument used to monitor the studied reactions

Experiment	**pH**	**Reactant(s)**	**Instrument**
GC-1	7.8 – 8.1	10 mg/L as Cl_2 of $^{15}NH_2Cl$ in treated surface water before disinfection	GC-MS
GC-2	7.8	1 mM NH_2Cl and 10 mM $C_{T,aldehyde}$	GC-MS
GC-3	9.5	1 mM NH_2Cl and 10 mM $C_{T,aldehyde}$	GC-MS
GC-4	5.5 – 7.0	1 mM NH_2Cl and 10 mM $C_{T,aldehyde}$	GC-MS
UV-1	7.8	1 mM NH_2Cl and 10 mM $C_{T,aldehyde}$	UV-VIS
UV-2	9.5	1 mM NH_2Cl and 10 mM $C_{T,aldehyde}$	UV-VIS
HR-1	7.0 – 9.9	1 mM DCAN	UV-VIS
HR-2	7.5	1 mM DCAN and 0.4-1.2 mM NH_2Cl	UV-VIS
SF-1	7.8	1 mM NH_2Cl and 10-90 mM $C_{T,aldehyde}$	Stopped flow

Table 2.2. Molar extinction coefficients ($M^{-1}cm^{-1}$) used in this study

	Wavelength (nm)			
Compound	**210**	**215**	**220**	**243**
NH_2Cl	77	108	164	461
$Cl_2CHCH(OH)NHCl$	35.1	95.1	150	318
$Cl_2CHC(O)NH_2$	1953	1042	517	45
Cl_2CHCN	328	217	132	26.3
$Cl_2CHC(O)NHCl$	6320	6320	5600	882

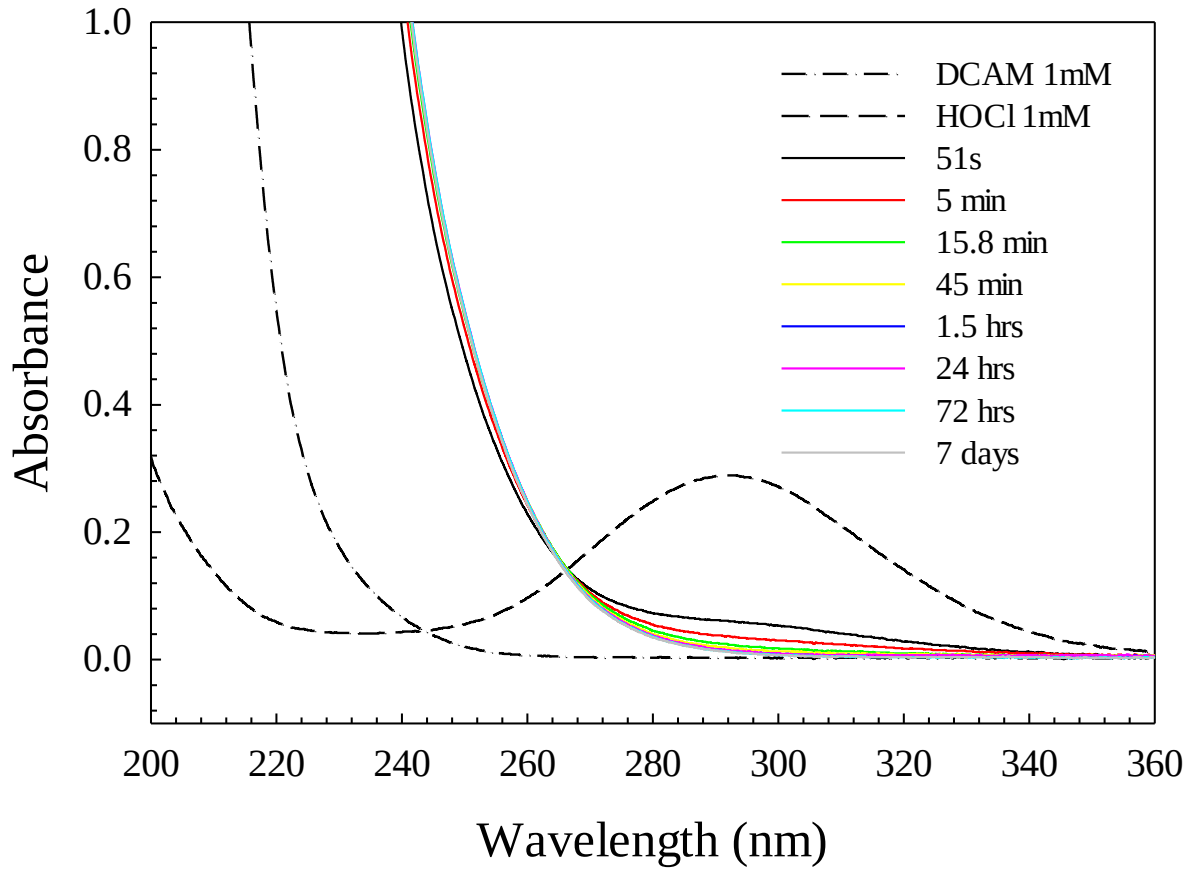

Figure 2.1. N,2,2-trichloroacetamide formation over time monitored with UV-Vis spectroscopy from the reaction between 2,2-dichloroacetamide and hypochlorous acid. Experimental conditions: $[HOCl]_o$ = 1 mM, $[Cl_2CHC(O)NH_2]_o$ = 1 mM, phosphate buffer 20 mM, pH 7.8 ± 0.1, μ = 0.1 M, Temp = 25 ± 0.1°C.

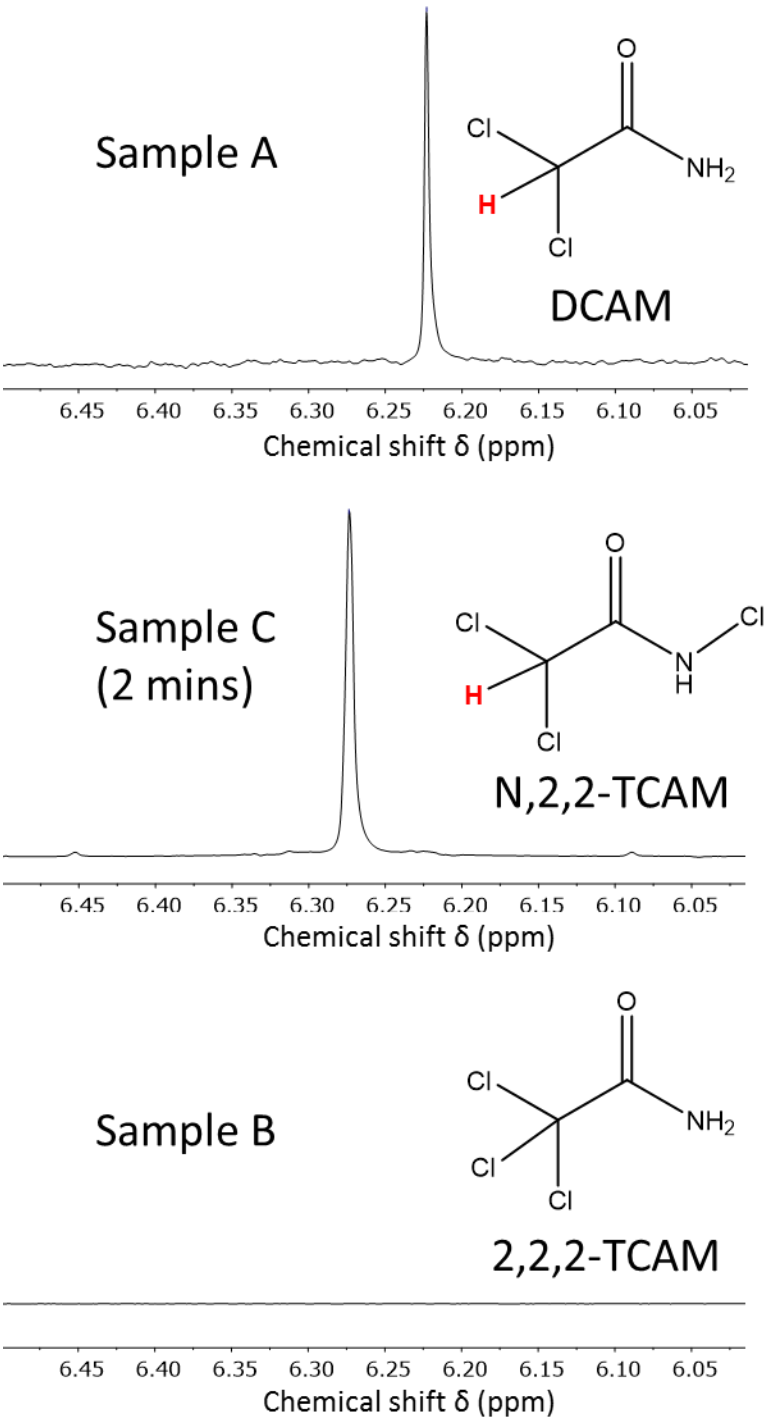

Figure 2.2. ^{1}H NMR spectra of 2,2-dichloroacetamide (sample A), the reaction of dichloroacetamide and hypochlorous acid after 2 minutes with the product N,2,2-trichloroacetamide (sample C), and the control 2,2,2-trichloroacetamide (sample B). Experimental conditions: $[HOCl]_o$ = 0.15 M, $[Cl_2CHC(O)NH_2]_o$ = 0.15 M, 25^{o}C.

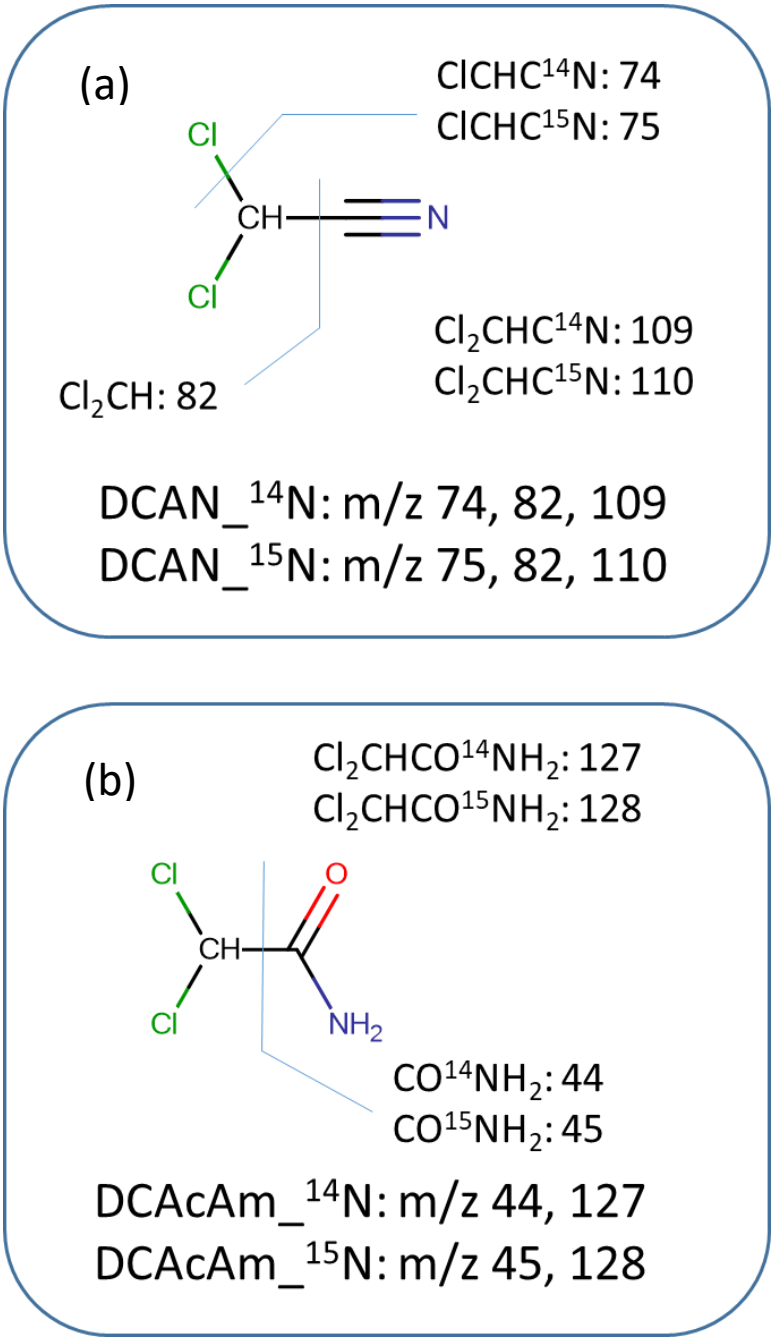

Figure 2.3. Fragment ions monitored to distinguish ^{14}N-DCAN vs ^{15}N-DCAN (a), ^{14}N-DCAM vs ^{15}N-DCAM (b).

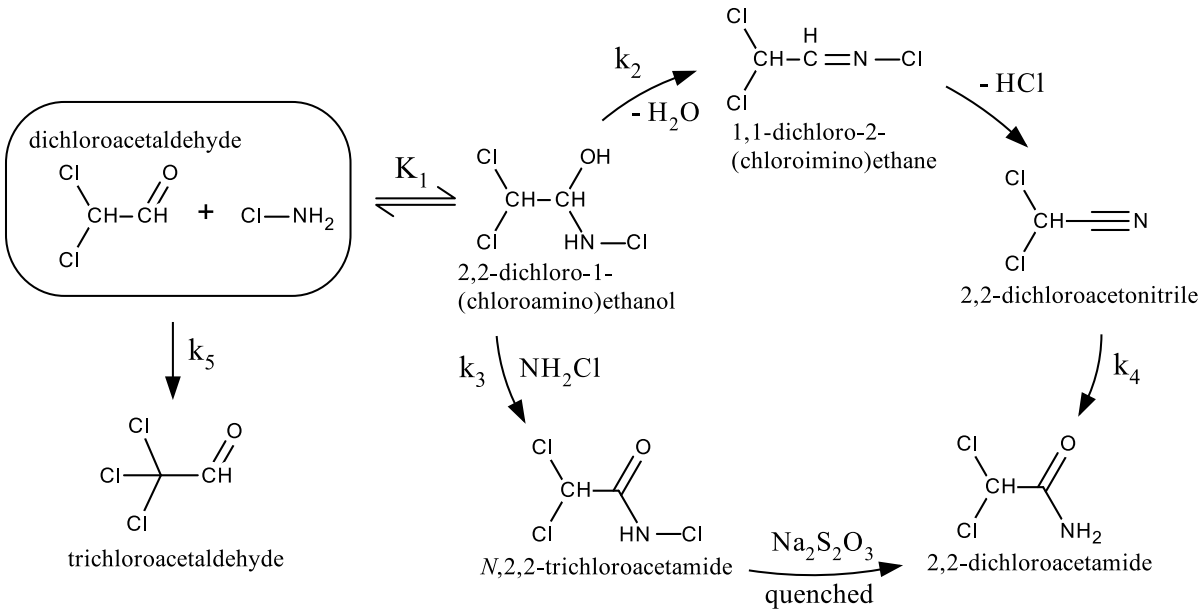

Figure 2.4. Proposed formation pathway of 2,2-dichloroacetonitrile, *N*,2,2-trichloroacetamide and TCAL

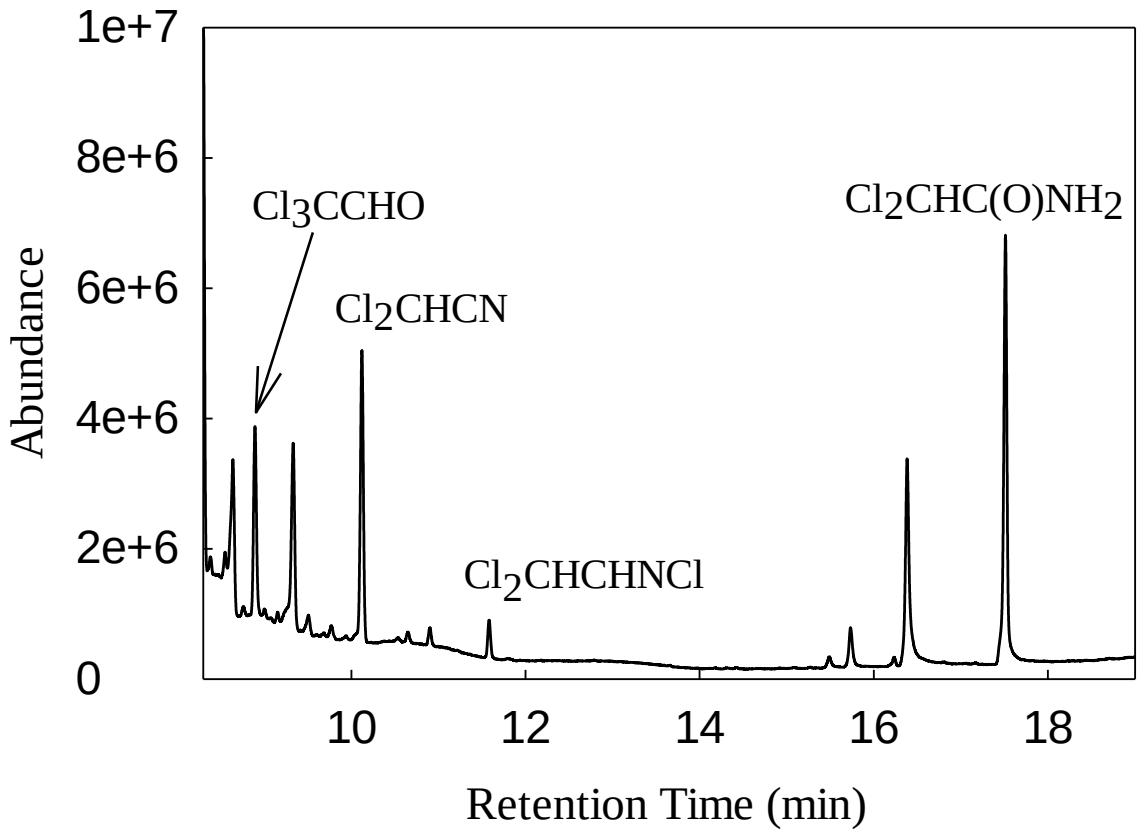

Figure 2.5. GC-EI-MS total ion chromatogram of reaction extracts by LLE using MTBE after 30 minutes in which dichloroacetonitrile (Cl_2CHCN), dichloroacetamide ($Cl_2CHC(O)NH_2$), 1,1-dichloro-2-(chloroimino)ethane (Cl2CHCHNCl), and trichloroacetaldehyde (Cl_3CCHO) were identified. Experimental conditions: $[NH_2Cl]_o$ = 1 mM and $[Cl_2CHCHO]_{T,0}$ = 10 mM, phosphate buffer 20 mM, pH 9.5 ± 0.1, μ = 0.1 M, Temp = 25 ± 0.1°C.

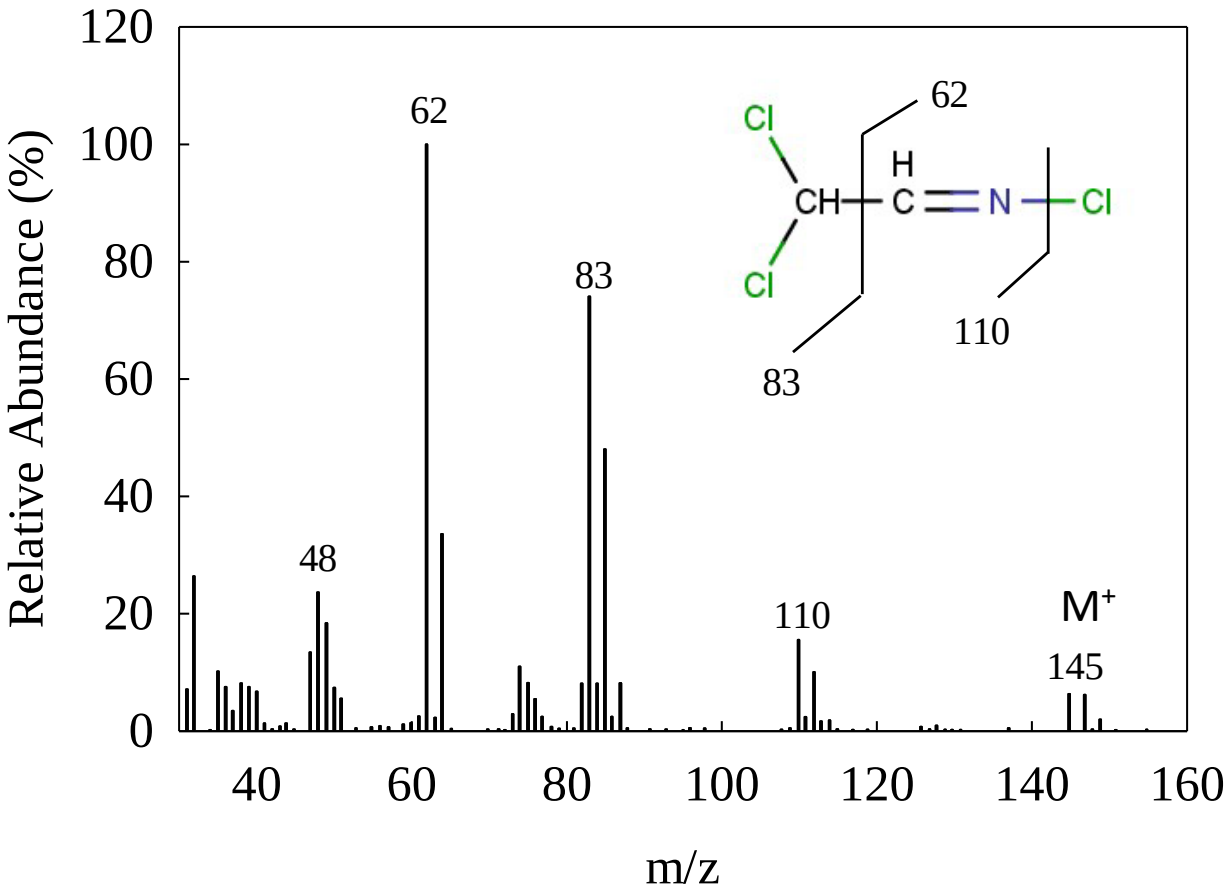

Figure 2.6. Mass spectra of imine 1,1-dichloro-2-(chloroimino)ethane; m/z 48 (23.6%), m/z 62 (100%), m/z 64 (33.6%), m/z 83 (74.1%), m/z 85 (48.0%), m/z 87 (8.2%), m/z 110 (15.6%), m/z 112 (10.1%), m/z 114 (1.9%), M^+ m/z 145 (6.3%), m/z 147 (6.2%), m/z 149 (0.29%).

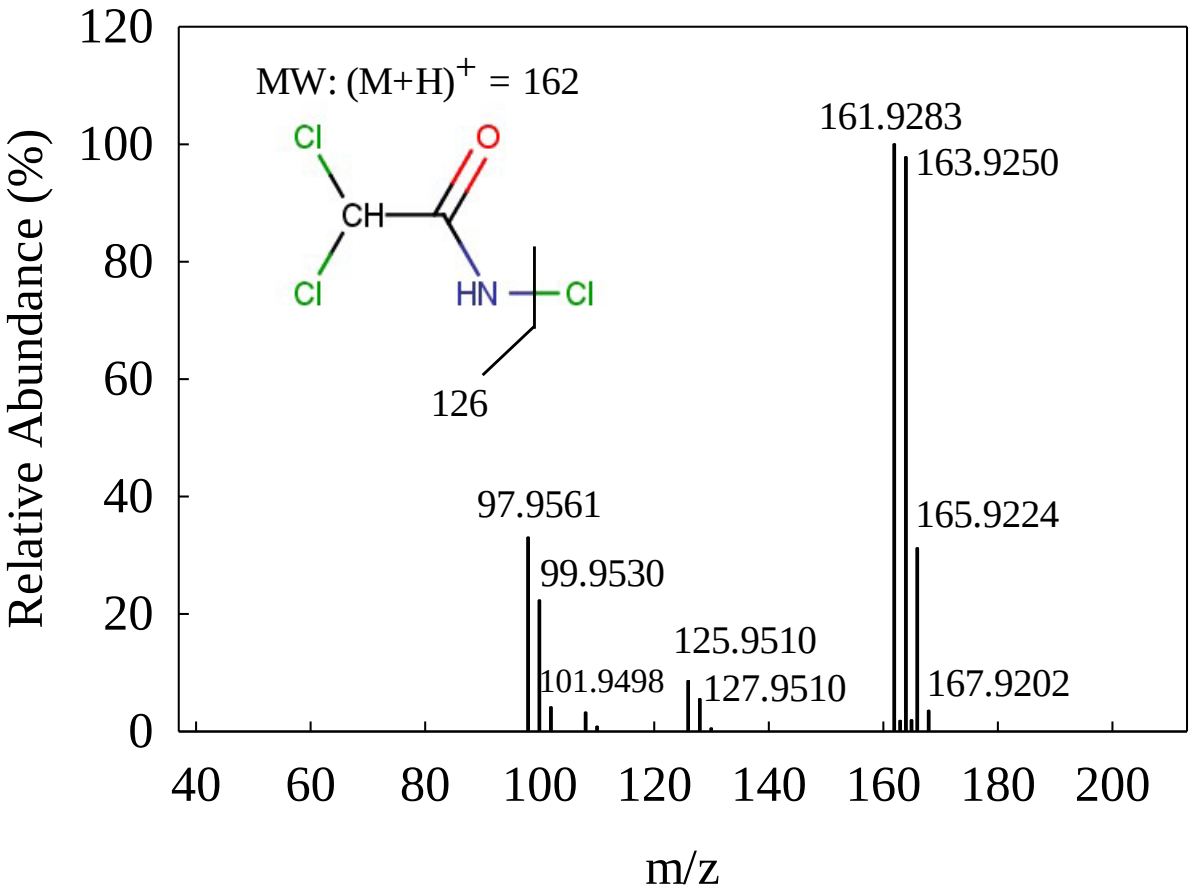

Figure 2.7. Mass spectrum of *N*,2,2-trichloroacetamide analyzed by GC-APCI-HRMS. *N*,2,2-trichloroacetamide m/z: 161.9283 (100%), 163.9250 (97.8%), 165.9224 (31.2%), 167.9202 (3.5%), 125.9510 (8.6%), 127.9510 (5.5%), 97.9561 (33%), 99.9530 (22.3%) and 101.9498 (4.1%).

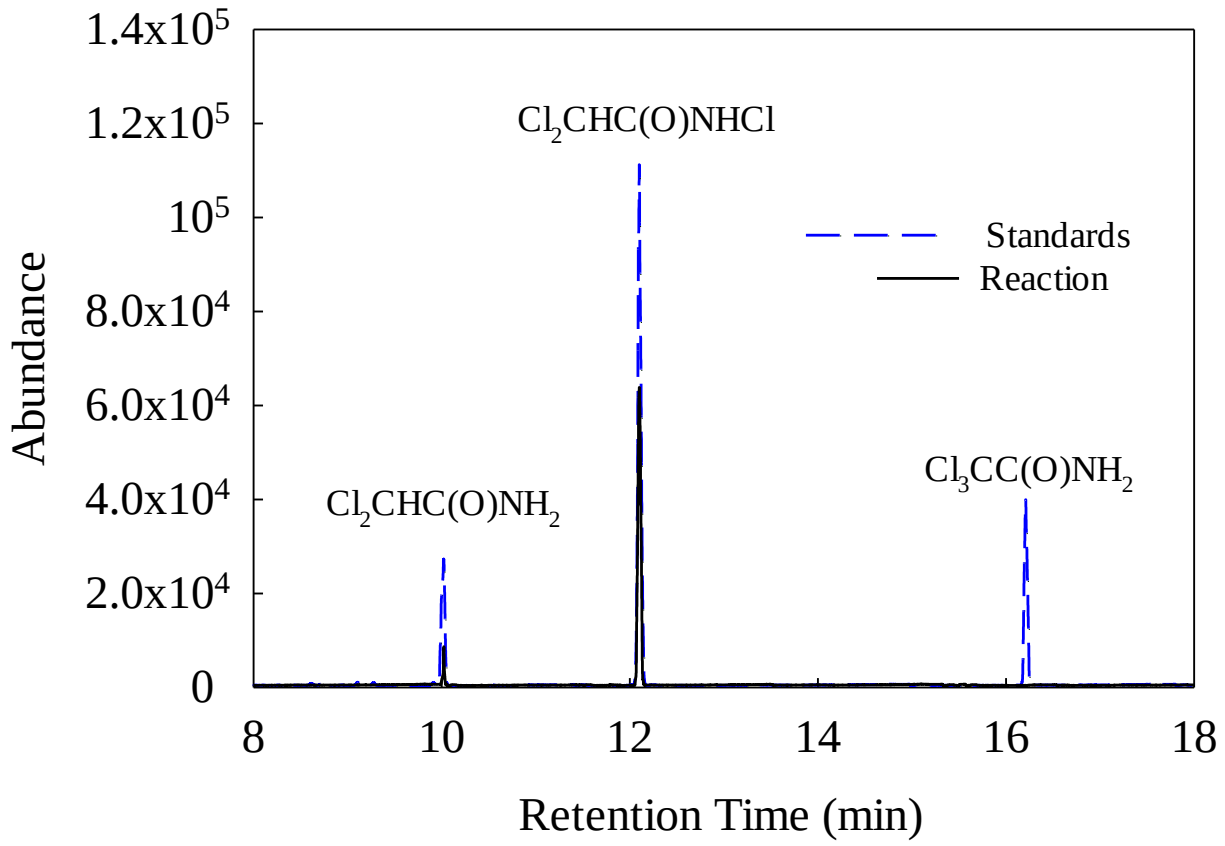

Figure 2.8. GC-APCI-HRMS total ion chromatogram of pure standards containing 2,2,2-trichloroacetamide (Cl_3CCONH_2), 2,2-dichloroacetamide ($Cl_2CHCONH_2$), and *N*,2,2-trichloroacetamide ($Cl_2CHCONHCl$) and reaction extract after 24 hours. Experimental conditions: $[NH_2Cl]_o$ = 15 mM, $[Cl_2CHCHO]_{T,0}$ = 50 mM, total phosphate buffer of 20 mM, pH 9.5 ± 0.1, μ = 0.1 M, Temp = 25 ± 0.1 ^oC.

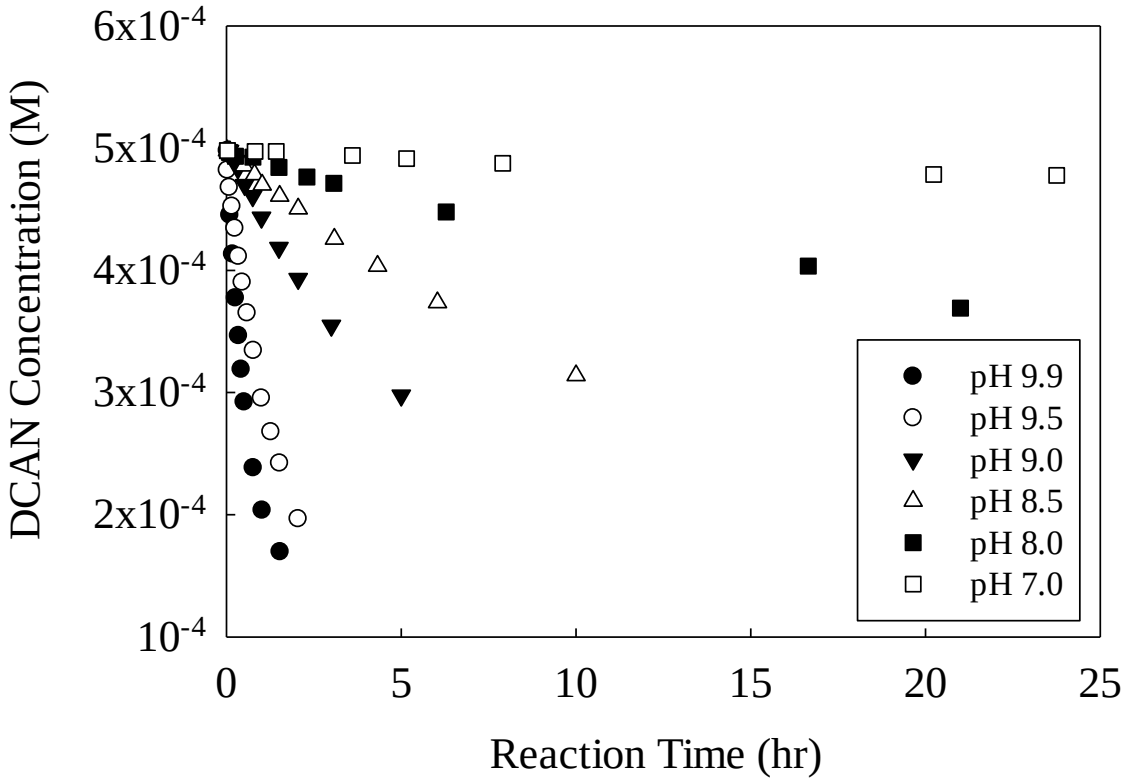

Figure 2.9. Hydrolysis of dichloroacetonitrile (DCAN) at different pHs (7.0 – 9.9). Total phosphate buffer 0.02 M, μ = 0.1 M, Temp = 25 ± 0.1 ºC.

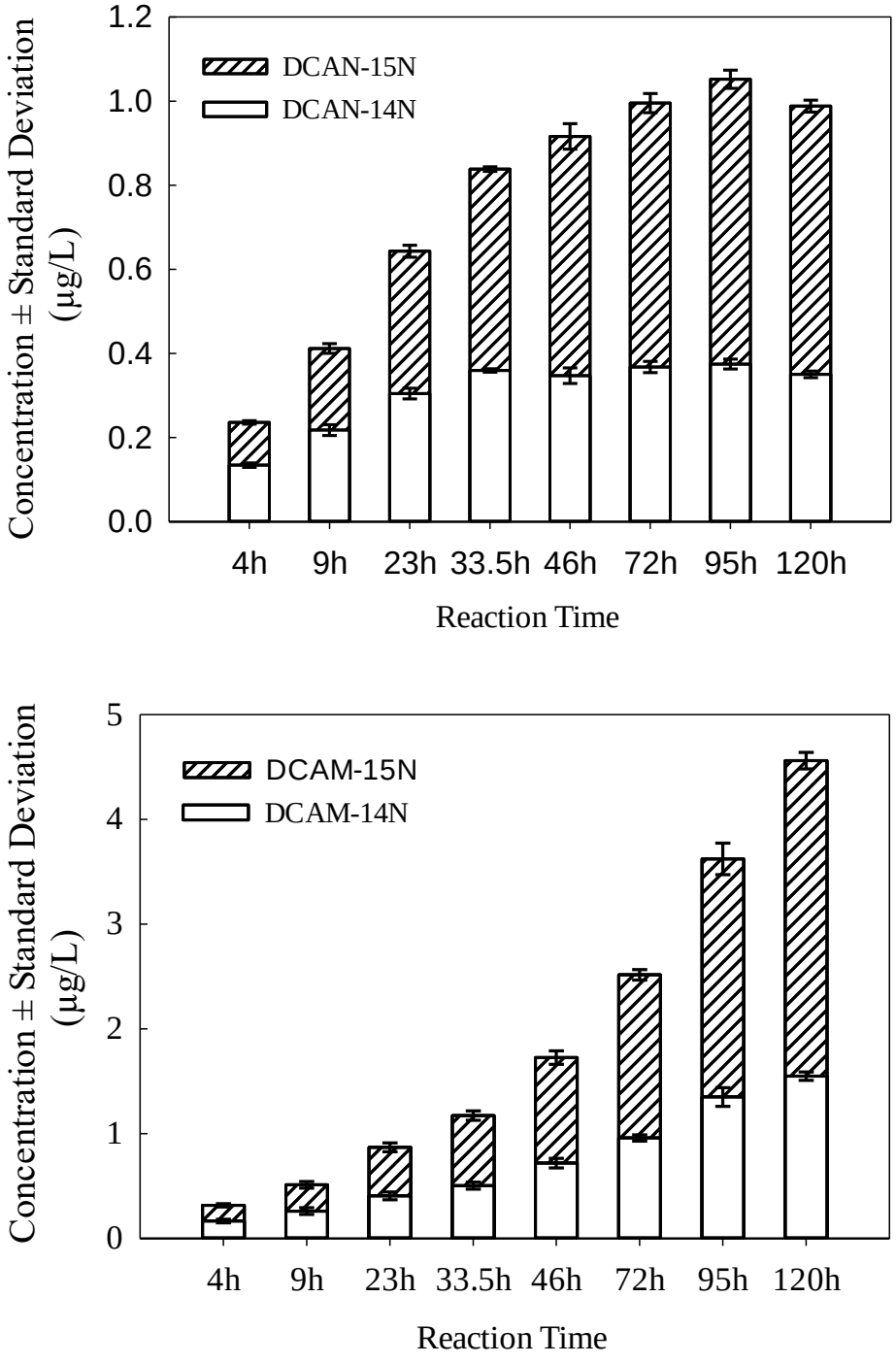

Figure 2.10. Formation of ^{15}N labelled and unlabeled DCAN and DCAM during chloramination of Bloomington water at pH 7.8 – 8.1.

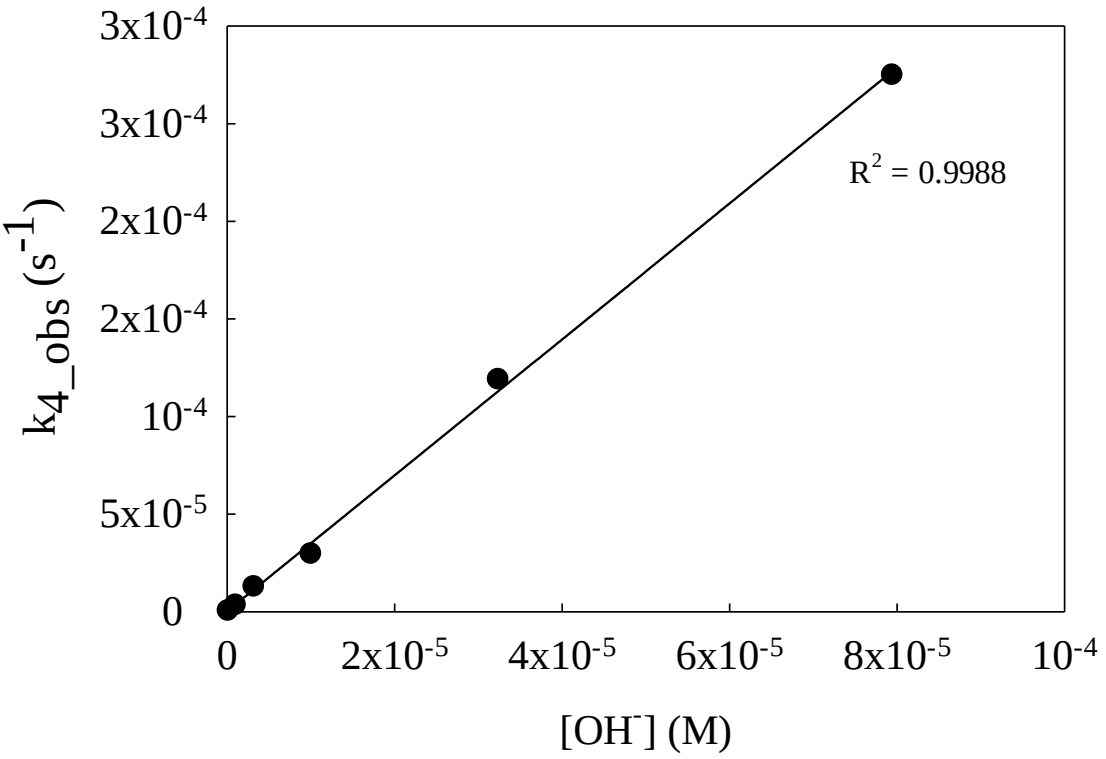

Figure 2.11. A linear relationship between (1/τ) and unhydrated dichloroacetaldehyde concentration. Experimental conditions: $[NH_2Cl]_o$ = 1 mM, $[Cl_2CHCHO]_{T,0}$ = 10-90 mM, total phosphate buffer = 20 mM, pH 7.8 ± 0.1, μ = 0.1 M, Temp = 25 ± 0.1 °C.

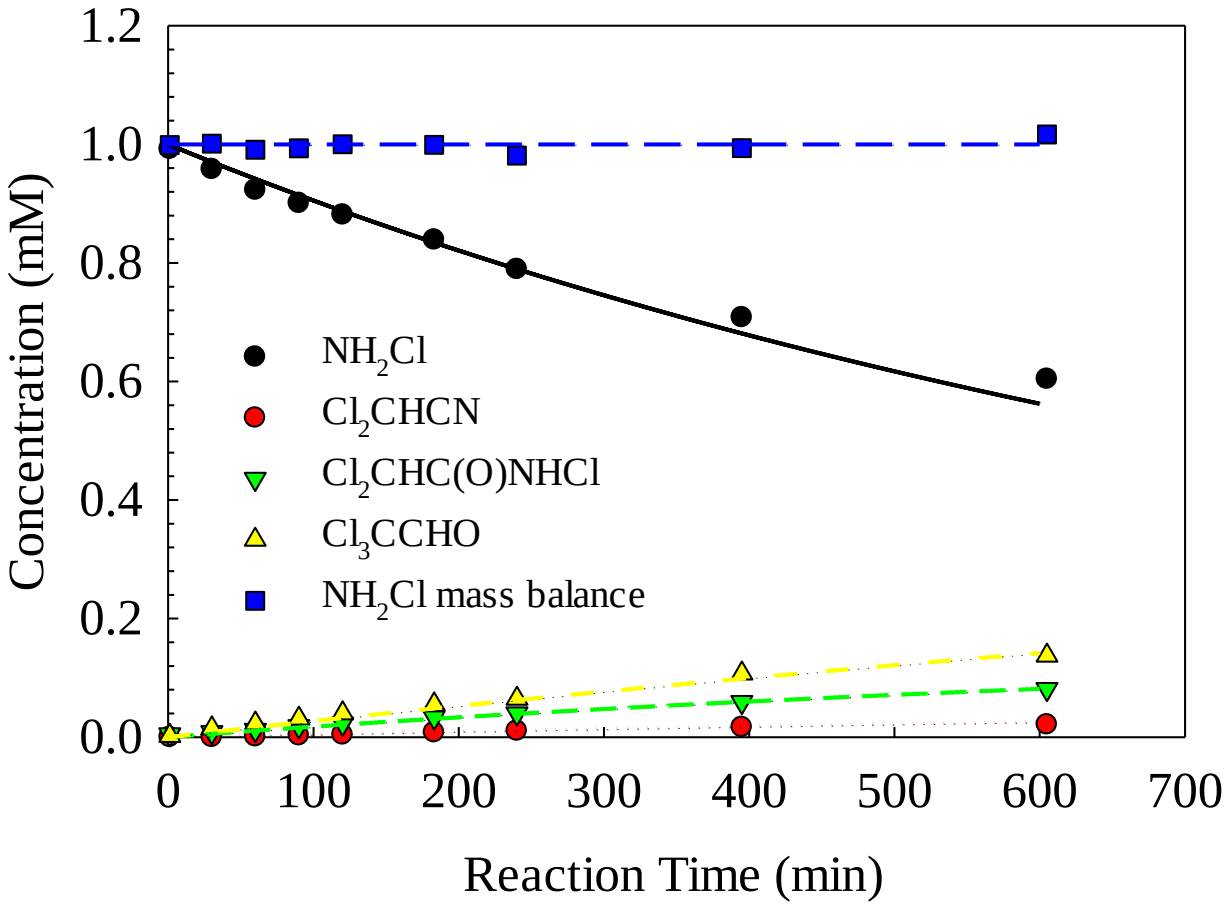

Figure 2.12. Experimental and modeled concentrations of monochloramine, dichloroacetonitrile, *N*,2,2-trichloroacetamide and TCAL over time (UV-1 and GC-1). Symbols are experimental data and lines are kinetic model fitting curves. Experimental conditions: [NH_2Cl] = 1 mM, [$C_{T,Cl2CHCHO}$] = 10 mM, total phosphate buffer 20 mM, pH 7.8 ± 0.1, μ = 0.1 M, Temp = 25 ± 0.1 °C.

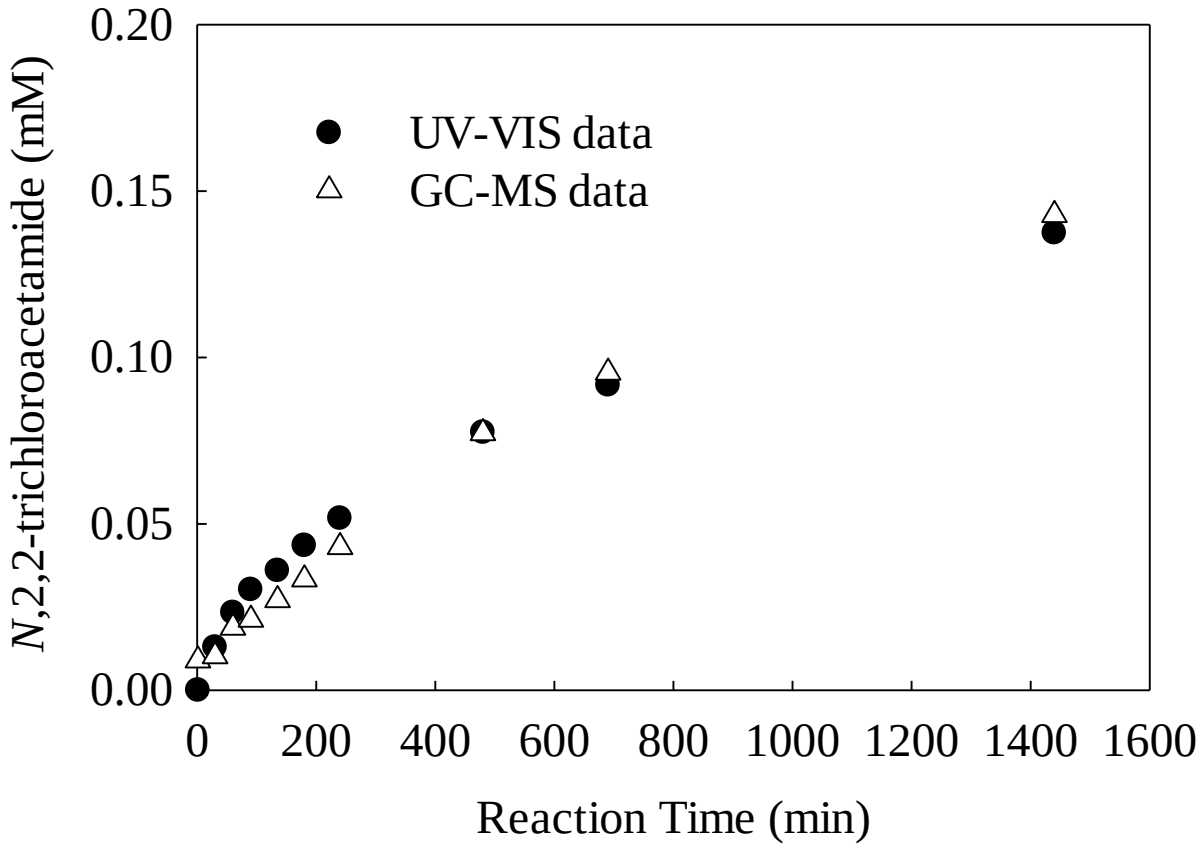

Figure 2.13. *N*,2,2-trichloroacetamide formation from the reaction between dichloracetaldehyde and monochloramine analyzed by UV-VIS data (UV-1) in compared with GC-MS data (GC-2). Experimental conditions: $[NH_2Cl]_o$ = 1 mM, $Cl_2CHCHO]_{T,0}$ = 10 mM, total phosphate buffer 0.02 M, pH 7.8 ± 0.1, μ = 0.1 M, Temp = 25 ± 0.1 ºC.

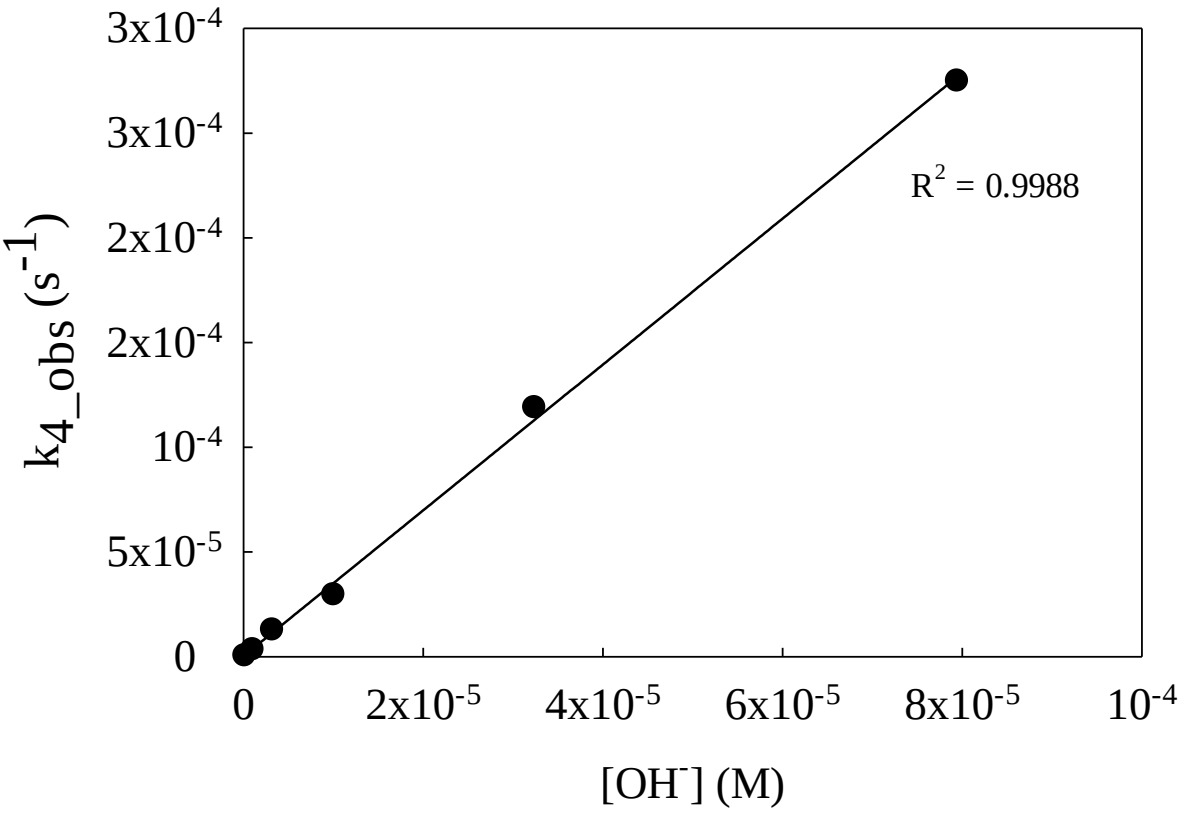

Figure 2.14. Linear relationship between the observed hydrolysis rate constant k_{4_obs} (s^{-1}) and the hydroxide concentration [OH^-]. Experimental conditions: [Cl_2CHCN] = 1 mM, pH ranged from 7 – 9.9, μ = 0.1 M, Temp = 25 ± 0.1 ºC.

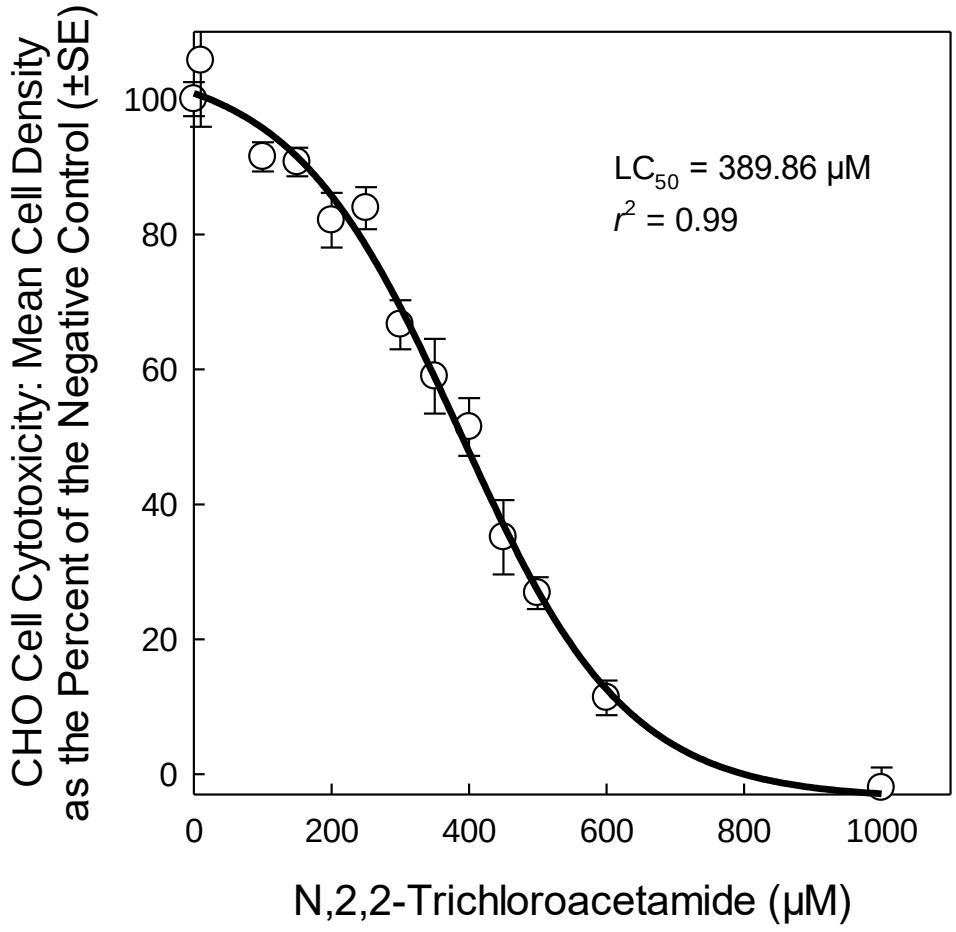

Figure 2.15. *N*,2,2-trichloroacetamide concentration response curve and regression curve for chronic CHO cell cytotoxicity.

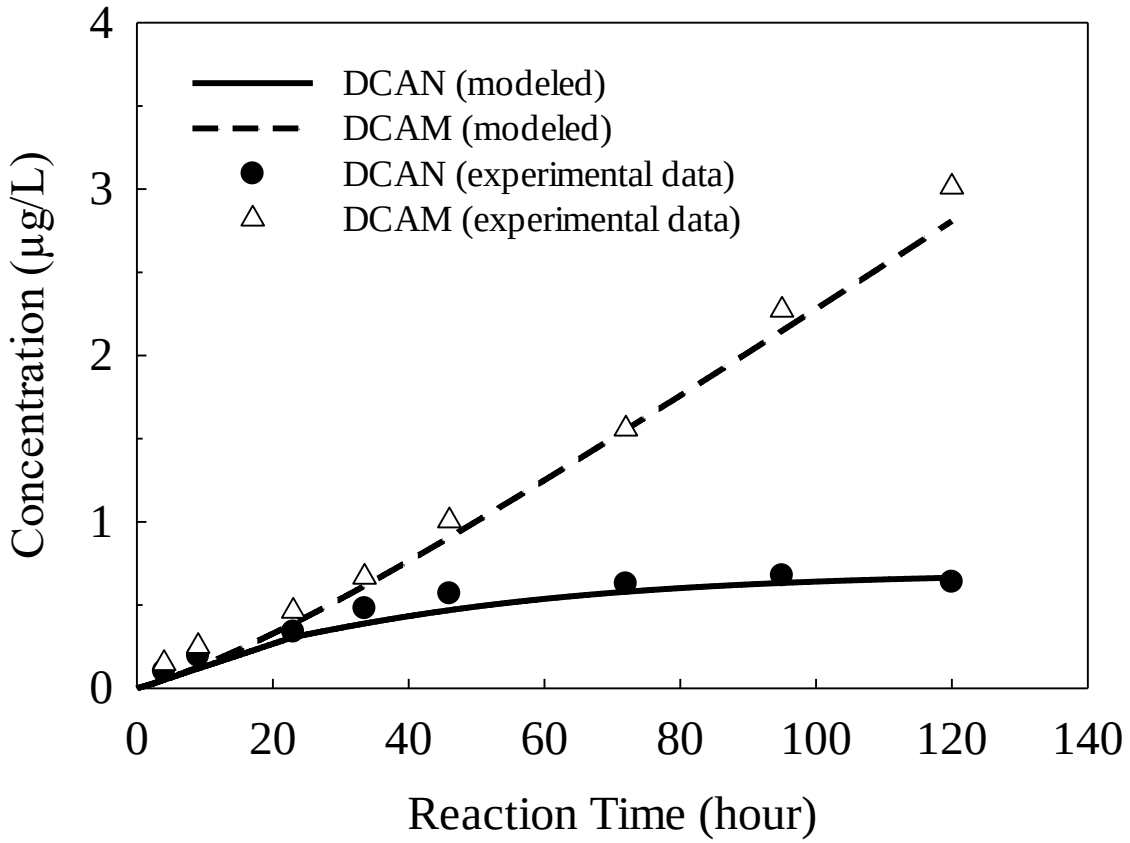

Figure 2.16. Experimental (GC-1) and modeled concentrations of dichloroacetonitrile (DCAN) and dichloroacetamide (DCAM) over time. Symbols are experimental data and lines are the simulation from the kinetic model.

References

1. Calderon, R., *The epidemiology of chemical contaminants of drinking water.* Food Chem. Toxicol., 2000. **38**: p. S13-S20.
2. Bellar, T.A., J.J. Lichtenberg, and R.C. Kroner, *The occurrence of organohalides in chlorinated drinking waters.* J. Am. Water Works Assoc., 1974. **66**: p. 703-706.
3. Rook, J.J., *Haloforms in drinking water.* J. Am. Water Works Assoc., 1976. **68**: p. 168-172.
4. Richardson, S.D., et al., *Occurrence, genotoxicity, and carcinogenicity of regulated and emerging disinfection by-products in drinking water: a review and roadmap for research.* Mutat. Res., 2007. **636**(1): p. 178-242.
5. Page, N.P., *Report on carcinogenesis bioassay of chloroform*. 1976, Bethesda, MD: U.S. Dept. of Health, Education, and Welfare, Public Health Service, National Institutes of Health, National Cancer Institute, Division of Cancer Cause and Prevention, Carcinogenesis Program, Carcinogen Bioassay and Program Resources Branch.
6. Fawell, J., *Risk assessment case study—chloroform and related substances.* Food Chem. Toxicol., 2000. **38**: p. S91-S95.
7. U.S.EPA, *National interim primary drinking water regulations: control of trihalomethanes in drinking water: final rules.* Federal register, 1979. **44**: p. 68624-68705.
8. U.S.EPA, *National primary drinking water regulations: disinfectants and disinfection by-products: final rule.* Fed. Regist., 1998. **63**: p. 69390-69476.
9. U.S.EPA, *National primary drinking water regulations: Stage 2 disinfectants and disinfection byproducts rule.* Fed. Regist., 2006. **71**: p. 387-493.
10. Weinberg, H.S., et al., *The occurrence of disinfection by-products (DBPs) of health concern in drinking water: results of a nationwide DBP occurrence study*. 2002, EPA National Exposure Research Laboratory: Athens, GA.
11. Krasner, S.W., et al., *Occurrence of a new generation of disinfection byproducts.* Environ. Sci. Technol., 2006. **40**(23): p. 7175-7185.

12. Chu, W., et al., *Formation and speciation of nine haloacetamides, an emerging class of nitrogenous DBPs, during chlorination or chloramination.* J. Hazard. Mater., 2013. **260**: p. 806-812.

13. Plewa, M.J., et al., *Occurrence, synthesis, and mammalian cell cytotoxicity and genotoxicity of haloacetamides: an emerging class of nitrogenous drinking water disinfection byproducts.* Environ. Sci. Technol., 2008. **42**(3): p. 955-961.

14. Plewa, M., et al., *Occurrence, formation, health effects and control of disinfection by-products in drinking water*, in *Comparative Mammalian Cell Toxicity of N-DBPs and C-DBPs*. 2008, American Chemical Society Washington, DC. p. 36-50.

15. Komaki, Y., B.J. Mariñas, and M.J. Plewa, *Toxicity of drinking water disinfection byproducts: cell cycle alterations induced by the monohaloacetonitriles.* Environ. Sci. Technol., 2014. **48**(19): p. 11662-11669.

16. Muellner, M.G., et al., *Haloacetonitriles vs. regulated haloacetic acids: are nitrogen-containing DBPs more toxic?* Environ. Sci. Technol., 2007. **41**(2): p. 645-651.

17. Plewa, M.J., E.D. Wagner, and S.D. Richardson, *TIC-Tox: A preliminary discussion on identifying the forcing agents of DBP-mediated toxicity of disinfected water.* J. Environ. Sci., 2017.

18. Wagner, E.D. and M.J. Plewa, *CHO cell cytotoxicity and genotoxicity analyses of disinfection by-products: An updated review.* J. Environ. Sci., 2017.

19. Lee, W., P. Westerhoff, and J.-P. Croué, *Dissolved organic nitrogen as a precursor for chloroform, dichloroacetonitrile, N-nitrosodimethylamine, and trichloronitromethane.* Environ. Sci. Technol., 2007. **41**(15): p. 5485-5490.

20. Mitch, W.A., et al., *Occurrence and formation of nitrogenous disinfection by-products*. 2009, Denver, CO: Water Research Foundation.

21. Huang, H., et al., *Dichloroacetonitrile and dichloroacetamide can form independently during chlorination and chloramination of drinking waters, model organic matters, and wastewater effluents.* Environ. Sci. Technol., 2012. **46**(19): p. 10624-10631.

22. Nihemaiti, M., J. Le Roux, and J.-P. Croué, *Formation of Emerging Disinfection By-products by Chlorination/Chloramination of Seawater Impacted by Algal Organic Matter*, in *Recent Progress in Desalination, Environmental and Marine Outfall Systems*. 2015, Springer. p. 285-294.

23. Yu, Y. and D.A. Reckhow, *Kinetic Analysis of Haloacetonitrile Stability in Drinking Waters.* Environ. Sci. Technol., 2015. **49**(18): p. 11028-11036.

24. Chu, W., et al., *The formation of haloacetamides and other disinfection by-products from non-nitrogenous low-molecular weight organic acids during chloramination.* Chem. Eng. J., 2016. **285**: p. 164-171.

25. Pedersen, E.J., et al., *Formation of cyanogen chloride from the reaction of monochloramine with formaldehyde.* Environ. Sci. Technol., 1999. **33**(23): p. 4239-4249.

26. Kimura, S.Y., et al., *Chloroacetonitrile and n,2-dichloroacetamide formation from the reaction of chloroacetaldehyde and monochloramine in water.* Environ. Sci. Technol., 2013. **47**(21): p. 12382-90.

27. Kimura, S.Y., et al., *Acetonitrile and N-chloroacetamide formation from the reaction of acetaldehyde and monochloramine.* Environ. Sci. Technol., 2015. **49**(16): p. 9954-9963.

28. Yang, X., et al., *Nitrogenous disinfection byproducts formation and nitrogen origin exploration during chloramination of nitrogenous organic compounds.* Water Res., 2010. **44**(9): p. 2691-2702.

29. Joo, S.H. and W.A. Mitch, *Nitrile, aldehyde, and halonitroalkane formation during chlorination/chloramination of primary amines.* Environ. Sci. Technol., 2007. **41**(4): p. 1288-1296.

30. Chuang, Y.-H., et al., *Formation pathways and trade-offs between haloacetamides and haloacetaldehydes during combined chlorination and chloramination of lignin phenols and natural waters.* Environ. Sci. Technol., 2015. **49**(24): p. 14432-14440.

31. Le Roux, J., M. Nihemaiti, and J.-P. Croué, *The role of aromatic precursors in the formation of haloacetamides by chloramination of dissolved organic matter.* Water Res., 2016. **88**: p. 371-379.

32. Krasner, S.W., et al., *The occurrence of disinfection by-products in US drinking water.* J. Am. Water Works Assoc., 1989. **81**(8): p. 41-53.

33. Schechter, D.S. and P.C. Singer, *Formation of aldehydes during ozonation.* Ozone Sci. Eng., 1995. **17**(1): p. 53-69.

34. Richardson, S.D., et al., *Identification of new ozone disinfection byproducts in drinking water.* Environ. Sci. Technol., 1999. **33**(19): p. 3368-3377.

35. Koudjonou, B.K. and G.L. LeBel, *Halogenated acetaldehydes: Analysis, stability and fate in drinking water.* Chemosphere, 2006. **64**(5): p. 795-802.

36. Kumar, K., R.A. Day, and D.W. Margerum, *Atom-transfer redox kinetics: general-acid-assisted oxidation of iodide by chloramines and hypochlorite.* Inorg. Chem., 1986. **25**(24): p. 4344-4350.

37. Yu, Y. and D.A. Reckhow, *Formation and Occurrence of N-Chloro-2, 2-dichloroacetamide, a Previously Overlooked Nitrogenous Disinfection Byproduct in Chlorinated Drinking Waters.* Environ. Sci. Technol., 2017. **51**(3): p. 1488-1497.

38. Cuthbertson, A.A., et al., *Method Optimization for Quantification of Priority Disinfection By-Products: Finding a Good Compromise*, in *Drinking Water Disinfection By-Products Gordon Research Conference*. August 2015: Hadley, MA.

39. Jeong, C.H., et al., *Occurrence and comparative toxicity of haloacetaldehyde disinfection byproducts in drinking water.* Environ. Sci. Technol., 2015. **49**(23): p. 13749-13759.

40. Plewa, M.J., et al., *Mammalian cell cytotoxicity and genotoxicity analysis of drinking water disinfection by-products.* Environ. Mol. Mutagen., 2002. **40**(2): p. 134-142.

41. Glezer, V., et al., *Hydrolysis of haloacetonitriles: linear free energy relationship, kinetics and products.* Water Res., 1999. **33**(8): p. 1938-1948.

42. Valentine, R.L. and C.T. Jafvert, *General acid catalysis of monochloramine disproportionation.* Environ. Sci. Technol., 1988. **22**(6): p. 691-696.

43. Jafvert, C.T. and R.L. Valentine, *Reaction scheme for the chlorination of ammoniacal water.* Environ. Sci. Technol., 1992. **26**(3): p. 577-586.

44. Speitel, G., et al., *Disinfection by-product formation and control during chloramination*. 2005, Denver, CO: American Water Works Association.

45. Greenzaid, P., Z. Luz, and D. Samuel, *A nuclear magnetic resonance study of the reversible hydration of aliphatic aldehydes and ketones. I. Oxygen-17 and proton spectra and equilibrium constants.* J. Am. Chem. Soc., 1967. **89**(4): p. 749-756.

46. Bernasconi, C.F., *Investigation of rates and mechanisms of reactions Part I*. 4th ed. Vol. Techniques of Chemistry VI. 1986, New York, NY: John Wiley & Sons. 1041.

47. Reckhow, D.A., et al., *Formation and degradation of dichloroacetonitrile in drinking waters.* J. Water Supply Res. T., 2001. **50**(1): p. 1-13.

CHAPTER 3

EFFEECT OF CHLORINE PRETREATMENT ON THE FORMATION OF DICHLOROACETONITRILE AND DICHLOROACETAMIDE VIA THE ALDEHYDE PATHWAY UNDER DRINKING WATER CONDITION

Abstract

Haloacetonitrile and haloacetamide, two main N-DBP groups commonly found in drinking water, were proved to be more toxicity than regulated DBPs mostly produced via chlorination process. Alternative disinfection strategies such as chloramination may promote the formation of these unregulated DBPs with severe health risks. The aldehyde pathway, where aldehydes react with monochloramine, has been proposed as a major reaction scheme leading to the formation of N-DBPs (i.e. dichloroacetonitrile (DCAN), dichloroacetamide (DCAM) and *N*,2,2-trichloroacetamide (*N*,2,2-TCAM)) under drinking water condition. In this study, the relevance of the aldehyde pathway was further examined at different experimental conditions which imitated the common disinfection practices at water utilities.

Free chlorine exposure (4mg/L as Cl_2 and 30 mins) followed by chloramination enhanced the formation of dichloroacetaldehyde, the initial reactant of the aldehyde pathway, and thereby increase the yield of ^{15}N-DCAN and ^{15}N-DCAM by 30-40% over a period of 5 days compared to the chloramination process only. Extending the exposure time of the free chlorine pretreatment increased the formation of ^{14}N-DBPs produced but decreased the production of their ^{15}N counter parts during the whole treatment process. Additionally, pH also had a strong effect on the formation of DCAN and DCAM because it determines the hydrolysis rate of DCAN to form DCAM. High pH range favored the formation of DCAM by accelerating the hydrolysis whereas DCAN still occurred at high concentration at low pH range. Lastly, a simplified kinetic model was developed based on this hydrolysis reaction to predict the formation of ^{14}N-DCAN and ^{14}N-DCAM which also co-occurred with ^{15}N-DBP formation via the aldehyde pathway.

Introduction

According to the recent national occurrence and toxicity studies, HANs and HAMs are two major unregulated N-DBP groups commonly found in drinking water [1, 2] and they were shown to be more cytotoxic and genotoxic than the regulated DBPs such as THMs and HAAs [3-7]. Although, HANs and HAMs may cause some negative health impact on consumers by significantly contributing to the overall toxicity of the post-disinfected waters, their formation mechanism under drinking water conditions has not been well characterized. Previous researches have focused on two main hypotheses about the formation pathway these N-DBP classes based on the source of nitrogen atom in their molecular structures [8-11]. In the formation mechanism referred to as decarboxylation pathway, nitrogenous organic compounds, commonly found at high levels in waters impacted by wastewater effluents, were chlorinated to form organic chloramines and then decomposed into several products including aldehydes and nitriles [10, 12-16]. In the decarboxylation pathway, the nitrogen of the nitrile or amide group was contributed by a nitrogen-containing organic precursor, organic-N source. On the other hand, another hypothesis suggests that HANs and HAMs could be produced from the reaction between an aldehyde and monochloramine [17-19]. The aldehyde could be naturally occurring in the waters or subsequently produced from the chloramination of the organic matters in source waters. In the reaction scheme referred to as aldehyde pathway, the nitrogen of the nitrile or amide group originated from monochloramine, inorganic-N source.

In natural water, the decarboxylation pathway and the aldehyde pathway were shown to occur simultaneously and significantly lead to the formation of HANs and HAMs in finished water [11, 20, 21]. A brief summary of these formation pathways was shown in Figure 3.1. Prevalence of each pathway in drinking water condition are mostly determined by several factors such as pH, reaction time, chloramine to organic-N ratio, and the structure of the organic-N precursors [11]. As these properties are widely different for each natural water source, the dominant scheme between the decarboxylation pathway and the aldehyde pathway may vary for each scenario. Therefore, labelled $^{15}NH_2Cl$ technique was employed in previous studies to identify the dominant pathway at a certain condition. Some studies reported that a majority of N-DBP products (i.e. DCAN and cyanogen chloride) contains ^{15}N atom in their structures which can only be provided by ^{15}N labelled monochloramine. These results have confirmed the importance of the aldehyde pathway on the formation of HANs and HAMs in real drinking water conditions. Additionally, in

chapter 2 of this work, labelled $^{15}NH_2Cl$ experiments using natural water collected at Bloomington water plant also reveal that 60-70% DCAN and DCAM incorporate ^{15}N atom meaning they were produced via the aldehyde pathway.

According to a national occurrence study, N-DBP formation in drinking water may be promoted by employing alternative disinfection strategies in order to reduce the formation of regulated DBPs. The highest occurrences of these priority DBPs such as HANs and HAMs were observed at a treatment plant using prechlorination followed by chloramination [2]. Therefore, common disinfection practices at the water utilities should be considered in DBP studies as it may provide a critical condition leading to the formation of some specific unregulated DBP classes. For example, pH may play a key role in the DBP formation pathway as some reactions (i.e. hydrolysis of haloacetonitrile to form haloacetamide) are acidic or basic catalyzed. Particularly, the hydrolysis of mono-, di- and tri-chloroacetonitrile at different pH levels (5.4, 7.2 and 8.7) was studied and the rates were shown to be fastest at high pH (8.7), intermediate at neutral pH (7.2) and slowest at low pH (5.4) [22].

The objective of this study is to further investigate the relevance of the aldehyde pathway on the formation of DCAN and DCAM under some practical conditions that imitate the real common treatment processes at many water utilities and distribution systems. ^{15}N-labelled monochloramine was spiked on natural source water which was previously exposure to free chlorine. First, the effect of free chlorine pretreatment followed by the ^{15}N-labelled chloramination process on N-DBP formation was examined under some scenarios with different chlorination concentration and time (CT) values. Second, pH effect on the formation of DCAN and DCAM produced from the chloramination with prior free chlorine exposure was investigated. Lastly, a simplified kinetic model based on the hydrolysis reaction of DCAN was applied as a prediction tool for the formation of ^{14}N-DBP species such as ^{14}N-DCAN and ^{14}N-DCAM.

Experimental methods

Reagents and solutions

All chemical reagents with the highest purity grade commercially available were purchased from Sigma-Aldrich (St. Louis, MO) and Fisher Scientific (Pittsburgh, PA). Sodium hydroxide (97%), perchloric acid (70%), ammonium chloride (99.9%), sodium hypochlorite (5-6%), sodium thiosulfate (99%), sodium sulfate (99%), chloral hydrate (>97%), 2,2-dichloroacetonitrile

(>99.5%), 2,2-dichloroacetamide (>98%), methanol (HPLC grade 99%), methyl tertiary butyl ether (HPLC grade 99.9%), acetonitrile (HPLC grade 99%) and hexane (>98.5%) were used in this study. Ammonium chloride labelled ^{15}N (99%) used to prepare $^{15}NH_2Cl$ solution in the labelled $^{15}NH_2Cl$ experiments was purchased from Cambridge Isotope Laboratories (Tewksbury, MA).

Commercial dichloroacetaldehyde hydrate solid stock (> 99%) was purchased from Tokyo Chemical Industry (TCI) – America (Portland, OR). When preparing sub-stock solution used for calibration curve, the amount of dichloroacetaldehyde hydrate and other chemicals obtained from the pure stock was weighed with an analytical balance (Mettler Toledo AB104, Columbus, OH). Haloacetamide stocks were prepared with methanol as the solvent and haloacetonitrile stocks were prepared with acetonitrile as the solvent.

All aqueous solutions were prepared with MiliQ water (>18 MΩ), a phosphate buffer concentration of 0.02 M and ionic strength of 0.1 M. Phosphate buffer solution was prepared with potassium biphosphate salt (ACS reagent) and adjusted to specific pH values. Ionic strength was adjusted with sodium perchlorate (ACS reagent) purchased from Sigma-Aldrich. Specific pH values of all solutions were adjusted with concentrated perchloric acid and sodium hydroxide (ACS reagent). Phosphate buffer solution was prepared daily for the experiments while sodium perchlorate solutions and sodium hydroxide were prepared monthly.

Monochloramine stock solution was freshly prepared on-site for each set of experiments by slow drop-wise addition of sodium hypochlorite solution into ammonium chloride solution under fast stirring. The mixing volume ratio for these solutions was 1:1 with a slightly higher concentration of ammonium chloride (N/Cl molar ratio = 1.1). These solutions were prepared with a phosphate buffer concentration of 0.02 M at pH 8.5 to minimize the undesired formation of dichloramine. Sodium hypochlorite solutions were prepared by diluting sodium hypochlorite liquid stock which was standardized with a spectrophotometer (λ_{max} = 292 mn, molar absorptivity ε_{292} = 362 $M^{-1}cm^{-1}$) [23]. Similarly, ammonium chloride solutions and labelled ^{15}N ammonium chloride solutions were prepared by dissolving ammonium chloride salt and labelled ^{15}N ammonium chloride salt in MiliQ water. After mixing, the concentration of monochloramine stock solution was standardized with a spectrophotometer (λ_{max} = 243 mn, molar absorptivity ε_{243} = 461 $M^{-1}cm^{-1}$) [24].

Experimental matrix

Detail conditions of each experiment set are described were shown in Table 3.1. A natural water experiment included two steps, (1) free chlorine exposure and followed by (2) chloramination where labelled ^{15}N ammonium chloride was consequently added to produce monochloramine. Procedure of each experiment set were illustrated in Figure 3.2. The feed water used for these natural water experiments is the surface water collected from the water treatment plant of Bloomington, IL treated with conventional treatment by sedimentation and recarbonation with no disinfection (TOC = 1.8 mg/L, pH= 7.8-8.1). The experiments were monitored for 5 days. Samples were taken at the beginning and after every 24 hours.

Instruments and methods

A Thermo Electron Orion ROSS Ultra pH electrode and an Accumet AB15 Plus pH meter were used to measure pH values for all solutions. The pH meter was calibrated daily for the tests with commercial pH standard solution (pH value 4, 7, and 10). The Davis equation was applied to calculate the effect of activity coefficient caused by 0.1 M ionic strength on the theoretical pH. Then, pH meter values (activity of hydrogen ion) were adjusted to the actual hydrogen ion concentration for measured solutions. A PolyScience water bath re-circulator was used to maintain a constant temperature (25^oC) for all of the reactors.

A 2550 UV-Vis spectrophotometer (Shimadzu Scientific Instruments, Columbia, MD) was used to standardize the monochloramine solution and monitor reactions to determine kinetic rates. Samples were placed in 10 mm quartz cuvettes and absorbance spectra were taken at wavelengths in the range of 200 – 400 nm.

Gas chromatography with mass spectrometry detection (GCMS) (Agilent Technologies GC 6850/ MSD 5975C) was employed to quantify the reaction products from the experiment sets C01, C02, R01, R02, R03, R04 and R05 shown in Table 3.1. Labelled ^{15}N-monochloramine technique and GC-MS analysis were used to evaluate the relevance of the aldehyde pathway under some practical drinking water conditions.

At each sampling time, an aliquots of total 200 mL were quenched by sodium thiosulfate and analyzed for HANs, HAMs, and HALs over time. For determination of HANs and HAMs, an aliquot of 100 mL was extracted by liquid liquid extraction (LLE) method with 2 mL of methyl

tert-butyl ether (MTBE), 30 g of sodium sulfate, and 1,2-dibromopropane used as an internal standard. The mixture was shaken for 30 min and the top layer was transferred to a GC-MS vial after a 5 min rest [25]. For determination of HALs, the aldehydes were derivatized with O-2,3,4,5,6-pentafluorobenzylhydroxylamine (PFBHA) and extracted from another 100 mL aliquot according to a procedure described elsewhere [26]. A 30 m Rtx-200 column (Restek Corporation, Bellefonte, PA) was used for GC-MS analysis. A 2 µL extract was injected into the inlet under split mode (2:1 split ratio) at 230^{o}C. The oven was programed to be initially held at 40^{o}C for 3 min, increased to 70^{o}C (ramped 10^{o}C/min) and held for 2 min, then risen to 240^{o}C (ramped 10^{o}C/min) and held for 5 min. Electron impact (EI) was used as the ionization mode and the scan range was m/z 30-450. For DCAN, the fragments m/z 74 and 75 were used to distinguish DCAN containing ^{14}N and DCAN containing ^{15}N, respectively. Similarly, m/z 127 and 128 were applied to differentiate DCAM containing ^{14}N and DCAM containing ^{15}N, respectively.

Results and discussions

Effect of free chlorine pretreatment on formation of DCAN and DCAM during the chloramination

Results from experiment sets R01 and C01 (chloramination with and without free chlorine pre-treatment) revealed the effect of free chlorine exposure on the later chloramination process. This pre-treatment showed a strong impact on the formation of commonly found N-DBPs such as DCAN and DCAM. Their concentrations during the chloramination were multiplied 3-5 times if a chlorination step was previously used. In term of the total concentration including both ^{14}N and ^{15}N fractions, at 48 hours, DCAN has increased from 0.51 µg/L to 2.43 µg/L (Figure 3.4a and 3.4c) and DCAM has increased from 1.05 µg/L to 2.94 µg/L (Figure 3.4b and 3.4d) under the effect of free chlorine exposure.

In addition to the main target compounds DCAN and DCAM, another DBP species, dichloroacetaldehyde (DCAL) formation was also affected by free chlorine pre-treatment. Although DCAL was not initially detected in the feed water, its concentration was significantly increased with free chlorine exposure to 0.75 µg/L after 30 mins pre-treatment (as shown in Figure 3.3). As being a strong oxidizing agent, free chlorine could react with organic matter naturally occurring in the feed water to produce DCAL. Furthermore, DCAL formation during the chloramination was always higher when free chlorine exposure was formerly applied. Maximum

DCAL concentrations in experiment sets R01 and C01 were 2.03 µg/L and 0.76 µg/L, respectively (Figure 3.3). During the pre-treatment, free chlorine might have broken the organic matter in the source water to smaller and simpler molecules which could serve as DCAL precursors. Then, these precursors may continue to react with monochloramine to form DCAL during the chloramination process.

As DCAL was the major reactant of the aldehyde pathway along with monochloramine previously shown in Chapter 2, the enhancement of DCAL and DCAL precursor formation due to free chlorine pre-treatment resulted in higher yield of ^{15}N-DCAN and ^{15}N-DCAM during the subsequent chloramination with ^{15}N-labelled monochloramine (experiment R01 and C01). Significant effect of free chlorine pre-treatment on the formation of N-DBPs was indicated in Figure 1 where ^{15}N-DCAN and ^{15}N-DCAM formation increases about 2.7 times and 1.4 times with previous chlorination being used, respectively.

Thanks to the labelled ^{15}N monochloramine technique, percentage of ^{15}N-DBP products over the total including both ^{15}N and ^{14}N species would determine which pathway dominates. In experiment C01 where free chlorine exposure was not used, the fraction ^{15}N of N-DBP products counted for 60-65% of the total (Figure 3.4a and 3.4b). This finding is consistent with the results from a similar experiment setup in a previous work (Chapter 2) where the dominance of the aldehyde pathway in drinking water conditions was confirmed.

Furthermore, the aldehyde pathway still dominated with free chlorine pre-treatment as ^{15}N-DBPs took up larger fraction than ^{14}N-DBPs (Experiment R01). The percentage ratio of ^{15}N/^{14}N fractions was not accurately comparable because significant amounts ^{14}N-DBPs had been already formed after 30 min free chlorine exposure leading to a relative low percentage of ^{15}N fraction over the total. As shown in Figure 3.4c, ^{15}N-DCAN only counts for 19-35% of the total DCAN but its fraction can increase to 52-100% if we set aside the amount ^{14}N-DCAN formed by chlorination step from the total DCAN. After free chlorine pre-treatment, ^{14}N-DCAN was quickly produced and most of ^{14}N-DCAN precursors might be used up during the pretreatment step. Then, the aldehyde pathway became dominant when $^{15}NH_2Cl$ was added to the water as ^{15}N-DCAN was produced predominantly compared to ^{14}N-DCAN during chloramination process. Similarly, ^{15}N-DCAM only counts for 16-52% of the total DCAM but it can increase to 49-64% if we set aside the amount ^{14}N-DCAM formed by chlorination pretreatment from the total DCAM (Figure 3.4d).

Unlike DCAN trend, ^{14}N-DCAM precursors were not used up during the free chlorine pretreatment and the amount of ^{14}N-DCAM produced by decarboxylation pathway was still in comparable to the amount of ^{15}N-DCAM via the aldehyde pathway.

A previously developed kinetic model for the aldehyde pathway in Chapter 2 was applied to predict the concentration of ^{15}N-DCAN and ^{15}N-DCAM (indirectly indicate N,2,2-TCAM) for an experimental period of 5 days. The inputs of the kinetic model such as DCAL apparent formation rate and $^{15}NH_2Cl$ concentration (4 mg/L as Cl_2) were modified to the specific condition of these experiment sets C01 and R01. The modeled values and experimental data of ^{15}N-DCAN and ^{15}N-DCAM for two scenarios (with and without 30 mins free chlorine pre-treatment) were plotted in Figure 3.5a and 3.5b. A good agreement between the measured data and prediction values provided by the kinetic model was observed in two sets of the experiment. The formation mechanisms of these N-DBPs via the aldehyde pathway under drinking water condition were confirmed by this result.

Effect of CT value of free chlorine pretreatment on the formation of DCAN and DCAM produced from the chloramination with prior free chlorine exposure

Effect of the chlorination step at different conditions on the subsequent chloramination was examined in experiment sets R01, R02 and R03. Three conditions of free chlorine pre-treatment varied by different CT values were tested as shown in Table 3.1. CT value of the chlorination step in experiment R01 (120 mg/L.min) was two times less than experiment R02 (240 mg/L.min). CT values in experiments R01 and R03 were the same but the contacting time in experiment R03 was doubled than in R01. The following ^{15}N-labelled chloramination condition was kept the same in all of these experiment sets.

In term of the total concentrations of DCAN and DCAM including both ^{14}N and ^{15}N species, results of R02 were mostly higher than R03. At higher chlorination CT condition (experiment R02), free chlorine could react with organic matters in the feed water for a longer time, and thus enhanced the formation of these N-DBPs during the first step - chlorination. It was observed in Figure 3.6a and 3.6b that DCAN and DCAM concentrations produced after 60 mins of chlorination (R02) were about 30-40% higher than after 30 mins of chlorination (R01). Although experiment sets R01 and R03 have the same CT value condition, total DCAN and DCAM formations of R03 were slightly higher due to the different at the chlorine exposure time. There were no sufficient

evidence to conclude about the effect of CT value of the chlorination step on the total concentration of DCAN and DCAM. ^{14}N and ^{15}N species were involved with different formation mechanisms which might vary distinctly under the effect of different chlorination condition.

Unlike the total ^{14}N-DBPs and ^{15}N-DBPs, the ^{15}N species followed a different formation trend. It is interesting that at condition 4 mg/L 30 mins of free chlorine pretreatment ^{15}N-DCAN and ^{15}N-DCAM was formed as the highest amount during the chloramination (Figure 3.6c and 3.6d). Extending the exposure time of free chlorine pretreatment led to a decrease in the formation of these ^{15}N-DBPs regardless the chlorine concentration was applied. It was also observed that DCAL was formed at the highest at 4mg/L 30 mins HOCl pretreatment, second at the condition 4mg/L 60 mins and lowest at 2mg/L 60 mins. DCAL concentration was well correlated with the formation of ^{15}N-DCAN and ^{15}N-DCAM during the chloramination experiment as DCAL was the main reactant in the aldehyde pathway which would further produce these ^{15}N-DBPs. The aldehyde pathway mechanism was again confirmed by a kinetic model developed in Chapter 2 and showing a good match with the real measured data about ^{15}N-DCAN and ^{15}N-DCAM concentration.

Effect of pH on the formation of DCAN and DCAM produced from the chloramination with prior free chlorine exposure

Experiment sets R01, R04 and R05 were conducted to investigate the effect of the chloramination step's pH on the formation of N-DBP via this stage. Condition of the first step – free chlorine exposure was kept the same in these sets of experiment and pH of the following ^{15}N-labelled chloramination was adjusted to 5.8, 7.8 and 9.2 (Table 3.1).

In general, the total concentration of DCAN including ^{14}N-DCAN and ^{15}N-DCAN was higher whereas the total concentration of DCAM was lower at low pH than the corresponding values at higher pH because of the hydrolysis reaction of DCAN (Figure 3.7a and 3.7b). At high pH range (about >8), DCAN quickly hydrolyzed to form DCAM which could be further converted into DCAA [22, 27, 28]. Both of ^{14}N-DCAN and ^{15}N-DCAN were assumed to hydrolyze at the same rate at a certain pH condition. Low pH favors the formation of DCAN whereas high pH will enhance the formation of DCAM, the hydrolysis product of DCAN. pH choice should be determined by taking the toxicity of each species into consideration because they may contribute differently to the overall toxicity of the finished waters.

At low pH 5.8, the formation of ^{15}N-DCAN and ^{15}N-DCAM was always less than their ^{14}N counter parts suggesting the dominance of the decarboxylation pathway under this condition (Figure 3.7c and 3.7d). Little amount of ^{15}N-DBPs was formed by the aldehyde pathway may be explained by the fact that the reactions in this pathway were not favored at low pH range. As shown in Figure 3.7c, ^{15}N-DCAN at pH 5.8 is much lower than ^{15}N-DCAN at pH 7.8, especially at the beginning period where the hydrolysis of DCAN at neutral was insignificantly. However, ^{15}N-DCAN at high pH 9.2 was the lowest among three pHs though its formation rate at this pH may be higher than neutral and low pH due to the effect of hydrolysis consumption.

Simplified model predicting the formation of ^{14}N-DCAN and ^{14}N-DCAM

Although characterizing the formation of ^{14}N-DCAN and ^{14}N-DCAM via the decarboxylation pathway was not a target in this study, a simplified model based on the hydrolysis of DCAN was also developed to predict the formation of these ^{14}N-DBPs under drinking water conditions. The hydrolysis reaction occurred for both ^{14}N-DCAN and ^{15}N-DCAN and should be considered in both of these pathways, decarboxylation and aldehyde pathway. The hydrolysis rate constant has been reported in literature and also determined in Chapter 2 of this study (k_4).

In the decarboxylation pathway, there are several reactions involved to the formation of ^{14}N-DCAN as well as its consumption. Figure 3.8 showed the ^{14}N-DCAN concentration during 5 days of chloramination (10 mg/L as Cl_2 and natural water was used as the feed water). There were two stages in which the DCAN formation rate varied differently. First, ^{14}N-DCAN was quickly formed during the initial period up to 9 hours. Then, ^{14}N-DCAN formation rate became slower in the second stage, and it was in stable with the hydrolysis rate as ^{14}N-DCAN concentration did not changed much. During this stable period (after the first 9 hours), we made an assumption that DCAN hydrolysis reaction is the major source leading to ^{14}N-DCAM formation. A simple chain of reactions was proposed starting with ^{14}N-DCAN precursors to form ^{14}N-DCAN and further produce ^{14}N-DCAM.

The rate expressions for the formation of ^{14}N-DCAN and ^{14}N-DCAM are:

$$\frac{d[DCAN]}{dt} = k_{DCAN,form} - k_4 \times [DCAN]$$

$$\frac{d[DCAM]}{dt} = k_4 \times [DCAN]$$

Where $k_{DCAN,form}$ is the apparent rate constant of the ^{14}N-DCAN formation reaction from ^{14}N-DCAN precursors. This rate constant was determined experimentally from the concentrations of ^{14}N-DCAN and ^{14}N-DCAM with the assumption that a majority of ^{14}N-DCAM formation was contributed by ^{14}N-DCAN hydrolysis. To match the mass balance for this reaction chain, the total amounts of ^{14}N-DCAN and ^{14}N-DCAM would be equal to ^{14}N-DCAN precursors. Consequently, the concentration of ^{14}N-DCAN precursors over time were used to calculate $k_{DCAN,form}$.

Additionally, k_4 is the hydrolysis rate constant of DCAN, the value of which was reported in a previous study (20^{o}C) and also in Chapter 2. This rate constant varies significantly with pH condition of the hydrolysis reaction as it was determined by the equation k_4^0 = (2.86 ± 0.90) x 10^{-7} s^{-1} and k_4^{OH} = 3.69 ± 0.09 $M^{-1}s^{-1}$ for 25^{o}C. At a certain pH condition, k_4 value would be calculated only for each period of reaction time instead of using the value determined by the average pH during 5 days of the real water experiment.

A simplified kinetic model was developed using the above rate expressions and rate constants to predict the formation of ^{14}N-DCAN and ^{14}N-DCAM from the experiment. As plotted in Figure 3.9, simulation values calculated by the kinetic model and the experimental data measured from the water sample showed a good match between them. The modeled values of ^{14}N-DCAM were slightly lower than measured data (about 5-15%) and this small discrepancy may be caused by the contribution of other ^{14}N-DCAM precursors beside the hydrolysis of ^{14}N-DCAN.

Practical Implications

N-DBP species are drawing more attention from research communities and public because of their occurrences in the drinking water samples and higher toxicity than the regulated DBPs. Some studies has elucidated the formation mechanisms of DCAN and DCAM which are commonly found among N-DBPs. However, it is difficult to determine their formation level as a large number of kinetic rate constants in these pathways have not been well characterized in the natural water conditions. This brings many challenges in developing regulations and control strategies to minimize the effect of DCAN, DCAM and other N-DBPs in drinking waters. For this reason, the experiments in this study were designed to imitate the practical processes at the water utilities and aim to close the gap between kinetic works with synthetic water and real water treatment scenarios. The simulated models can be adjusted by chloramine concentration providing the prediction of DCAN and DCAM via the aldehyde pathway.

From regulators' view, predicting the formation of these N-DBPs along with their toxicity are essential references for establishing the maximum contaminant level and recommended operating conditions. Furthermore, results of these experiments are also useful for water engineers to avoid moderated formation of HANs and HAMs or promote less toxic compounds when designing the treatment processes and setting up the operating parameters. In the future work, different water types such as ground waters or surface waters impacted by secondary effluent will be examined to provide more insight about the formation of these N-DBPs in a variety of source waters. In addition to free chlorine pre-treatment, other oxidants (i.e. UV, O_3 or ClO_2) will also be studied to understand the effect of different processes on N-DBP formation.

Tables and Figures

Table 3.1. Natural water experiment conditions

Experiment	First step: free chlorine exposure Free chlorine condition		Second step: chloramination Labelled ^{15}N chloramination condition	
	Concentration (mg/L as Cl_2)	Time (mins)	Concentration (mg/L as Cl_2)	pH
C01	0	0	4	7.8 – 8.0
C02	0	0	10	7.8 – 8.0
R01	4	30	4	7.8 – 8.0
R02	4	60	4	7.8 – 8.0
R03	2	60	4	7.8 – 8.0
R04	4	30	4	5.7 – 5.9
R05	4	30	4	9.0 – 9.2

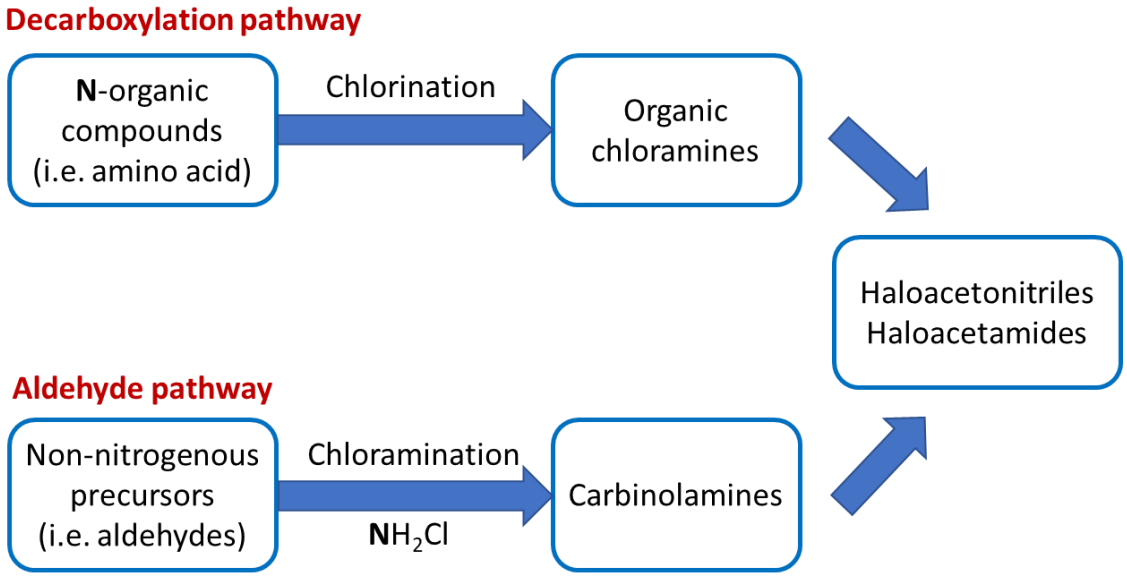

Figure 3.1. Simplified summary of two major pathways leading to the formation of haloacetonitriles and haloacetamides.

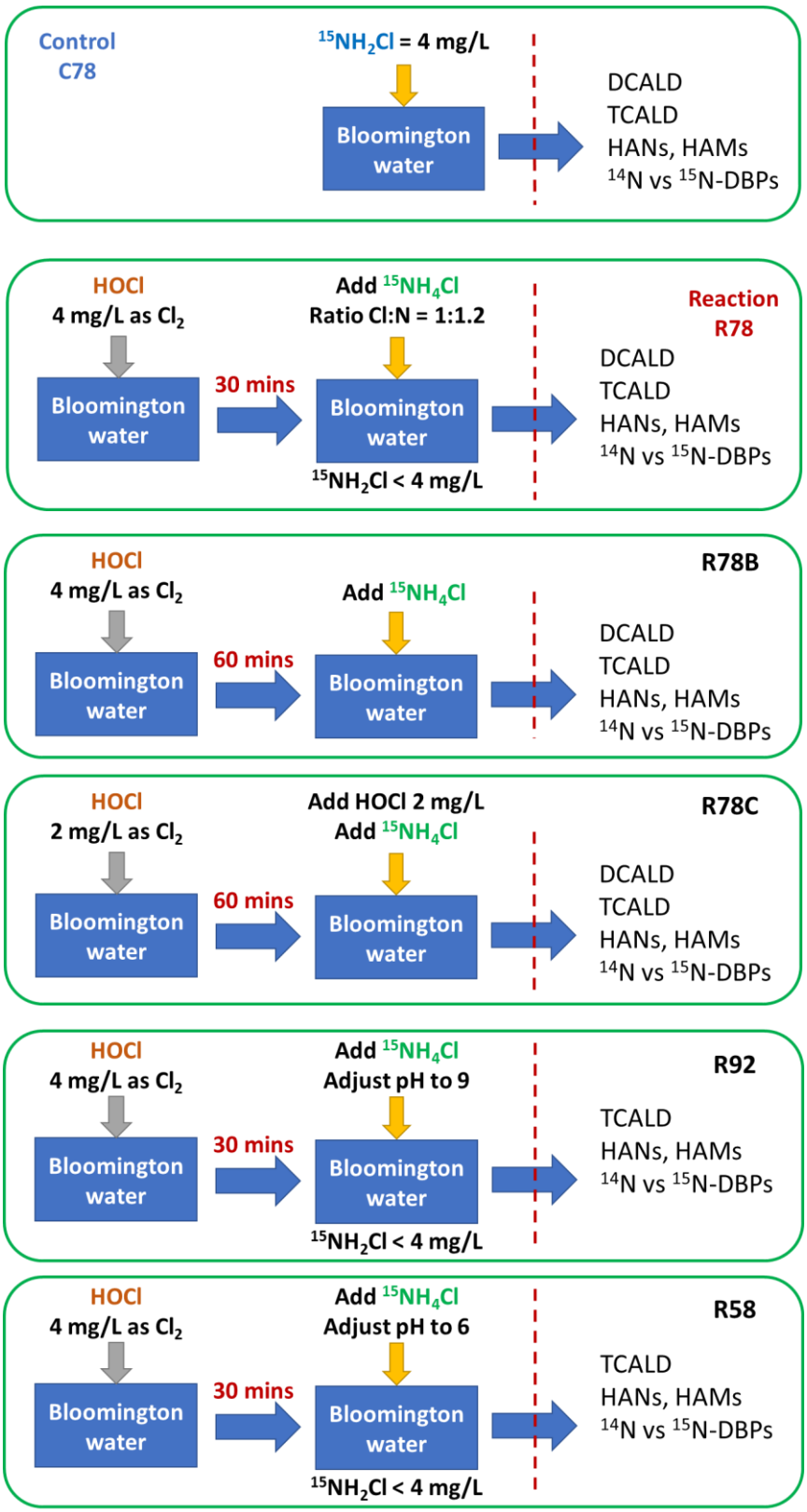

Figure 3.2. Experimental conditions of natural water experiments

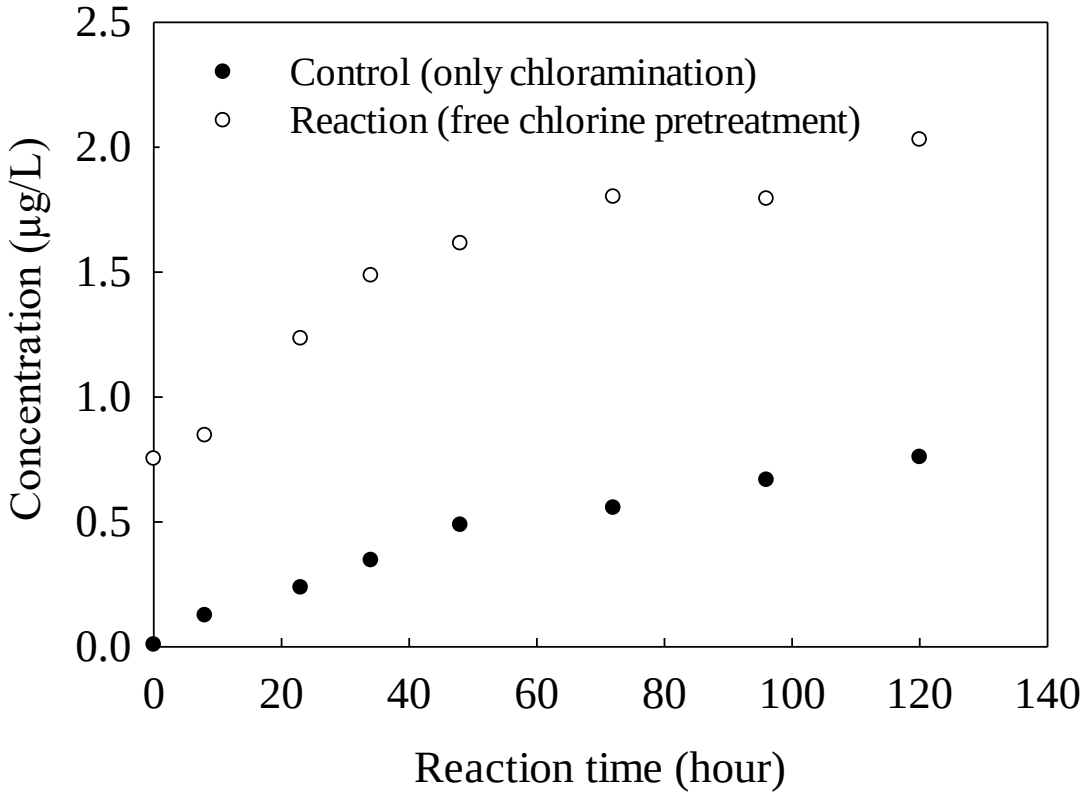

Figure 3.3. Dichloroacetaldehyde formation during control C01 and reaction R01 experiments. Experimental condition: only $^{15}NH_2Cl$ 4mg/L (control – C01); HOCl 4mg/L for 30 mins and followed by $^{15}NH_2Cl$ 4mg/L (reaction – R01). pH 7.8 – 8.1 and 25±0.1^oC.

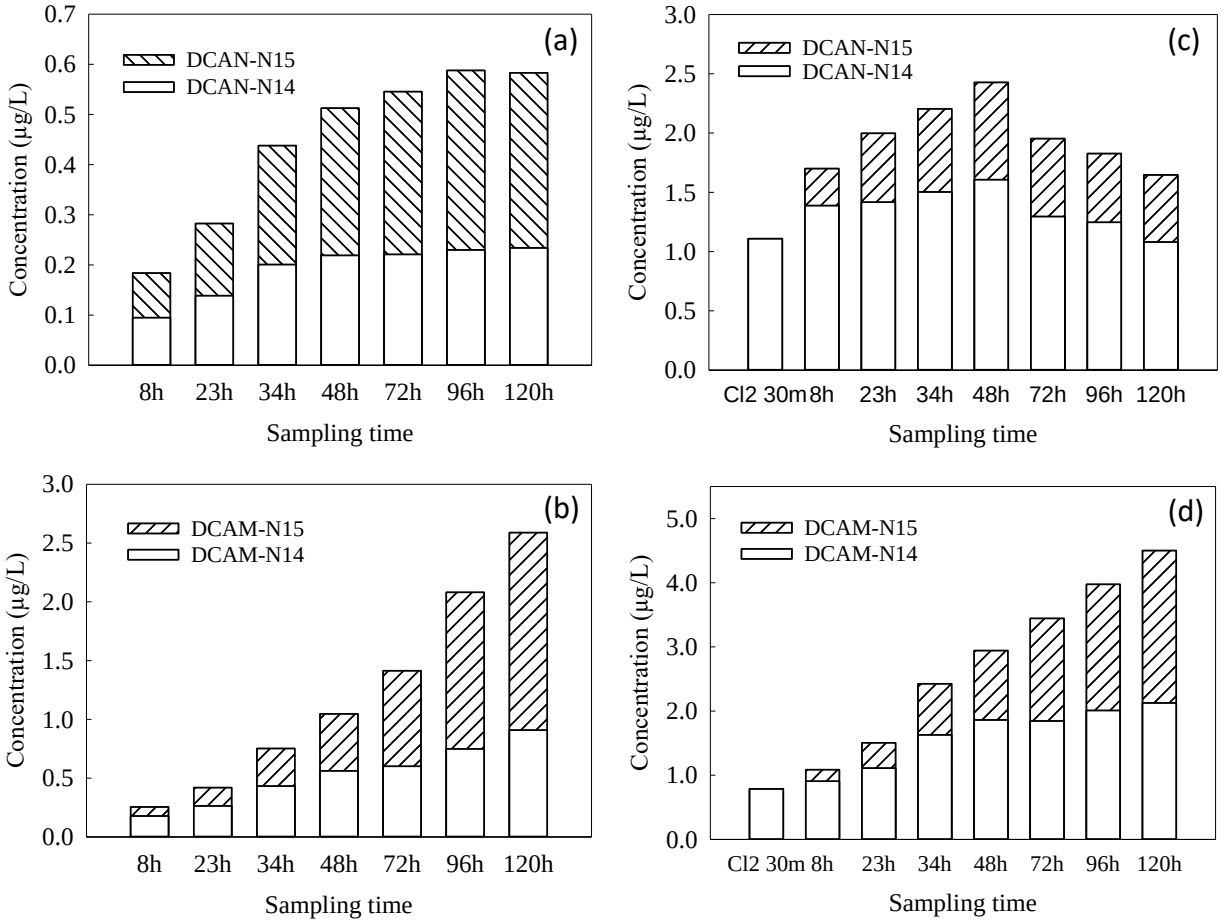

Figure 3.4. Formation of ^{15}N labelled and unlabeled DCAN (1a) and DCAM (1b) with chloramination of Bloomington water (Experiment C01: $^{15}NH_2Cl$ 4mg/L, pH 7.8 – 8.1, 25±0.1°C). Formation of ^{15}N labelled and unlabeled DCAN (1c) and DCAM (1d) with chloramination of Bloomington water after a 30 min contact time with free chlorine (Experiment R01: HOCl 4 mg/L for 30 mins).

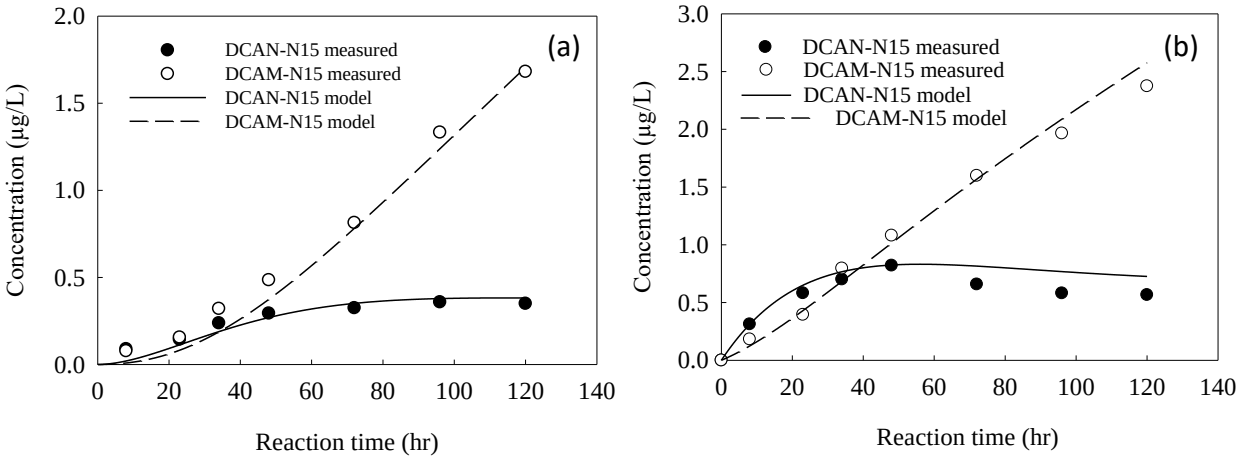

Figure 3.5. Experimental and modeled concentrations of DCAN and DCAM in experiment C01 (a) and R01 (b). Symbols are experimental data and lines are the simulation from kinetic models.

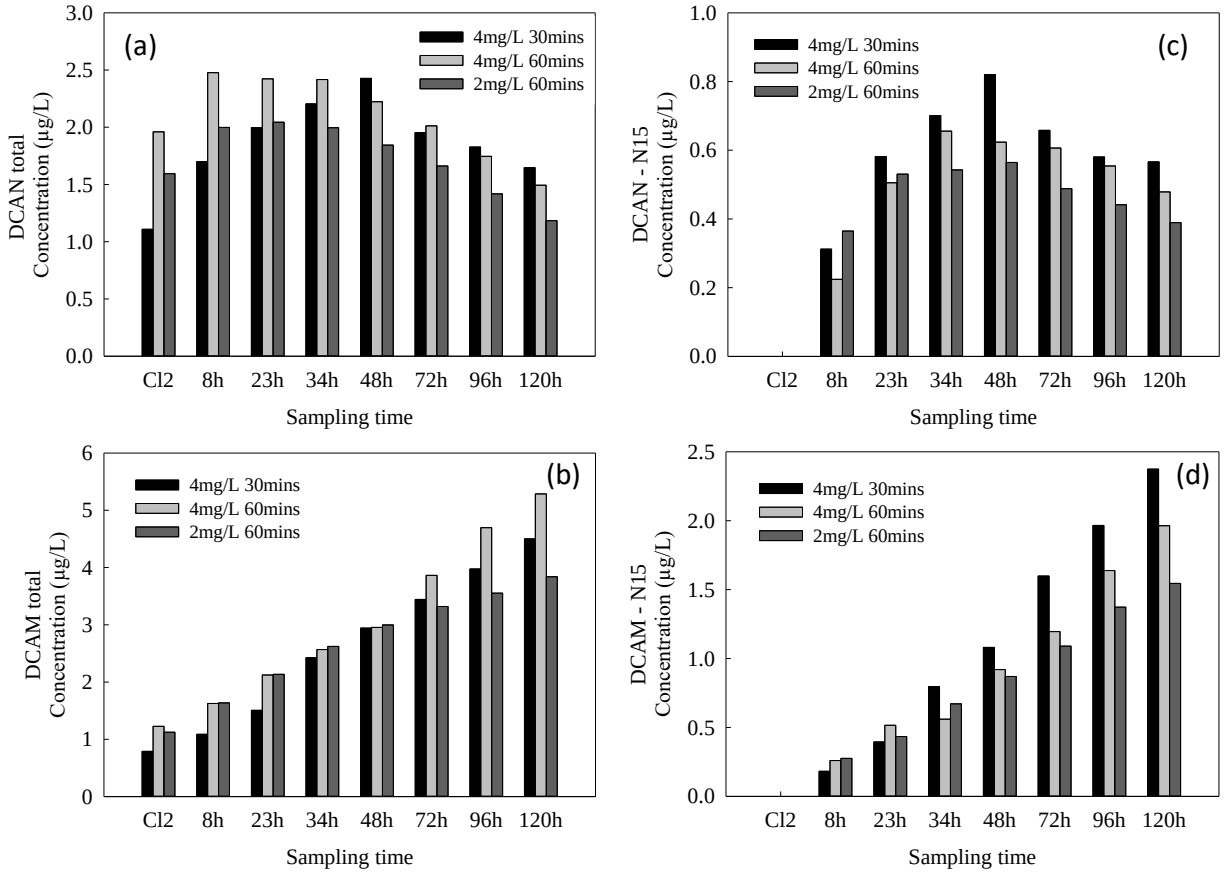

Figure 3.6. Formation of DCAN and DCAM during the chlorination + chloramination process at different CT conditions in experiment R01, R02 and R03; (a) total DCAN; (b) total DCAM; (c) labelled ^{15}N-DCAN; (d) labelled ^{15}N-DCAM.

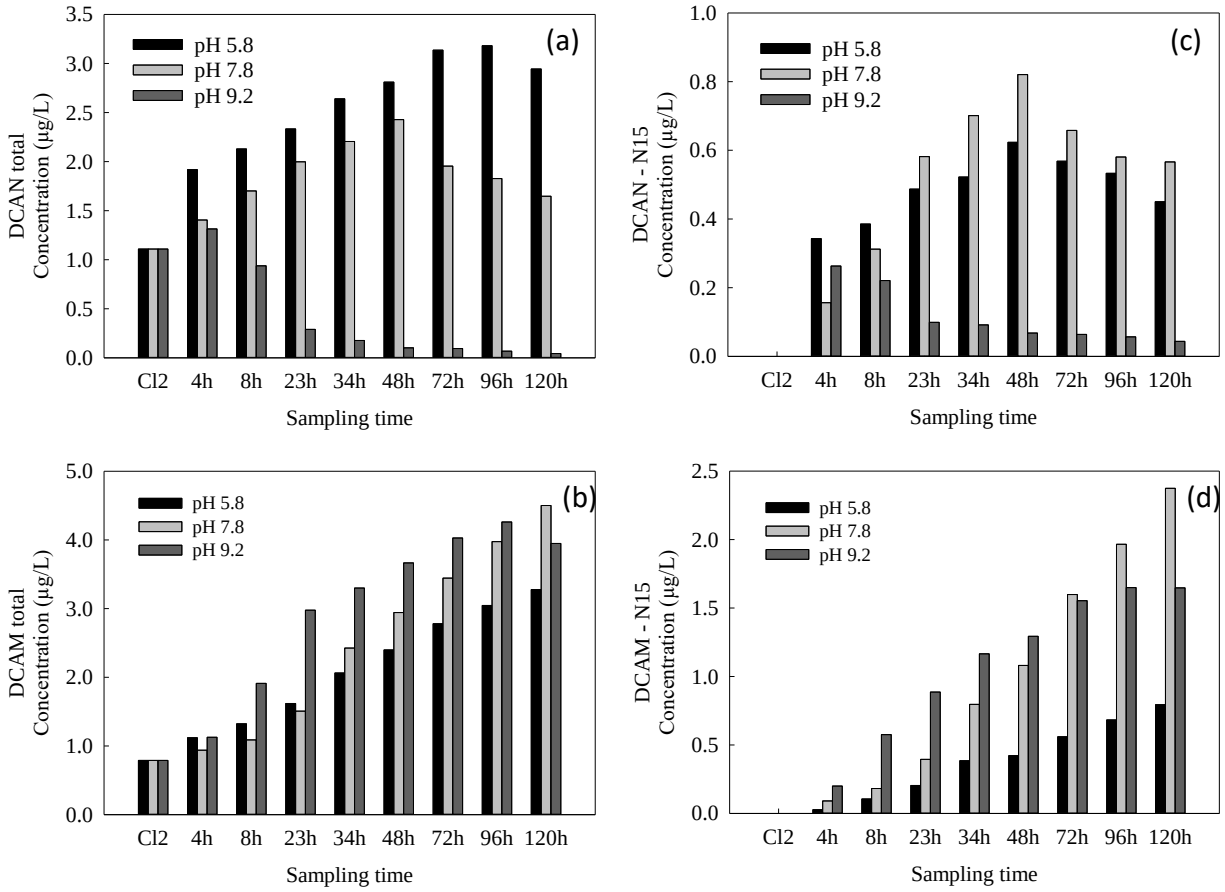

Figure 3.7. Formation of DCAN and DCAM during the chlorination + chloramination process at different pH conditions in experiment R01, R04 and R05; (a) total DCAN; (b) total DCAM; (c) labelled ^{15}N-DCAN; (d) labelled ^{15}N-DCAM.

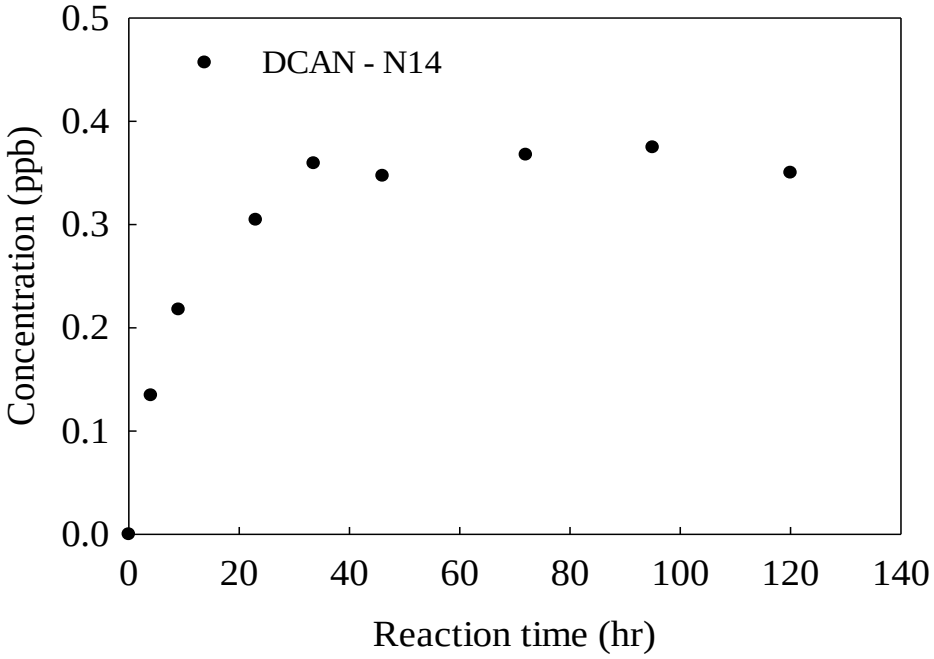

Figure 3.8. Formation of ^{14}N unlabeled DCAN during chloramination of Bloomington water. Experimental condition: $^{15}NH_2Cl$ 10mg/L, pH 7.8 – 8.1, 25±0.1°C.

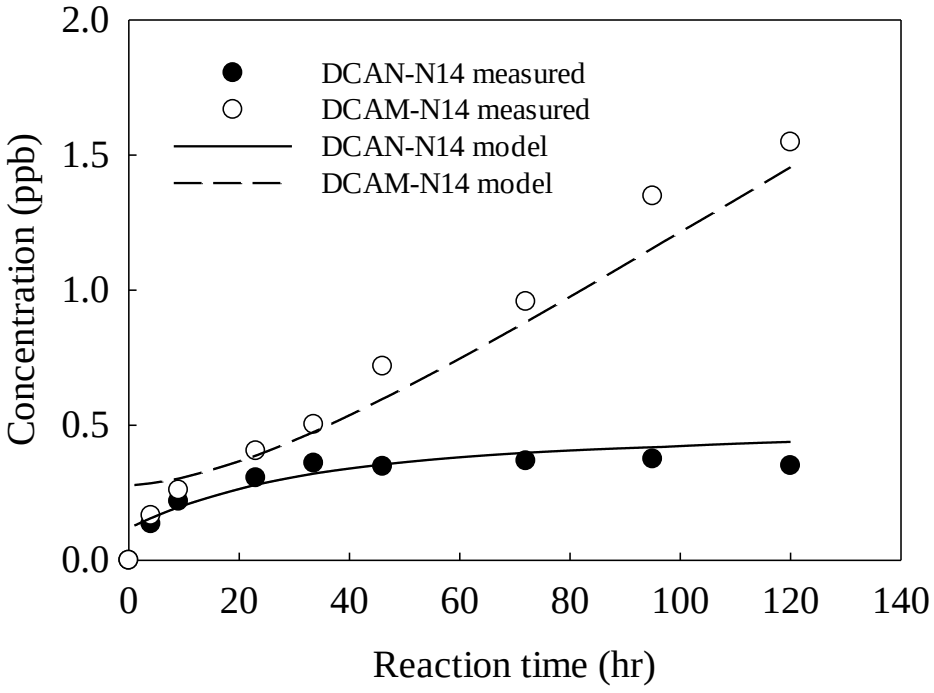

Figure 3.9. Experimental and modeled concentrations of DCAN and DCAM (N14 fraction) over time. Symbols are experimental data and lines are the simulation from the kinetic model. Experimental condition: $^{15}NH_2Cl$ 10mg/L, pH 7.8 – 8.1, 25±0.1°C.

References

1. Weinberg, H.S., et al., *The occurrence of disinfection by-products (DBPs) of health concern in drinking water: results of a nationwide DBP occurrence study*. 2002, EPA National Exposure Research Laboratory: Athens, GA.

2. Krasner, S.W., et al., *Occurrence of a new generation of disinfection byproducts.* Environ. Sci. Technol., 2006. **40**(23): p. 7175-7185.

3. Richardson, S.D., et al., *Occurrence, genotoxicity, and carcinogenicity of regulated and emerging disinfection by-products in drinking water: a review and roadmap for research.* Mutat. Res., 2007. **636**(1): p. 178-242.

4. Plewa, M., et al., *Occurrence, formation, health effects and control of disinfection by-products in drinking water*, in *Comparative Mammalian Cell Toxicity of N-DBPs and C-DBPs*. 2008, American Chemical Society Washington, DC. p. 36-50.

5. Plewa, M.J., et al., *Occurrence, synthesis, and mammalian cell cytotoxicity and genotoxicity of haloacetamides: an emerging class of nitrogenous drinking water disinfection byproducts.* Environ. Sci. Technol., 2008. **42**(3): p. 955-961.

6. Komaki, Y., B.J. Mariñas, and M.J. Plewa, *Toxicity of drinking water disinfection byproducts: cell cycle alterations induced by the monohaloacetonitriles.* Environ. Sci. Technol., 2014. **48**(19): p. 11662-11669.

7. Muellner, M.G., et al., *Haloacetonitriles vs. regulated haloacetic acids: are nitrogen-containing DBPs more toxic?* Environ. Sci. Technol., 2007. **41**(2): p. 645-651.

8. Joo, S.H. and W.A. Mitch, *Nitrile, aldehyde, and halonitroalkane formation during chlorination/chloramination of primary amines.* Environ. Sci. Technol., 2007. **41**(4): p. 1288-1296.

9. Lee, W., P. Westerhoff, and J.-P. Croué, *Dissolved organic nitrogen as a precursor for chloroform, dichloroacetonitrile, N-nitrosodimethylamine, and trichloronitromethane.* Environ. Sci. Technol., 2007. **41**(15): p. 5485-5490.

10. Mitch, W.A., et al., *Occurrence and formation of nitrogenous disinfection by-products*. 2009, Denver, CO: Water Research Foundation.

11. Yang, X., et al., *Nitrogenous disinfection byproducts formation and nitrogen origin exploration during chloramination of nitrogenous organic compounds.* Water Res., 2010. **44**(9): p. 2691-2702.

12. Chu, W., et al., *Formation and speciation of nine haloacetamides, an emerging class of nitrogenous DBPs, during chlorination or chloramination.* J. Hazard. Mater., 2013. **260**: p. 806-812.

13. Chuang, Y.-H., et al., *Formation pathways and trade-offs between haloacetamides and haloacetaldehydes during combined chlorination and chloramination of lignin phenols and natural waters.* Environ. Sci. Technol., 2015. **49**(24): p. 14432-14440.

14. Chu, W., et al., *The formation of haloacetamides and other disinfection by-products from non-nitrogenous low-molecular weight organic acids during chloramination.* Chem. Eng. J., 2016. **285**: p. 164-171.

15. Le Roux, J., M. Nihemaiti, and J.-P. Croué, *The role of aromatic precursors in the formation of haloacetamides by chloramination of dissolved organic matter.* Water Res., 2016. **88**: p. 371-379.

16. Zeng, T., M.J. Plewa, and W.A. Mitch, *N-Nitrosamines and halogenated disinfection byproducts in US Full Advanced Treatment trains for potable reuse.* Water research, 2016. **101**: p. 176-186.

17. Pedersen, E.J., et al., *Formation of cyanogen chloride from the reaction of monochloramine with formaldehyde.* Environ. Sci. Technol., 1999. **33**(23): p. 4239-4249.

18. Kimura, S.Y., et al., *Chloroacetonitrile and n,2-dichloroacetamide formation from the reaction of chloroacetaldehyde and monochloramine in water.* Environ. Sci. Technol., 2013. **47**(21): p. 12382-90.

19. Kimura, S.Y., et al., *Acetonitrile and N-chloroacetamide formation from the reaction of acetaldehyde and monochloramine.* Environ. Sci. Technol., 2015. **49**(16): p. 9954-9963.

20. Huang, H., et al., *Dichloroacetonitrile and dichloroacetamide can form independently during chlorination and chloramination of drinking waters, model organic matters, and wastewater effluents.* Environ. Sci. Technol., 2012. **46**(19): p. 10624-10631.

21. Yang, X., et al., *Precursors and nitrogen origins of trichloronitromethane and dichloroacetonitrile during chlorination/chloramination.* Chemosphere, 2012. **88**(1): p. 25-32.

22. Glezer, V., et al., *Hydrolysis of haloacetonitriles: linear free energy relationship, kinetics and products.* Water Res., 1999. **33**(8): p. 1938-1948.

23. Hussain, A., P. Trudell, and A.J. Repta, *Quantitative spectrophotometric methods for determination of sodium hypochlorite in aqueous solutions.* Journal of Pharmaceutical Sciences, 1970. **59**(8): p. 1168-1170.

24. Kumar, K., R.A. Day, and D.W. Margerum, *Atom-transfer redox kinetics: general-acid-assisted oxidation of iodide by chloramines and hypochlorite.* Inorg. Chem., 1986. **25**(24): p. 4344-4350.

25. Cuthbertson, A.A., et al., *Method Optimization for Quantification of Priority Disinfection By-Products: Finding a Good Compromise*, in *Drinking Water Disinfection By-Products Gordon Research Conference*. August 2015: Hadley, MA.

26. Jeong, C.H., et al., *Occurrence and comparative toxicity of haloacetaldehyde disinfection byproducts in drinking water.* Environ. Sci. Technol., 2015. **49**(23): p. 13749-13759.

27. Reckhow, D.A., et al., *Formation and degradation of dichloroacetonitrile in drinking waters.* J. Water Supply Res. T., 2001. **50**(1): p. 1-13.

28. Yu, Y. and D.A. Reckhow, *Kinetic Analysis of Haloacetonitrile Stability in Drinking Waters.* Environ. Sci. Technol., 2015. **49**(18): p. 11028-11036.

CHAPTER 4

CONCLUSIONS

First, this study has shown that dichloroacetonitrile and dichloroacetamide, two prevalent species among HAN and HAM groups, were produced from the reaction between dichloroacetaldehyde and monochloramine via the aldehyde pathway. The finding was in a good agreement with previous studies on the reaction between haloacetaldehyde (i.e chloroacetaldehyde, acetaldehyde) and monochloramine. Initially, dichloroacetaldehyde reacted with monochloramine to form the carbinolamine 2,2-dichloro-1-(chloroamino)ethanol in a reversible reaction. Then, 2,2-dichloro-1-(chloroamino)ethanol underwent two parallel reactions where, (1) it dehydrates to the imine 1,1-dichloro-2-(chloroimino)ethane which further decomposed to dichloroacetonitrile, and (2) it was oxidized by monochloramine to form *N*,2,2-trichloroacetamide, a newly found species of *N*-haloacetamide group. At high pH range, the product dichloroacetonitrile was converted into dichloroacetamide by a hydrolysis reaction. Besides, trichloroacetaldehyde was also found as a product of the reaction between dichloroacetaldehyde and monochloramine at low and neutral pH range where the presence of monochlorammonium ion, a product of monochloramine disproportionation, was significant. Additionally, the kinetic rate constants for this reaction scheme were determined at neutral pH and high pH range only for the hydrolysis reaction of dichloracetonitrile. Kinetic constant values at a wider pH range will be identified in future work as the current experimental and calculation methods are adjusted to fix the UV data interference caused by carbonate buffer.

Second, labelled $^{15}NH_2Cl$ technique was employed in this study to evaluate the relevance of the aldehyde pathway in the competition with other pathways (i.e. decarboxylation pathway) under real drinking water conditions. It was shown that 60-70% DCAN and DCAM produced from the labelled ^{15}N chloramination has the ^{15}N atom in their structures only contributed by the initial $^{15}NH_2Cl$ spike. This results confirmed the dominance of aldehyde pathway which is consistent with the findings in other studies working the nitrogen origin of HANs and HAMs. In addition, a kinetic model was developed with reaction rate constants determined previously in this study to predict the formation of ^{15}N-DCAN and ^{15}N-DCAM via the aldehyde pathway. Simulated values calculated by the kinetic model show a very good agreement with the real measured data (^{15}N

fractions of these DBPs) confirming again the reaction mechanism of the aldehyde pathway and suggesting that this kinetic model could be used as a valuable tool to predict the formation of DCAN and DCAM, the most commonly found N-DBPs in drinking water.

Third, different scenarios imitating some common practices at drinking water utilities were examined to evaluate the effect of free chlorine pretreatment, CT value of the free chlorine exposure, and pH on the chloramination of natural waters. Free chlorine pretreatment shows significant effect on the formation of N-DBPs via the aldehyde pathway as it increases the formation of DCAL and thereby enhances the formation of DCAN, N,2,2-TCAM and DCAM through this pathway. pH value plays a key role to determine which specie is dominant between DCAN and DCAM as the hydrolysis rate of DCAN to form DCAM is significantly base catalyzed. Other factors such as temperature, bromide or iodide concentration may have strong effects on the formation of HANs and HAMs in drinking water condition that need to be explored in future research. Better understanding about the formation mechanism of these N-DBPs is critical to develop appropriate control strategies to minimize their formation in waters as well as their impacts on human health consumers.

APPENDIX A

EXPERIMENTAL DATA FOR CHAPTER 2

A.1. Chemical relaxation analysis to obtain equilibrium constant K_1.

Equilibrium experiments consisted of dichloroacetaldehyde in excess from 10 mM to 90 mM and monochloramine fixed at 1mM. For this reason, the reaction would be characterized as a pseudo first order reaction as described below.

$$NH_2Cl \overset{k'_1}{\rightleftharpoons} Cl_2CHCH(OH)NHCl \tag{A.1}$$

Where, $k'_1 = k_1 \times [Cl_2CHCHO]_0$, is an apparent or pseudo first-order rate constant at a fixed dichloroacetaldehyde concentration assuming that the consumed amount of aldehyde in the reaction is negligible.

According to mass conservation, the amount monochloramine consumed is equal to the amount of product (carbinolamine) formed.

$$[NH_2Cl]_t - [NH_2Cl]_e = [Cl_2CHCH(OH)NHCl]_e - [Cl_2CHCH(OH)NHCl]_t \tag{A.2}$$

Where, subscript "*t*" refers to concentration at a given time t and "*e*" means at equilibrium. If we substitute monochloramine consumption with variable x, we will obtain.

$$[NH_2Cl]_t = [NH_2Cl]_e + x \tag{A.3a}$$

$$[Cl_2CHCH(OH)NHCl]_t = [Cl_2CHCH(OH)NHCl]_e - x \tag{A.3b}$$

The change in monochloramine concentration is expressed as:

$$-\frac{d[NH_2Cl]}{dt} = \frac{d[Cl_2CHCH(OH)NHCl]}{dt} = k'_1[NH_2Cl] - k_{-1}[Cl_2CHCH(OH)NHCl] \tag{A.4}$$

Substituting equation 6a and 6b, equation 7 is re-written to:

$$-\frac{d([NH_2Cl]_e + x)}{dt} = -k_1'([NH_2Cl]_e + x) + k_{-1}([Cl_2CHCH(OH)NHCl]_e - x) \quad \text{(A.5)}$$

$$-\frac{d([NH_2Cl]_e)}{dt} - \frac{dx}{dt} = -k_1'[NH_2Cl]_e + k_{-1}[Cl_2CHCH(OH)NHCl]_e - (k_1' + k_{-1})x \quad \text{(A.6)}$$

At equilibrium, the concentrations of reactants and product do not change or $d([NH_2Cl]_e)/dt = 0$. Also, from the equilibrium constant expression, we obtain $k_1'[NH_2Cl]_e = k_{-1}[CH_3CH(OH)NHCl]_e$. Therefore equation 9 is reduced to:

$$\frac{dx}{dt} = -(k_1' + k_1)\,.\,x = -\frac{1}{\tau}x \quad \text{(A.7)}$$

Where, τ is the relaxation time expressed as:

$$\frac{1}{\tau} = k_1' + k_{-1} = k_1 \times [Cl_2CHCHO] + k_{-1} \quad \text{(A.8)}$$

After integrating equation 10 and combining with equation 5, 6a, 6b, we obtain:

$$[NH_2Cl]_t = [NH_2Cl]_e + ([NH_2Cl]_0 - [NH_2Cl]_e) \times exp\left(-\frac{t}{\tau}\right) \quad \text{(A.9)}$$

Reaction absorbance values at a time *t* and at a specific wavelength obtained from experiments and is expressed according to Beers Law as:

$$Abs_t = \varepsilon_{NH_2Cl}[NH_2Cl]_t + \varepsilon_{Cl_2CHCHO}[Cl_2CHCHO]_t + \varepsilon_{Cl_2CHCH(OH)NHCl}[Cl_2CHCH(OH)NHCl]_t \quad \text{(A.10)}$$

It is assumed that the excess aldehyde consumed is not significant. The differences in the absorbance at a time *t* and at equilibrium and between equilibrium and initial conditions are expressed as:

$$Abs_t - Abs_e = \left(\varepsilon_{NH2Cl} - \varepsilon_{Cl2CHCH(OH)NHCl}\right) \times ([NH_2Cl]_t - [NH_2Cl]_e) \quad \text{(A.11)}$$

$$Abs_0 - Abs_e = \left(\varepsilon_{NH2Cl} - \varepsilon_{Cl2CHCH(OH)NHCl}\right) \times ([NH_2Cl]_0 - [NH_2Cl]_e) \quad \text{(A.12)}$$

After replacing equation 14 and 15 into equation 12 and rearranging:

$$Abs_t = (Abs_0 - Abs_e).\exp\left(-\frac{t}{\tau}\right) + Abs_e \quad \text{(A.13)}$$

The monochloramine and dichloroacetaldehyde reaction reached equilibrium within a time scale of a few seconds. Therefore, the SX20 stopped flow spectrophotometer was needed to monitor the fast reaction. Absorbance values at wavelength 243nm over time (Abs_t and t) were fitted to obtain Abs_0, Abs_e and $1/\tau$. For each initial dichloroacetaldehyde concentration, a $1/\tau$ value was obtained.

A.2. Data set GC-1.1

Experimental condition: 10 mg/L as Cl_2 of $^{15}NH_2Cl$ in treated surface water before disinfection at pH 7.8 – 8.1

No.	Time	DCAN (ppb)			DCAM (ppb)		
		total	N14	N15	total	N14	N15
1	Blank	0	0	0	0	0	0
2	4 hr	0.236	0.134	0.102	0.315	0.165	0.149
3	9 hr	0.412	0.218	0.194	0.511	0.259	0.251
4	23 hr	0.643	0.305	0.339	0.868	0.405	0.464
5	33.5 hr	0.839	0.359	0.479	1.171	0.503	0.668
6	46 hr	0.916	0.347	0.569	1.725	0.718	1.007
7	72 hr	0.995	0.368	0.628	2.516	0.958	1.558
8	95 hr	1.052	0.375	0.677	3.623	1.349	2.274
9	5 days	0.988	0.350	0.638	4.561	1.548	3.013
10	7 days	0.902	0.341	0.561	5.778	1.783	3.995

A.3. Data set GC-1.2

Experimental condition: 10 mg/L as Cl_2 of unlabeled $^{14}NH_2Cl$ in treated surface water before disinfection at pH 7.8 – 8.1

No.	Time	TCAL (ppb)	DCAN (ppb)	CAN (ppb)	DCAM (ppb)	TCAM (ppb)
1	Blank	0	0	0	0	0
2	4 hr	0.145	0.236	0.014	0.315	0.095
3	9 hr	0.155	0.412	0.007	0.511	0.107
4	23 hr	0.153	0.643	0.006	0.868	0.106
5	33.5 hr	0.173	0.839	0.015	1.171	0.056
6	46 hr	0.166	0.916	0.013	1.725	0.118
7	72 hr	0.217	0.995	0.011	2.516	0.094
8	95 hr	0.244	1.052	0.019	3.623	0.113
9	5 days	0.289	0.988	0.015	4.561	0.135
10	7 days	0.290	0.902	0.019	5.778	0.116

A.4. Data set GC-2

Experimental condition: 1 mM NH_2Cl and 10 mM $C_{T,aldehyde}$ at pH 7.8

Run 1

Time (min)	Concentration TCAL (uM)	DCAN (uM)	DCAM (uM)
1	2.15	0.00	2.37
30	18.16	0.00	4.25
60	28.33	0.91	6.10
90	38.95	2.49	9.20
120	50.06	4.10	11.45
183	68.70	7.60	16.62
240	80.73	10.37	19.93
395	113.83	16.60	29.64
605	161.53	21.11	40.50
1380	174.58	24.07	74.44
2760	157.11	14.30	70.96

Run 2

Time (min)	Concentration (uM) TCAL (uM)	DCAN (uM)	DCAM (uM)
1	3.53	0.00	4.48
30	17.91	0.00	5.11
60	33.04	0.09	9.39
90	41.54	0.46	10.59
135	53.25	1.83	13.53
180	63.58	2.94	16.64
240	76.58	5.80	21.50
480	112.30	13.29	38.62
690	129.18	16.08	47.73
1440	162.45	16.31	71.41
1920	164.88	13.18	77.71
2880	179.17	7.67	88.84
4320	177.44	0.59	96.42
7200	177.94	0.00	98.92
10080	172.42	0.00	94.29

A.5. Data set GC-3

Experimental condition: 1 mM NH_2Cl and 10 mM $C_{T,aldehyde}$ at pH 9.5

Time (min)	Concentration TCAL (uM)	DCAN (uM)	DCAM (uM)
1	14.64	2.03	8.68
5	16.21	10.5	27.6
10	16.39	21.41	50.03
20	18.78	30.89	92.68
30	19.97	30.49	124.47
45	18.83	23.85	144.64
60	19.82	16.76	166.2
120	18.89	2.78	185.93

A.6. Data set GC-4

Experimental condition: 1 mM NH_2Cl and 10 mM $C_{T,aldehyde}$ at pH 5.8

Time (min)	Concentration (uM) TCAcAl
1	4.40
5	8.95
15	12.88
30	25.80
90	70.87
240	160.18
1140	482.70
1440	527.83

A.7. Data set UV-1

Experimental conditions: 1 mM NH_2Cl and 10 mM $C_{T,aldehyde}$ at pH 7.8, phosphate buffer 0.02 M

Time (s)	Time (h)	WL 210 nm	WL 215 nm	WL 220 nm	WL 243 nm
95	0.03	0.1022	0.1233	0.1700	0.4473
325	0.09	0.1022	0.1246	0.1726	0.4429
655	0.18	0.1100	0.1284	0.1739	0.4392
950	0.26	0.1159	0.1330	0.1734	0.4359
1234	0.34	0.1189	0.1345	0.1735	0.4303
1875	0.52	0.1331	0.1379	0.1776	0.4261
2765	0.77	0.1383	0.1454	0.1753	0.4117
3600	1.00	0.1565	0.1512	0.1779	0.4039
5400	1.50	0.1716	0.1645	0.1811	0.3869
7200	2.00	0.1838	0.1699	0.1823	0.3717
9000	2.50	0.1934	0.1733	0.1814	0.3551
10800	3.00	0.2024	0.1768	0.1783	0.3389
14400	4.00	0.2197	0.1866	0.1795	0.3167
18000	5.00	0.2302	0.1906	0.1764	0.2941
21600	6.00	0.2416	0.1951	0.1776	0.2765
25320	7.03	0.2556	0.2016	0.1789	0.2610
35400	9.83	0.2856	0.2154	0.1763	0.2212
85560	23.77	0.3643	0.2526	0.1739	0.1138
109200	30.33	0.3737	0.2577	0.1721	0.0871
172800	48.00	0.4225	0.2818	0.1828	0.0639

A.8. Data set UV-2

Experimental conditions: 1 mM NH_2Cl and 10 mM $C_{T,aldehyde}$ at pH 9.5, phosphate buffer 0.02 M

Time(s)	WL 243 nm	WL 215 nm	WL 210 nm
50	0.4559	0.1322	0.1249
120	0.4537	0.1357	0.1327
244	0.4455	0.1401	0.1422
319	0.443	0.143	0.1469
455	0.4369	0.1486	0.1555
600	0.4324	0.1546	0.1664
914	0.4209	0.1614	0.1746
1260	0.4109	0.1697	0.1872
1858	0.3939	0.1856	0.2183
2715	0.3744	0.1968	0.2287
3600	0.3559	0.2054	0.2487
5460	0.3254	0.2192	0.2673
7200	0.3058	0.2287	0.2845

A.9. Data set UV-3

Experimental conditions: 1 mM NH_2Cl and 10 mM $C_{T,aldehyde}$ at pH 5.7, phosphate buffer 0.02 M

Time(s)	WL 243 nm	WL 215 nm	WL 210 nm
54	0.4601	0.1566	0.143
113	0.4577	0.1585	0.1452
238	0.454	0.1656	0.152
267	0.4498	0.1734	0.1616
352	0.4443	0.1808	0.1728
465	0.4385	0.1906	0.1857
596	0.4318	0.2028	0.2006
725	0.4243	0.21225	0.21355
902	0.4161	0.2258	0.2313
1193	0.40335	0.24555	0.25745
1502	0.3928	0.2678	0.2869
1803	0.3813	0.2847	0.3099
2326	0.3655	0.3139	0.3482
2723	0.3545	0.3332	0.3723
3605	0.3334	0.3708	0.4224
5503	0.3001	0.436	0.5056
7200	0.2774	0.4771	0.5579
14400	0.2186	0.5687	0.6812
21600	0.18375	0.6117	0.7383
86400	0.1141	0.6549	0.8045

A.10. Data set HR-1

Experimental condition: 1mM DCAN at pH 7.0 – 9.9

HR99 pH 9.9		HR95 pH 9.5		HR90 pH 9.0	
Time (hr)	**DCAN (M)**	**Time (hr)**	**DCAN (M)**	**Time (hr)**	**DCAN (M)**
0.021	0.000498	0.02167	0.000482	0.0828	0.000498
0.093	0.0004454	0.07917	0.000468	0.1292	0.0004954
0.172	0.0004134	0.15194	0.000453	0.1867	0.0004915
0.253	0.0003774	0.23611	0.000435	0.3211	0.0004837
0.341	0.0003467	0.33611	0.000411	0.5153	0.00047
0.419	0.0003191	0.44833	0.00039	0.7472	0.0004609
0.504	0.0002922	0.58528	0.000365	1.0000	0.0004434
0.763	0.0002383	0.76639	0.000335	1.5000	0.0004186
1.017	0.0002037	1	0.000295	2.0500	0.0003933
1.533	0.0001697	1.26667	0.000268	3.0000	0.0003549
2.167	0.0001626	1.51667	0.000242	5.0000	0.0002977
3.183	0.0001748	2.05	0.000197	8.1000	0.000245
		2.63333	0.000161	18.5167	0.0001682
		3.26667	0.000138	22.3667	0.0001246
		5.06667	0.000104	27.3167	0.0001032

HR85 pH 8.5		HR80 pH 8.0		HR70 pH 7.0	
Time (hr)	**DCAN (M)**	**Time (hr)**	**DCAN (M)**	**Time (hr)**	**DCAN (M)**
0.02472	0.000498	0.0228	0.000498	0.02278	0.000498
0.09222	0.0004973	0.0839	0.000497	0.81278	0.0004973
0.26667	0.0004928	0.2528	0.000493	1.41667	0.0004973
0.50000	0.0004856	0.7514	0.000493	3.6	0.0004941
0.80000	0.0004785	1.5000	0.000484	5.15	0.0004915
1.01667	0.00047	2.3000	0.000477	7.9	0.0004876
1.51667	0.0004609	3.0667	0.000471	20.2333	0.0004785
2.05000	0.0004505	6.2833	0.000448	23.75	0.0004778
3.08333	0.0004258	16.6500	0.000404	31.7	0.0004642
4.31667	0.0004037	21.0000	0.000369	43.1333	0.0004577
6.03333	0.0003738	25.8500	0.000344	50.9333	0.0004492
10.00000	0.0003139	29.5667	0.000322	56.35	0.0004434
21.43333	0.0002424	41	0.000289		
25.28333	0.0002124	47.6	0.00027		
29.23333	0.0001845	54	0.000252		

A.11. Data set HR-2

Experimental condition: 1mM DCAN at pH 8.5, NH_2Cl ranged from 0.4 – 1.2 mM

HRN1 - NH2Cl 0.4 mM		HRN2 - NH2Cl 0.7 mM		HRN3 - NH2Cl 1.0 mM		HRN4 - NH2Cl - 1.2 mM	
Time (hr)	DCAN (M)	Time (hr)	DCAN (M)	Time (hr)	DCAN (M)	Time (hr)	DCAN (M)
0.03	0.000498	0.03	0.000498	0.03	0.000498	0.03	0.000498
0.51	0.0004785	0.44	0.000485	0.47	0.0004856	0.39	0.000477185
0.76	0.0004707	1.00	0.0004694	0.78	0.0004759	0.71	0.000463525
1.00	0.0004629	1.50	0.0004551	1.10	0.0004668	1.02	0.000455719
1.50	0.0004525	2.00	0.0004466	1.50	0.000457	1.50	0.000441409
2.10	0.0004349	3.00	0.0004251	2.00	0.0004466	2.00	0.0004297
3.00	0.0004134	4.00	0.000405	3.08	0.0004206	3.00	0.000407584
4.10	0.0003926	6.00	0.0003705	4.00	0.000403	4.00	0.000390672
6.03	0.0003594	7.45	0.0003471	5.92	0.0003679	5.97	0.000358799
7.50	0.000336	9.00	0.0003243	7.50	0.0003438	7.50	0.000336032
9.07	0.0003139	12.00	0.0002853	9.00	0.0003217	8.93	0.000316518
12.03	0.0002762	23.75	0.000178	23.38	0.0001871	23.37	0.000177967
23.83	0.0001682						

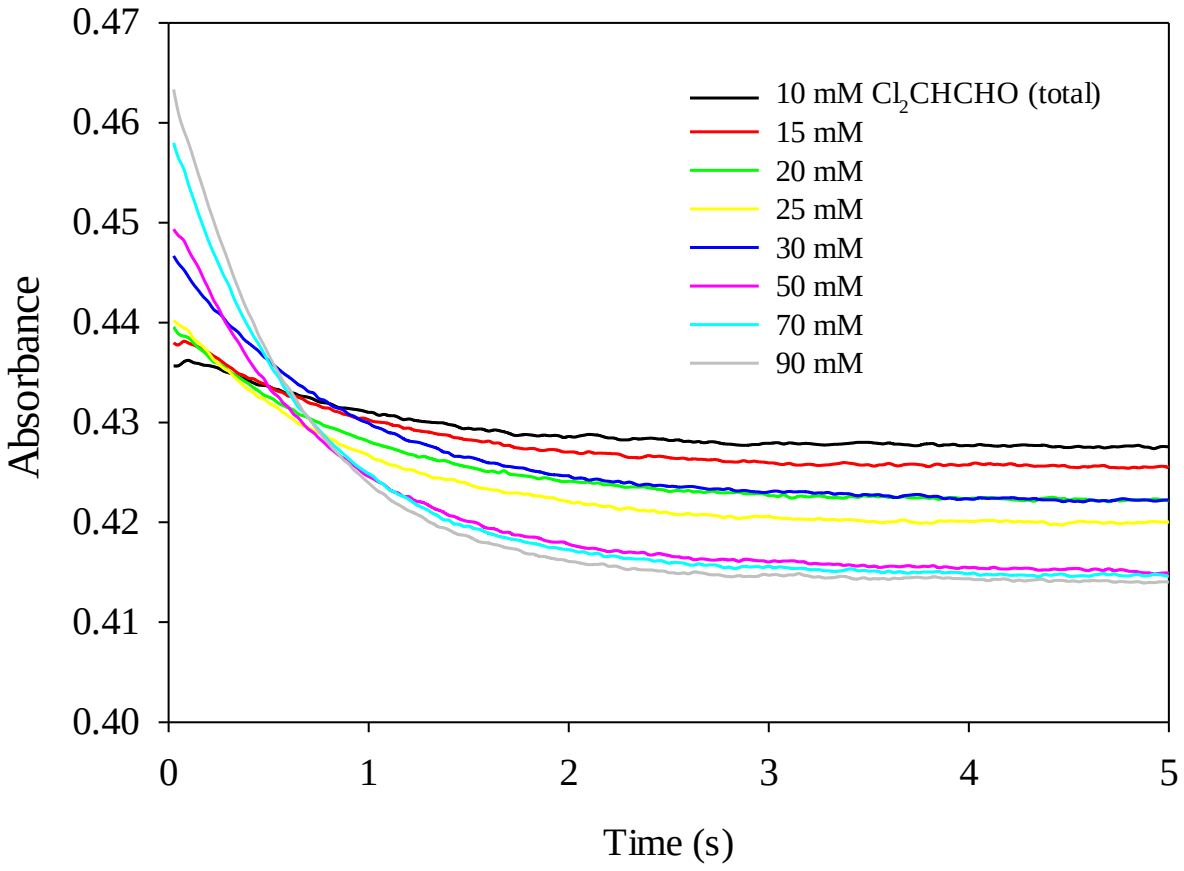

Figure A.1. Absorbance of the reaction between dichloroacetaldehyde and monochloramine within 5s. Experimental condition: dichloroacetaldehyde 10 – 90 mM, monochloramine 1 mM, Phosphate buffer 0.02 M, pH 7.8, 25ºC.

APPENDIX B

EXPERIMENTAL DATA FOR CHAPTER 3

B.1. Data set C01

Sample	Time (hour)	DCAN N14 (ppb)	DCAN N15 (ppb)	DCAN Total (ppb)	DCAM N14 (ppb)	DCAM N15 (ppb)	DCAM Total (ppb)
Blank	0	0.000	0.000	0.000	0.158	0.005	0.163
8h	8	0.095	0.089	0.184	0.178	0.078	0.255
23h	23	0.139	0.144	0.282	0.264	0.156	0.419
34h	34	0.201	0.237	0.438	0.432	0.320	0.752
48h	48	0.219	0.294	0.513	0.562	0.485	1.047
72h	72	0.221	0.324	0.545	0.600	0.813	1.414
96h	96	0.230	0.358	0.588	0.749	1.332	2.081
120h	120	0.234	0.349	0.583	0.908	1.681	2.589

Sample	Time (hour)	TCALD (ppb)	DCALD (ppb)
Blank	0	0.002	0.01
8h	8	0.511	0.13
23h	23	0.806	0.24
34h	34	1.092	0.35
48h	48	1.178	0.49
72h	72	1.306	0.56
96h	96	1.305	0.67
120h	120	1.296	0.76

B.2. Data set R01

Sample	Time (hour)	DCAN N14 (ppb)	DCAN N15 (ppb)	DCAN Total (ppb)	DCAM N14 (ppb)	DCAM N15 (ppb)	DCAM Total (ppb)
Blank	0	0	0	0.000	0.163	0.000	0.163
Cl_2 30mins	0	1.108	0.000	1.108	0.786	0.000	0.789
8h	8	1.388	0.312	1.700	0.905	0.182	1.087
23h	23	1.416	0.582	1.998	1.111	0.395	1.506
34h	34	1.503	0.701	2.204	1.629	0.796	2.425
48h	48	1.607	0.820	2.427	1.862	1.080	2.942
72h	72	1.295	0.658	1.953	1.845	1.598	3.444
96h	96	1.246	0.580	1.827	2.010	1.965	3.975
120h	120	1.081	0.566	1.647	2.127	2.374	4.501

Sample	Time (hour)	TCALD (ppb)	DCALD (ppb)
Blank	0	0.002	0
Cl_2 30mins	0	0.639	0.75
8h	8	1.380	0.85
23h	23	1.618	1.23
34h	34	1.926	1.49
48h	48	2.033	1.62
72h	72	2.175	1.80
96h	96	2.223	1.79
120h	120	2.277	2.03

B.3. Data set R02

Sample	Time (hour)	DCAN N14 (ppb)	DCAN N15 (ppb)	DCAN Total (ppb)	DCAM N14 (ppb)	DCAM N15 (ppb)	DCAM Total (ppb)
Blank	0	0	0	0.000	0.210	0.000	0.210
Cl_2 30mins	0	1.108	0.000	1.108	0.786	0.000	0.789
Cl_2 60mins	0	1.960	0.000	1.960	1.226	0.000	1.226
8h	8	2.252	0.224	2.477	1.366	0.260	1.626
23h	23	1.918	0.505	2.423	1.607	0.515	2.122
34h	34	1.761	0.655	2.416	2.008	0.560	2.568
48h	48	1.599	0.624	2.223	2.035	0.920	2.954
72h	72	1.406	0.606	2.012	2.668	1.195	3.863
96h	96	1.192	0.554	1.746	3.057	1.639	4.696
120h	120	1.015	0.479	1.493	3.323	1.963	5.286

B.4. Data set R03

Sample	Time (hour)	DCAN N14 (ppb)	DCAN N15 (ppb)	DCAN Total (ppb)	DCAM N14 (ppb)	DCAM N15 (ppb)	DCAM Total (ppb)
Blank	0	0	0	0.000	0.210	0.000	0.210
Cl_2 30mins	0	1.108	0.000	1.108	0.786	0.000	0.789
Cl_2 60mins	0	1.595	0.000	1.595	0.993	0.000	1.123
8h	8	1.634	0.365	1.999	1.362	0.275	1.637
23h	23	1.514	0.530	2.044	1.701	0.434	2.135
34h	34	1.453	0.543	1.996	1.951	0.671	2.622
48h	48	1.280	0.565	1.845	2.128	0.870	2.998
72h	72	1.174	0.488	1.662	2.231	1.089	3.320
96h	96	0.977	0.441	1.418	2.181	1.372	3.553
120h	120	0.795	0.389	1.184	2.295	1.544	3.839

B.5. Data set R04

Sample	Time (hour)	DCAN N14 (ppb)	DCAN N15 (ppb)	DCAN Total (ppb)	DCAM N14 (ppb)	DCAM N15 (ppb)	DCAM Total (ppb)
Blank	0	0	0	0.000	0.210	0.000	0.210
Cl_2 30mins	0	1.108	0.000	1.108	0.786	0.000	0.789
4h	4	1.575	0.343	1.918	1.093	0.027	1.120
8h	8	1.743	0.385	2.128	1.217	0.106	1.322
23h	23	1.845	0.487	2.332	1.414	0.204	1.618
34h	34	2.118	0.522	2.640	1.677	0.385	2.062
48h	48	2.186	0.623	2.809	1.976	0.422	2.398
72h	72	2.567	0.568	3.136	2.219	0.560	2.779
96h	96	2.647	0.533	3.180	2.362	0.682	3.045
120h	120	2.494	0.450	2.944	2.482	0.794	3.276

B.6. Data set R05

Sample	Time (hour)	DCAN N14 (ppb)	DCAN N15 (ppb)	DCAN Total (ppb)	DCAM N14 (ppb)	DCAM N15 (ppb)	DCAM Total (ppb)
Blank	0	0	0	0.000	0.210	0.000	0.210
Cl_2 30mins	0	1.108	0.000	1.108	0.786	0.000	0.789
4h	4	1.051	0.263	1.314	0.926	0.200	1.126
8h	8	0.717	0.221	0.938	1.335	0.576	1.910
23h	23	0.190	0.099	0.289	2.090	0.886	2.976
34h	34	0.085	0.092	0.176	2.133	1.165	3.299
48h	48	0.034	0.068	0.102	2.372	1.293	3.665
72h	72	0.031	0.064	0.095	2.475	1.553	4.028
96h	96	0.011	0.057	0.068	2.611	1.649	4.260
120h	120	0.000	0.044	0.044	2.301	1.647	3.948